

HELYBEN  
OLVASHATÓ

# Metamorphism in the Eastern Alps

GEORG HOINKES<sup>1\*</sup>, FRIEDRICH KOLLER<sup>2\*</sup>, ATTILA DEMÉNY<sup>3</sup>, RALF SCHUSTER<sup>4</sup>,  
CHRISTINE MILLER<sup>5</sup>, MARTIN THÖNI<sup>2</sup>, WALTER KURZ<sup>1</sup>, KURT KRENN<sup>1</sup> AND FRANZ WALTER<sup>1</sup>

<sup>1</sup> Institute of Earth Sciences, University of Graz, Universitätsplatz 2, A-8010 Graz, Austria; georg.hoinkes@uni-graz.at,

\*communicating author

<sup>2</sup> Universität Wien, Department für Lithosphärenforschung, Althanstraße 14, A-1090 Vienna, Austria;

friedrich.koller@univie.ac.at; \*communicating author

<sup>3</sup> Institute for Geochemical Research, Hungarian Academy of Sciences, Budaörsi út 45, H-1112 Budapest, Hungary

<sup>4</sup> Geological Survey of Austria, Neulinggasse 38, A-1030, Vienna, Austria

<sup>5</sup> University of Innsbruck, Institute of Mineralogy and Petrography, Innrain 52, A-6020 Innsbruck, Austria

## Table of contents

|   |    |
|---|----|
| 1. Introduction to the geology of the area visited .....  | 2  |
| 1.1 Plate tectonics .....   | 2  |
| 1.2 Description of the tectonic units of the Alps .....   | 4  |
| 1.3 Distribution and timing of metamorphism within the Alps .....   | 6  |
| 1.4 Geology of the Rechnitz Window unit .....   | 8  |
| 1.5 Geology of the Koralpe – Saualpe region .....   | 10 |
| 1.6 Geology of the Nockberge area .....   | 19 |
| 1.7 Geology of the Grossglockner area .....   | 20 |
| 2. Field stops .....  | 23 |
| 2.1 Field stop 1: Cák conglomerate, Cák, Rechnitz Window, Hungary .....   | 23 |
| 2.2 Field stop 2: View on Lockenhaus castle, Burgenland .....   | 24 |
| 2.3 Field stop 3: Gabbro at Glashütten, community of Lockenhaus, Burgenland .....   | 24 |
| 2.4 Field stop 4: Quarry Bienenhütte, Bernstein, Bernstein window, Burgenland .....   | 25 |
| 2.5 Field stop 5: Ophicalcite at Glashütten close to Schlaining, Rechnitz window, Burgenland .....  | 26 |
| 2.6 Field stop 5a: Dark calcareous micaschist, close to Unterkohlstätten, Rechnitz Window, Burgenland .....   | 27 |
| 2.7 Field stop 6: Greenschist, calcareous micaschists, quarry Freingruber, Rechnitz window, Burgenland .....  | 28 |
| 2.8 Field stop 7: "Plattengneis" – mylonite of the Koralpe complex at the Rath quarry, Rachling, W of Stainz, Styria .....  | 28 |
| 2.9 Field stop 8: Kyanite eclogite of the Koralpe complex at Hohl, S of Schwanberg, Styria .....  | 29 |
| 2.10 Field stop 9: Geopark, Glashütten, W of Deutschlandsberg, Styria .....   | 32 |
| 2.11 Field stop 10: "Paramorphosen"-Schists with pseudomorphs of kyanite after andalusite of the Koralpe<br>complex at Weinebene, W of Deutschlandsberg, Styria ..... | 32 |
| 2.12 Field stop 11: Panorama view towards the Southalpine Karawanken mountains and cultural stop,<br>Diex, N of Völkermarkt, Carinthia .....                          | 32 |
| 2.13 Field stop 12: Marbles of the Millstatt Complex at the Lauster quarry in Krastal, Puch, N of Villach, Carinthia .....  | 32 |
| 2.14 Field stop 13: Spodumene-bearing pegmatite and paragneisses of the Millstatt Complex at Lug-ins-Land,<br>Baldersdorf, S of Spittal a.d. Drau, Carinthia .....    | 34 |
| 2.15 Field stop 14: Coarse-grained garnet micaschists of the Radenthein complex,<br>Untertweg and Granatium at Radenthein, Carinthia .....                            | 35 |
| 2.16 Field stop 15: Coarse-grained micaschists and gneisses from the Radenthein Complex,<br>Nöringsattel (Millstätter Alpe), N of Radenthein, Carinthia .....         | 36 |



|  |    |
|--|----|
| 2.17 Field stop 16: Exhibition of minerals from the Hohe Tauern in the Mautturm at Winklarn, Carinthia .....   | 36 |
| 2.18 Field stop 17: Metapelites, metamarls and metabasites of the Glockner Nappe, Franz Josef Haus, Heiligenblut, Carinthia ...  | 36 |
| 2.19 Field stop 18: Retrogressed eclogite of the Glockner Nappe, Gamsgrube, Heiligenblut, Carinthia .....  | 37 |
| 2.20 Field stop 19: Serpentinites of the Glockner Nappe, Schönwand, Heiligenblut, Carinthia .....  | 38 |
| 2.21 Field stop 20: Metaclastic rocks of the Brennkogel group, Hochtorn Pass, Heiligenblut, Carinthia .....  | 38 |
| 2.22 Field stop 21: Thrust between Rote Wand – Modereck Nappe and Glockner Nappe, Elendgrube, Bruck/Fusch, Salzburg ....   | 38 |
| 2.23 Field stop 22: Chloritoid- and kyanite-bearing quartzitic schists, marbles and meta-evaporites of the Seidlwinkl<br>Triassic Group, Fuschertörl – Edelweißspitze, Bruck/Fusch, Salzburg ..... | 38 |
| 3. References .....  | 39 |
| Appendix – Itinerary for IMA2010 AT1 Field trip .....  | 46 |

## 1. Introduction to the geology of the area visited

The Alpine orogene formed during the convergence of the African and European plates, which has been more or less continuous since Cretaceous times. The geology of the Eastern Alps is complex, however, because of the existence of more than one oceanic realm and several microplates between Africa and Europe, and also because the interplay between shortening processes and lateral movements makes it difficult to determine the plate tectonic arrangement through time.

Models of Alpine tectonics have developed rapidly during recent decades, mainly as a result of modern structural, stratigraphic, petrological and geochronological investigations which, together with deep reflection seismic profiling and tomographic studies, have provided new insights into the present-day structures. Contrasting interpretations on the evolution of the Alpine orogen still remain, however, further complicated by the use of different nomenclatures. This summary of the geology of the Alps is based on the tectonic interpretation by Schmid *et al.* (2004) and on the recent review of Alpine metamorphic history by Oberhänsli (2004) together with all literature cited therein.

In a geographical sense the Alps are divided into the Southern Alps (to the south of the Periadriatic Lineament), the Eastern Alps, the Central Alps, and the arc of the Western Alps (Fig. 1). These divisions are each dominated by different paleogeographic elements, which were incorporated at different stages in the Alpine tectonic evolution, resulting in distinct geological structures and a specific geomorphology.

The excursion route passes through nearly all major tectonic units of the Eastern Alps and will also give a representative overview on the different landscapes, including the intramontane Pannonian Basin, the hilly areas of the eastern and mountainous regions of the central and

northern part of the Eastern Alps and the foreland Molasse Basin. The visited outcrops will give insight in the polyphase metamorphic history (Carboniferous, Permo-Triassic, Cretaceous and Tertiary) of the individual units.

In the following an overview on the plate tectonic evolution, the tectonic units of the Alps and the different metamorphic cycles is given.

### 1.1 Plate tectonic evolution

The Alpine orogen is subdivided into plate tectonic units reflecting the Mesozoic to Paleogene paleogeography. From north to south, respectively from bottom to the top, the Eastern Alps are formed by the following plate tectonic elements (Figs. 1, 2): The European plate is represented by the Helvetic and Ultrahelvetic nappes and the Subpenninic unit. Relics of the former Penninic Ocean (Piemont-Ligurian and Valais Ocean) are the overlying Lower and Upper Penninic nappes which form the Rhenodanubian Flysch belt and the Penninic nappes of the Engadin, Tauern and Rechnitz Window. The Middle Penninic nappes are the remnant of the Iberian-Briançonnais microcontinent which splitted in the western part of the Penninic

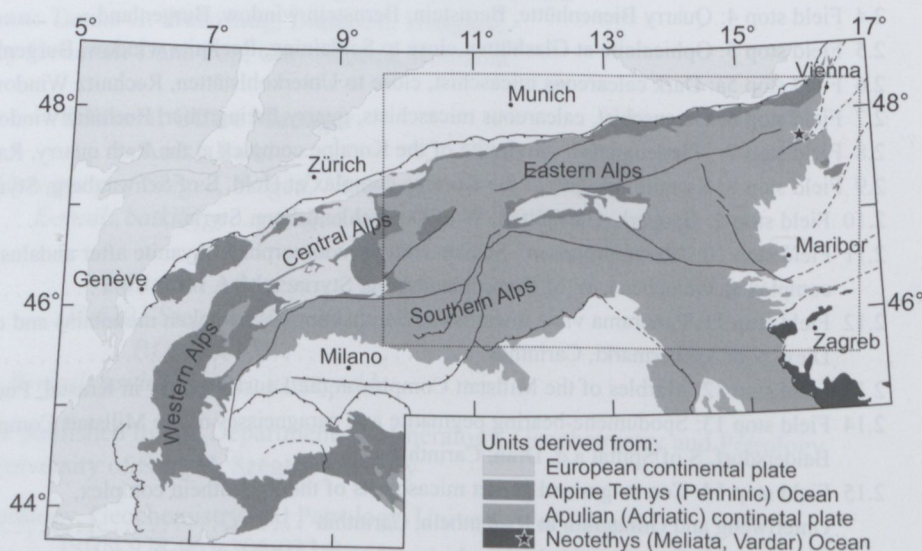
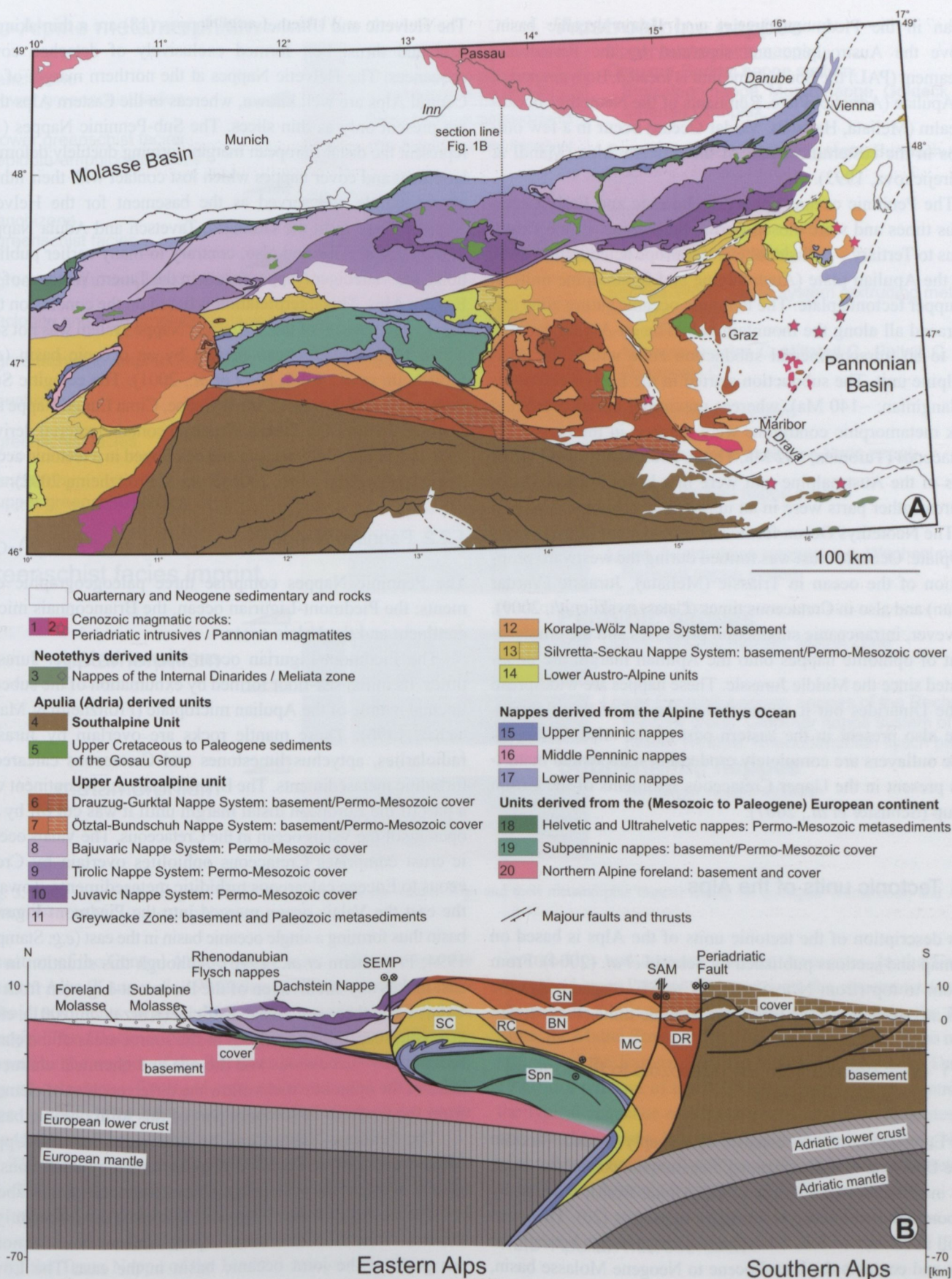


Fig. 1. Map of the major paleogeographic and tectonic units in the Alps according to Schmid *et al.* (2004).





**Fig. 2.** a) Tectonic map of the Eastern Alps according to the nomenclature in Schmid *et al.* (2004). The numbers of the units refer to the text; the squares show the areas visible in Fig. 7 and Fig. 15. b) Section through the Eastern Alps according to Schmid *et al.* (2004). GN – Gurktal nappe, DR – Drauzug Range, BN – Bundschuh nappe, RC – Radenthein Complex, MC – Millstatt Complex, SC – Schladming Complex, SEMP – Salzach-Ennstal-Mariazell-Puchberg fault, SAM – Southern border of Alpine Metamorphism (according to Hoinkes *et al.*, 1999), PAL – Periadriatic fault.



Ocean in the Piedmont-Ligurian and Valais oceanic basin. Above the Austroalpine and separated by the Periadriatic Lineament (PAL) the Southalpine unit is located. Both are part of the Apulian (Adriatic) Plate. Remnants of the Neotethys oceanic realm (Meliata, Hallstatt, Vardar Ocean) occur in a few outcrops in the easternmost part of the Eastern Alps (Mandl & Ondrejickova, 1993).

The Penninic oceans opened in Jurassic and Early Cretaceous times and were closed during the Alpine – Late Cretaceous to Tertiary – collisional event. Europe acted as the lower and the Apulian plate (Austroalpine and Southalpine unit) as the upper tectonic plate. The Penninic oceanic suture zone can be traced all along the mountain belt. The eo-Alpine event is due to an intracontinental subduction zone within the Austroalpine unit. The subduction started in the Early Cretaceous (Valanginian; ~140 Ma), whereas maximum burial depth and peak metamorphic conditions were reached in the early Late Cretaceous (Turonian; ~92 Ma, Thöni, 2006). During this event parts of the Austroalpine unit were in a lower plate position, whereas other parts were in an upper plate position.

The Neotethys Ocean formed an embayment into the Apulian plate. Oceanic crust was formed during the westward propagation of the ocean in Triassic (Meliata), Jurassic (Vardar Ocean) and also in Cretaceous times (Ustaszewski *et al.*, 2009). However, intraoceanic subduction processes and the emplacement of ophiolite nappes onto the Apulian margin are documented since the Middle Jurassic. These nappes are widespread in the Dinarides but it seems that outlayers of these nappes were also present in the eastern part of the Alps. Today all these outlayers are completely eroded but redeposited material is present in the Upper Cretaceous sediments of the Gosau Group (Schuster *et al.*, 2007).

## 1.2 Tectonic units of the Alps

This description of the tectonic units of the Alps is based on the map and sections published by Schmid *et al.* (2004). From bottom to top (from N to S, or NW to SE, respectively) the Alps are made up of the following tectonic units (Figs. 2, 3)

### 1.2.1 Units derived from the (Mesozoic to Paleogene) European continent

The European continent consists of a deeply eroded Variscan (Late Devonian to Carboniferous) metamorphic continental crust, rich in plutonic rocks (north of the Alpine front), covered by Carboniferous to Eocene sedimentary sequences (20). This crust is still in contact with its lithospheric mantle; it dips beneath the Alps and contains the Late Eocene to Neogene Molasse basin, which is the northern peripheral foreland basin of the orogene. The External massifs represent windows in the European plate within the Western and Central Alps. They comprise basement rocks and Late Carboniferous to Cretaceous cover sequences.

The Helvetic and Ultrahelvetic Nappes (18) are a thin-skinned fold and thrust belt formed exclusively of detached cover sequences. The Helvetic Nappes at the northern margin of the Central Alps are well known, whereas in the Eastern Alps they are present only as thin slices. The Sub-Penninic Nappes (19) represent the distal European margin, forming ductilely deformed basement and cover nappes which lost contact with their lithospheric mantle and served as the basement for the Helvetic Nappes. They form the Gotthard, Tavetsch and Adula Nappes in the Central Alps and also, contrary to many earlier publications, the Venediger Nappe system in the Tauern Window of the Eastern Alps. This interpretation is based on the conclusion that the crustal material of the Venediger Nappe system was not separated from the European margin by an oceanic basin (*e.g.* Froitzheim *et al.*, 1996; Kurz *et al.*, 2001). The eclogitic Sub-Penninic basement units (Adula Nappe, Cima Lunga Nappe and Eclogite Zone of the Tauern Window) contain material derived from the Alpine Tethys ocean and developed in a tectonic accretion channel (Engi *et al.*, 2001; Kurz & Froitzheim, 2002).

### 1.2.2 Penninic Nappes

The Penninic Nappes comprise three paleogeographic elements: the Piedmont-Ligurian ocean, the Briançonnais microcontinent and the Valais ocean.

The Piedmont-Ligurian ocean opened in Upper Jurassic times. Its initial sea-floor formed by exhumation of the subcontinental mantle of the Apulian microplate (Froitzheim & Manatschal, 1996). These mantle rocks are overlain by Jurassic radiolarites, aptychus limestones and Cretaceous calcareous turbiditic metasediments. The Briançonnais microcontinent was a part of the European distal margin until it was cut off by the opening of the Valais ocean in the Cretaceous. The Valais oceanic crust comprises Cretaceous ophiolites overlain by Cretaceous to Eocene calcareous turbiditic metasediments. Towards the east the Valais ocean merged into the Piedmont-Ligurian basin thus forming a single oceanic basin in the east (*e.g.* Stampfli, 1994; Froitzheim *et al.*, 1996). Although this situation in the east makes any subdivision of the Piedmont-Ligurian from the Valais basin there somewhat artificial (Kurz *et al.*, 2001), characteristic successions, analyses of the source areas of the clastic sedimentary successions and the age and chemical characteristics of the ophiolitic rocks allow the differentiation of elements from the northern or southern part of this joint oceanic basin.

The Penninic Nappes can be subdivided into the Upper, Middle and Lower Penninic Nappes, whereby each consists mainly of one of the paleogeographic elements mentioned above.

The Lower Penninic Nappes (17) consist predominantly of material from the Valais oceanic province and from the northern parts of the joint oceanic basin in the east. The Lower Penninic Nappes make up large parts of the Central Alps and the central part of the Lower Engadine Window. The lower nappes of the Rhenodanubian flysch zone, which are present along the northern margin of the Eastern Alps represent a con-



## Eo-Alpine metamorphism

## Austroalpine nappes

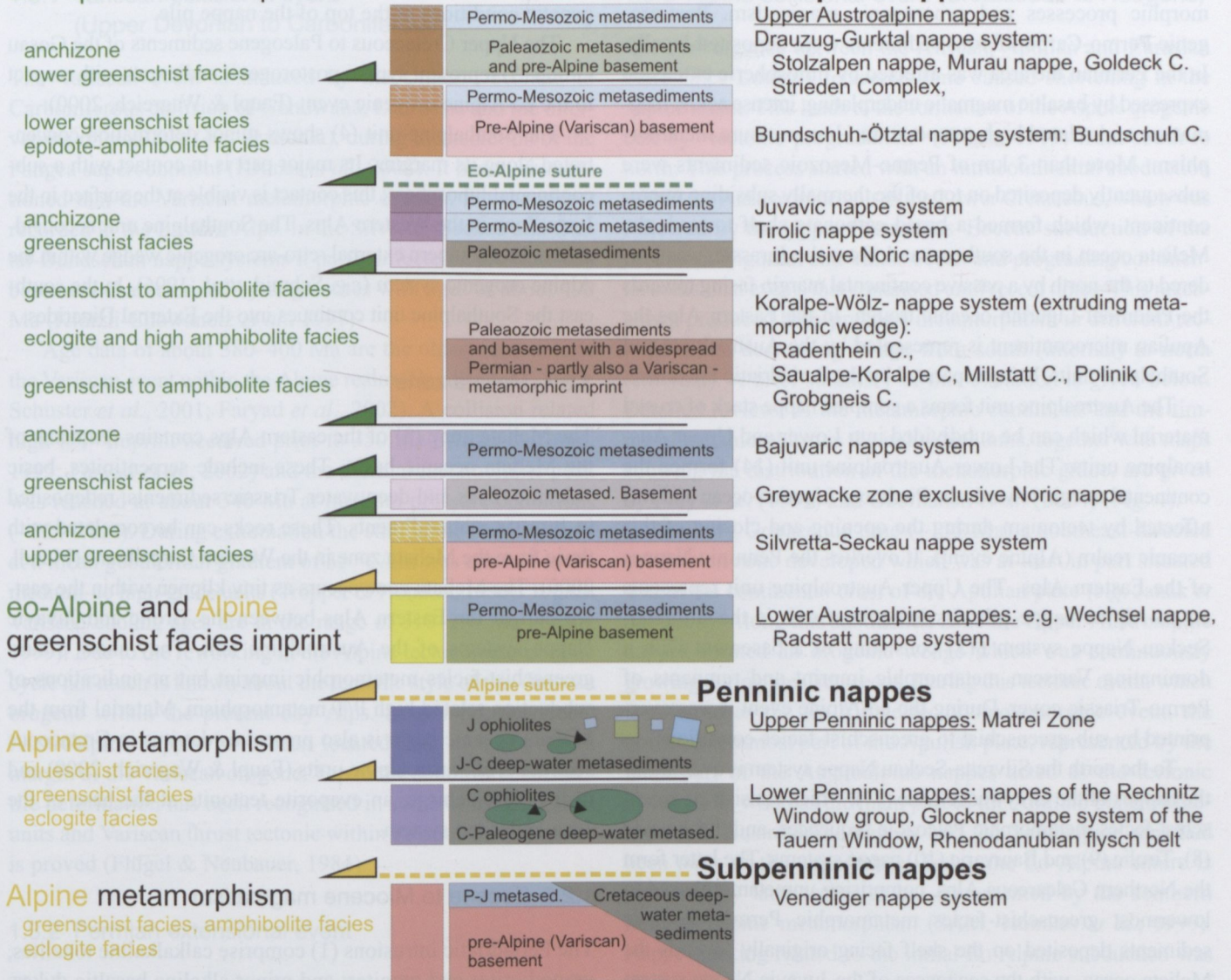


Fig. 3. Block diagram showing the major tectonic units of the Eastern Alps and their metamorphic imprint during the eo-Alpine (Cretaceous) and Alpine (Cenozoic) events.

tinuation of the Central Alpine Valais basin sediments into the Eastern Alps (Kurz *et al.*, 1998); they comprise Cretaceous flyschoid sediments deposited in a basin along the European margin. The Glockner Nappe system of the Tauern Window, as well as the nappes of the Rechnitz Window Group, consisting of calcareous flyschoid metasediments and metaophiolites, is thought to be a southern continuation of the lower nappes of the Rhenodanubian flysch zone.

The Middle Penninic Nappes (16) are mainly derived from the Briançonnais microcontinent and are common in the Western and Central Alps. The easternmost nappes to include material from the Briançonnais microcontinent are represented by the Tasna Nappe of the Lower Engadine Window.

Rocks derived from the Piedmont-Ligurian ocean and the accretionary wedge along the southern margin of the oceanic basin towards the Apulian microcontinent made up the Upper Penninic Nappes (15). They are widespread in the Western and

Central Alps and continue into the Apennines. In the Eastern Alps the Upper Penninic Nappes form the uppermost tectonic elements in the Engadine and Tauern windows (*e.g.* the Arosa Zone, the Matri Zone, and the Reckner Complex). In the northern part of the Eastern Alps the Ybbsitz klippen belt (Decker, 1990) is a remnant of the Piedmont-Ligurian ocean, containing the typical sequence of serpentinites, Jurassic radiolarites and aptychus limestones. It is in contact with the Kahlenberg Nappe of the Rhenodanubian flysch zone, which is also interpreted to be an Upper Penninic Nappe (Faupl & Wagreich, 1992).

### 1.2.3 Apulian microcontinent

The Apulian microcontinent consists of a Cadomian continental crust (Neubauer, 2002) with Paleozoic metasedimentary sequences and with magmatic activity related to rifting and subduction processes lasting until the Carboniferous. During the



Variscan orogeny large parts of this crust were affected by metamorphic processes and synorogenic magmatism. Post-orogenic Permo-Carboniferous sediments were deposited locally. In the Permian the area was affected by lithospheric extension expressed by basaltic magmatic underplating, intense acidic magmatism and related high-temperature / low-pressure metamorphism. More than 3 km of Permo-Mesozoic sediments were subsequently deposited on top of the thermally subsiding microcontinent, which formed a broad carbonate shelf towards the Meliata ocean in the southeast and, from the Jurassic, was bordered to the north by a passive continental margin facing towards the Piedmont-Ligurian oceanic trough. In the Eastern Alps the Apulian microcontinent is represented by the Austroalpine and Southalpine units, being separated by the Periadriatic lineament.

The Austroalpine unit forms a complex nappe stack of crustal material which can be subdivided into Lower and Upper Austroalpine units. The Lower Austroalpine unit (14) formed the continental margin towards the Piedmont-Ligurian ocean and was affected by tectonism during the opening and closing of this oceanic realm (Alpine event). It overlies the Penninic Nappes of the Eastern Alps. The Upper Austroalpine unit represents an eo-Alpine nappe pile. Its lowermost unit is the Silvretta-Seckau Nappe system (13) consisting of a basement with a dominating Variscan metamorphic imprint and remnants of Permo-Triassic cover. During the eo-Alpine event it was overprinted by sub-greenschist to greenschist-facies conditions.

To the north the Silvretta-Seckau Nappe system is overlain by the nappes of the Greywacke zone (11), which consists of greenschist-facies metamorphic Paleozoic sequences, and the Juvavic (8), Tirolic (9) and Bajuvaric (10) nappe systems. The latter form the Northern Calcareous Alps, comprising unmetamorphosed to lowermost greenschist-facies metamorphic Permo-Mesozoic sediments deposited on the shelf facing originally towards the Meliata ocean, with the sequences of the Juvavic Nappe system representing the most distal shelf towards the oceanic basin.

To the south the Silvretta-Seckau Nappe system is overlain by the Koralpe-Wölz Nappe system (12) which represents an eo-Alpine metamorphic extrusion wedge. Its Permo-Mesozoic cover was completely stripped off during an early phase of the eo-Alpine orogenic event (Lower Cretaceous) and it therefore consists exclusively of polymetamorphic basement nappes with a Permo-Triassic low P/T and an eo-Alpine high P/T metamorphic overprint (Schuster *et al.*, 2004).

The Ötztal-Bundschuh Nappe system (7) shows a similar lithological composition to the Silvretta-Seckau Nappe system, but is positioned on top of the Koralpe-Wölz Nappe system. The overlying Drauzug-Gurktal Nappe system (6) is made up of a Variscan metamorphic basement, anchizonal to greenschist-facies Paleozoic metasedimentary sequences and by unmetamorphosed Permo-Triassic sediments (Rantitsch & Russegger, 2000). Within the Ötztal-Bundschuh and Drauzug-Gurktal Nappe systems the eo-Alpine metamorphic grade

decreases upwards from amphibolite facies at the base to diagenetic conditions at the top of the nappe pile.

The Upper Cretaceous to Paleogene sediments of the Gosau Group (5) represent syn- to postorogenic sediments with respect to the eo-Alpine orogenic event (Faulpl & Wagreich, 2000).

The Southalpine unit (4) shows minor deformation concentrated along its margins. Its major part is in contact with a subcontinental lithosphere; this contact is visible at the surface in the Ivrea Zone in the Western Alps. The Southalpine unit is considered to be a southern external retro-arc orogenic wedge within the Alpine orogenic system (*e.g.* Schmid *et al.*, 1996). In the southeast the Southalpine unit continues into the External Dinarides.

#### 1.2.4 Meliata zone

The Meliata zone (3) of the eastern Alps contains remnants of the Meliata oceanic basin. These include serpentinites, basic volcanic rocks and deep water Triassic sediments, redeposited in Jurassic metasediments. These rocks can be correlated with those from the Meliata zone in the Western Carpathians (Mandl, 2000). The Meliata zone occurs as tiny klippen within the eastern part of the Eastern Alps between the Tirolic and Juvavic Nappe systems of the Austroalpine unit. They show a subgreenschist-facies metamorphic imprint but no indications of subduction related high P/T metamorphism. Material from the Meliata oceanic basin is also present as detritus in Cretaceous sediments of Austroalpine units (Faulpl & Wagreich, 2000) and in the Haselgebirge, an evaporite tectonite at the base of the Juvavic Nappe system.

#### 1.2.5 Eocene to Miocene magmatism

The Periadriatic intrusions (1) comprise calcalkaline tonalites, granodiorites and granites, and minor alkaline basaltic dykes. They are (Eocene to) Oligocene in age and related to the break-off of the Alpine Tethys oceanic lithosphere from the distal European margin (Davis & von Blanckenburg, 1995). Their intrusion is closely associated with contemporaneous strike-slip movements along the Periadriatic lineament.

The Pohorje pluton west of Maribor is not belonging to the Periadriatic intrusives. It is Miocene in age and related to the Pannonian magmatism (2) in the course of the extensional tectonics which leads to the development of the Pannonian basin (Fodor *et al.*, 2008).

### 1.3 Distribution and timing of metamorphism within the Alps

In the following chapter a brief summary of the metamorphic events of the Alps is given. In the Eastern Alps four major metamorphic cycles can be recognized since Paleozoic time.



### 1.3.1 Variscan collisional event (Upper Devonian to Carboniferous)

The Variscan event is induced by the Upper Devonian to Carboniferous collision of Gondwana, Laurussia and the intervening microplates (e.g. Avalonia), during the accretion of the Pangea supercontinent (Kroner *et al.*, 2008). It has to be mentioned that the Variscan metamorphic event is not the oldest recorded in the Eastern Alps. In the Silvretta-Seckau and Ötztal-Bundschuh nappe systems it partly affected a pre-Variscan basement characterized by migmatites with ages of about 490 Ma (Klötzli-Chowanetz *et al.*, 1997).

Age data of about 380–400 Ma are the oldest remnants of the Variscan event within the Alpine realm (Handler *et al.*, 1997; Schuster *et al.*, 2001; Faryad *et al.*, 2002). A collision related high P/T- imprint occurred prior to 350 Ma (Miller & Thöni, 1995; Faryad *et al.*, 2002) and the thermal metamorphic peak was reached at about 340 Ma at medium pressure conditions (~25 °C/km). During exhumation the sillimanite stability field at a mean geothermal gradient of 35 °C/km was crossed in the medium- to high-grade units (Tropper & Hoinkes, 1996). Typical Variscan cooling ages are in the range of 310–290 Ma (Thöni, 1999). Due to the reworking in the Alpine tectonometamorphic cycle not much is known about the tectonic style of the Variscan orogene within the present day Alps. In general, the recent Austroalpine nappes have been located near to the southern margin of the Variscan orogene. Top to the south-directed ductile deformation has been recognised in some of the basement units and Variscan thrust tectonic within Palaeozoic sequences is proved (Flügel & Neubauer, 1984).

### 1.3.2 Permian extensional event

The Permian event in the Alps followed in the wake of the Variscan tectonic evolution. Lithospheric extension affected the northern part of the Apulian microplate and caused magmatism and metamorphism in the Austroalpine, Southalpine and also in the Western Carpathian realm. The onset of the Permian event may be considered as when crustal thickness decreased below normal, and thus cannot be related to gravitational collapse of the Variscan orogen.

Evidence for active thinning in Permian time is the formation of grabens, intense magmatic activity and high temperature metamorphism (Thöni & Jagoutz, 1993; Habler & Thöni, 2001; Gaidies *et al.*, 2006; Schuster & Stüwe, 2008; Thöni & Miller, 2009). The metamorphic imprint reached a geothermal gradient of up to 45 °C/km. Peak metamorphic conditions were reached at about 280–260 Ma and accompanied by the formation of pegmatitic veins in upper amphibolite-facies metamorphic rocks. After that the rock pile was not exhumed and the lithosphere cooled down to the steady state geotherm of ~25 °C/km at about 200 Ma.

### 1.3.3 Alpine collisional event (Cretaceous to Neogene)

The convergence between the African, Apulian and Eurasian Plate since Lower Cretaceous time caused shortening in the Alpine realm. This leads to the formation of the Alpine orogenic belt by “tectonic progradation” (Frisch, 1979) from south to north. This process started with an intracontinental subduction within the Austroalpine unit in the Lower Cretaceous, which was followed by the Upper Cretaceous–Eocene subduction of the Piedmont-Ligurian and Valais ocean and prograding continental collisional events that continued until recent times. This mechanism produced high-pressure metamorphism in different tectonic units, decreasing in age from south (internal) to north (external). A brief summary of this evolution is given below. Detailed reviews of the metamorphic conditions and the timing of metamorphism in the individual units, together with maps showing the distribution of the metamorphic grade, are given by Frey *et al.* (1999) and Oberhänsli *et al.* (2004) (Fig. 4).

In Early Cretaceous time (~135 Ma) a southeast-directed subduction zone developed which was at least in part situated within the continental crust of the Apulian plate (e.g. Janák *et al.*, 2006). Along this subduction zone the Upper Austroalpine nappes formed an orogenic wedge which was continuously growing during the Cretaceous. During this tectonic event, which is referred as the Eo-Alpine tectonometamorphic event, the northwesternmost part of the Apulian plate, represented by the main part of the Austroalpine nappes acted as the tectonic lower plate, whereas the main part of the Apulian plate including some Austroalpine nappes and the Southalpine unit had been parts of the upper plate. Today the Eo-Alpine suture is obscured by later tectonics but documented by the southern limit of Alpine metamorphism (SAM, Hoinkes *et al.*, 1999). Nappe stacking related to the initial Eo-Alpine subduction was W to NW directed. Large parts of the sedimentary sequences of the Austroalpine unit have been stripped off from their basement, which has been buried and metamorphosed up to eclogite-facies conditions (Hoinkes *et al.*, 1991). Geochronological data suggest peak metamorphic conditions of the high-P metamorphic event at about 92 Ma (Thöni, 2006) and a subsequent medium pressure overprint during exhumation of the high-pressure rocks. In the eastern part of the Eastern Alps exhumation of the deeply buried units occurred by N or NW directed thrusting and S to SE directed extensional tectonics. During this process a metamorphic extrusion wedge formed. The latter shows a lower part with an inverted metamorphic field gradient and an upper part with an upright metamorphic field gradient. Cooling ages are in the range of 90 to 70 Ma (Hoinkes *et al.*, 1999; Thöni, 1999).

Ongoing subduction of the lithospheric plate caused the entrance of the Penninic oceanic domain into the subduction zone at about 100 Ma and after the closure of the ocean the European continent entered the subduction zone in the Paleogene at about 55 Ma. These processes are referred as the Alpine event, which



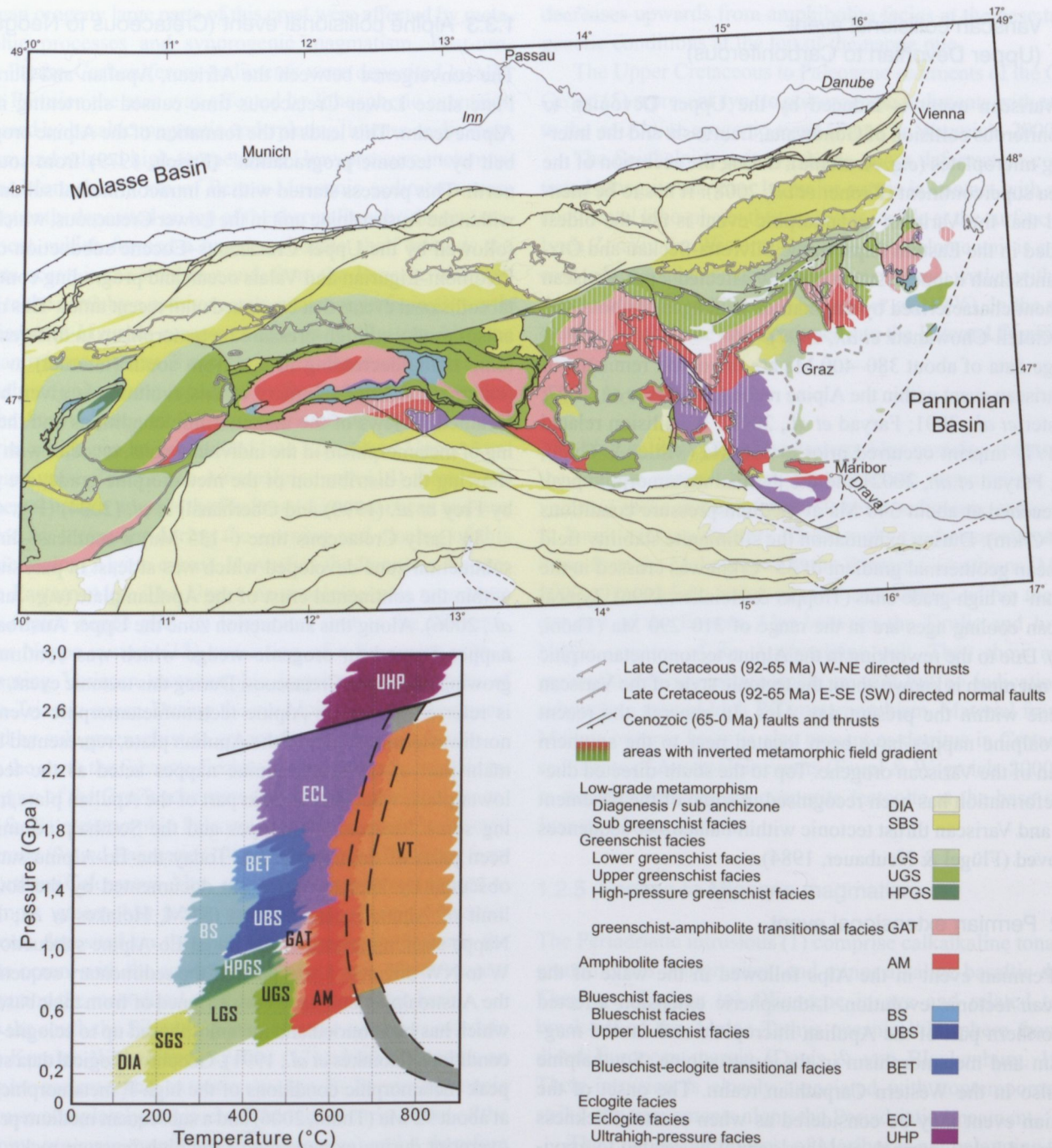


**Fig. 4.** Map of the Eastern Alps showing the distribution of the Alpine metamorphic imprint according to Oberhänsli (2004). Additionally areas with an inverted metamorphic field gradient and the most important Cretaceous and Cenozoic structures are given.

is the major event in the Western Alps. It is responsible for the formation of the Penninic and Subpenninic nappes. In the Eastern Alps the Alpine event caused a high P/T metamorphism in the Penninic and Subpenninic nappes at ~45 Ma (Thöni, 1999) and medium pressure overprint at about 30 Ma. Typical cooling ages are in the range of 25 to 15 Ma (Luth & Willingshofer, 2008). Exhumation of these units is related to E–W extension since Miocene time. It caused the formation of the Engadine-, Tauern- and Rechnitz- Windows. Adjacent to the windows the Austroalpine unit shows a structural and very low to low-grade Alpine metamorphic overprint (Hoinkes *et al.*, 1999).

## 1.4 Geology of the Rechnitz window unit

### 1.4.1 The Penninic zone at the eastern end of the Alps

The Penninic realm, widely distributed in the Western and Central Alps, can be followed along a series of windows across the whole range of the Eastern Alps. These are, from the W to the E the Lower Engadin Window, the Tauern Window and a group of small windows at the eastern margin of the Alps called the Rechnitz Window Group (RWG) (Höck & Koller, 1989; Koller & Höck, 1990).



The RWG (Fig. 5) at the eastern end of the Alps close to the Austrian-Hungarian border is formed by several small Penninic windows covered by the Lower Austroalpine nappes of the Variscan basement and more to the S also by young unmetamorphosed sediments (Pahr, 1980). From the north to the south they are called Möltener window, Bernstein window, Rechnitz window, and Eisenberg (Vashegy) window (Fig. 5). All these windows comprise huge masses of Mesozoic metasediments and locally some ophiolites (Koller & Pahr, 1980). The lithology consists of several km thick calcareous micaschists, quartz phyllites, graphite phyllites and locally breccias and few horizons of rauhwackes. From various outcrops of the calcareous micaschist a lower to mid-Cretaceous age is proven by fossils (Schönlaub, 1973). Within the ophiolitic section common remnants of oceanic metamorphism occur together with various degrees of oxidation in the most of the metagabbros, also in some of the metabasalts and ophicarbonates (Koller, 1985).

The metamorphic evolution is divided into an older LT/HP event and a younger one of Barrovian type. The following mineral parageneses have been described so far.

#### 1.4.2 Blueschist-facies event

Within the ophiolitic sequence, remnants of this HP/LT event are widespread. Typical minerals are alkali pyroxenes, glaucophane or "crossite", rare pseudomorphs of lawsonite, high-Si phengite (up to 3.5 pfu), Mg-rich pumpellyite with a  $\text{Fe}_{\text{tot}}/(\text{Fe}_{\text{tot}}+\text{Al})$

ratio of 0.03–0.06 or epidote, stilpnomelane, hematite and rutile. According to Koller (1985) the following mineral assemblages can be defined:

##### *Leucogabbro:*

- actinolite + Mg-pumpellyite + Mg-rich chlorite + albite

##### *Ferrogabbro:*

- aegerinaugite + epidote + albite + Fe-rich chlorite + hematite + rutile  $\pm$  stilpnomelane
- ferroglaucophane/crossite + epidote + albite + Fe-rich chlorite + magnetite + rutile  $\pm$  stilpnomelane

##### *Ferrodiorite and plagiogranite:*

- crossite + albite  $\pm$  Fe-rich chlorite  $\pm$  stilpnomelane  $\pm$  magnetite  $\pm$  rutile  $\pm$  phengite
- acmite + albite  $\pm$  Fe-rich chlorite  $\pm$  stilpnomelane  $\pm$  hematite  $\pm$  rutile  $\pm$  phengite
- albite + hematite + Mg-rich chlorite  $\pm$  talc  $\pm$  phengite

##### *Ophicarbonates:*

- aegerinaugite + Cr-rich phengite + Cr-epidote + hematite  $\pm$  stilpnomelane

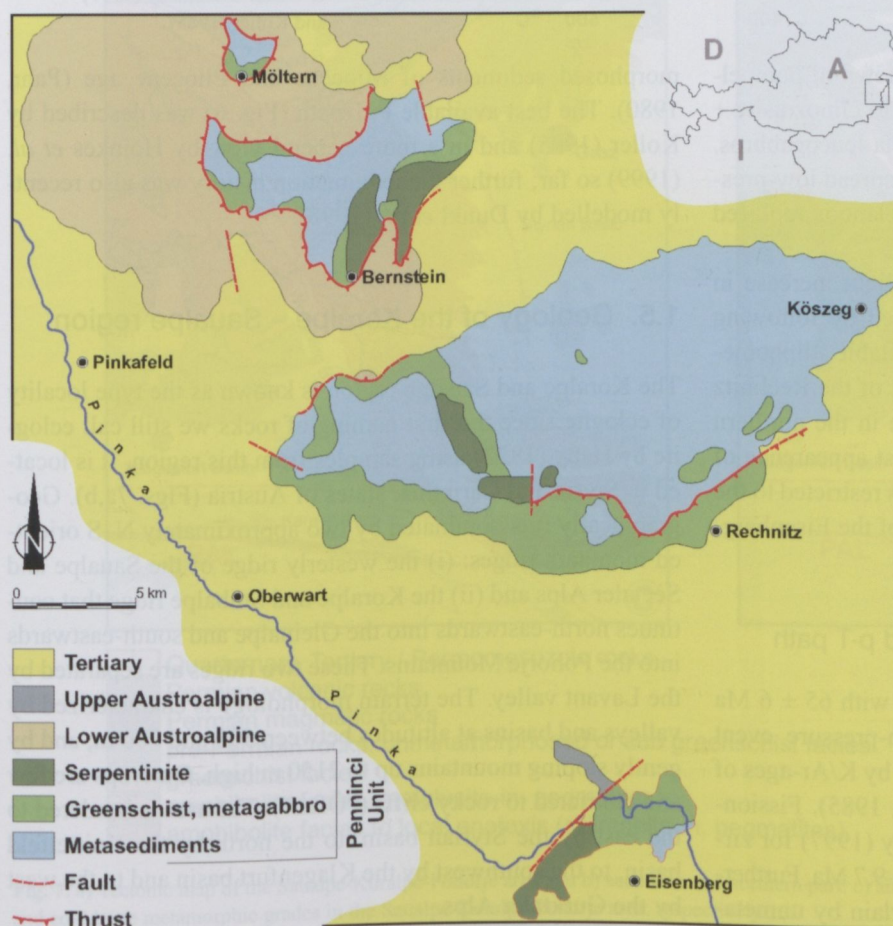
No clear high-pressure assemblage can be defined for the metabasalts containing very rare relics of blue amphibole, stilpnomelane and pseudomorphs after lawsonite. High-Si phengite is also observable in metabasalts and common in metasediments. In general only few data from the sedimentary rocks exist. Koller (1985) defines temperatures of 330–370 °C at a minimum pressure of 6–8 kbar for this high-pressure event (Fig. 6). The different mineral parageneses mentioned above are related to various degrees of oxidation.

#### 1.4.3 Low-pressure greenschist event

The high-pressure event is followed by a common greenschist-facies overprint forming the general assemblages (metabasalts, metasediments):

- Chlorite + albite + epidote + actinolite  $\pm$  titanite  $\pm$  magnetite  $\pm$  green biotite  $\pm$  muscovite
- Calcite + muscovite + paragonite  $\pm$  chlorite  $\pm$  quartz  $\pm$  albite  $\pm$  graphite  $\pm$  clinozoisite

Fig 5. Schematic geology of the Penninic unit at the eastern end of the Alps according to Pahr (1980) and Koller (1985).





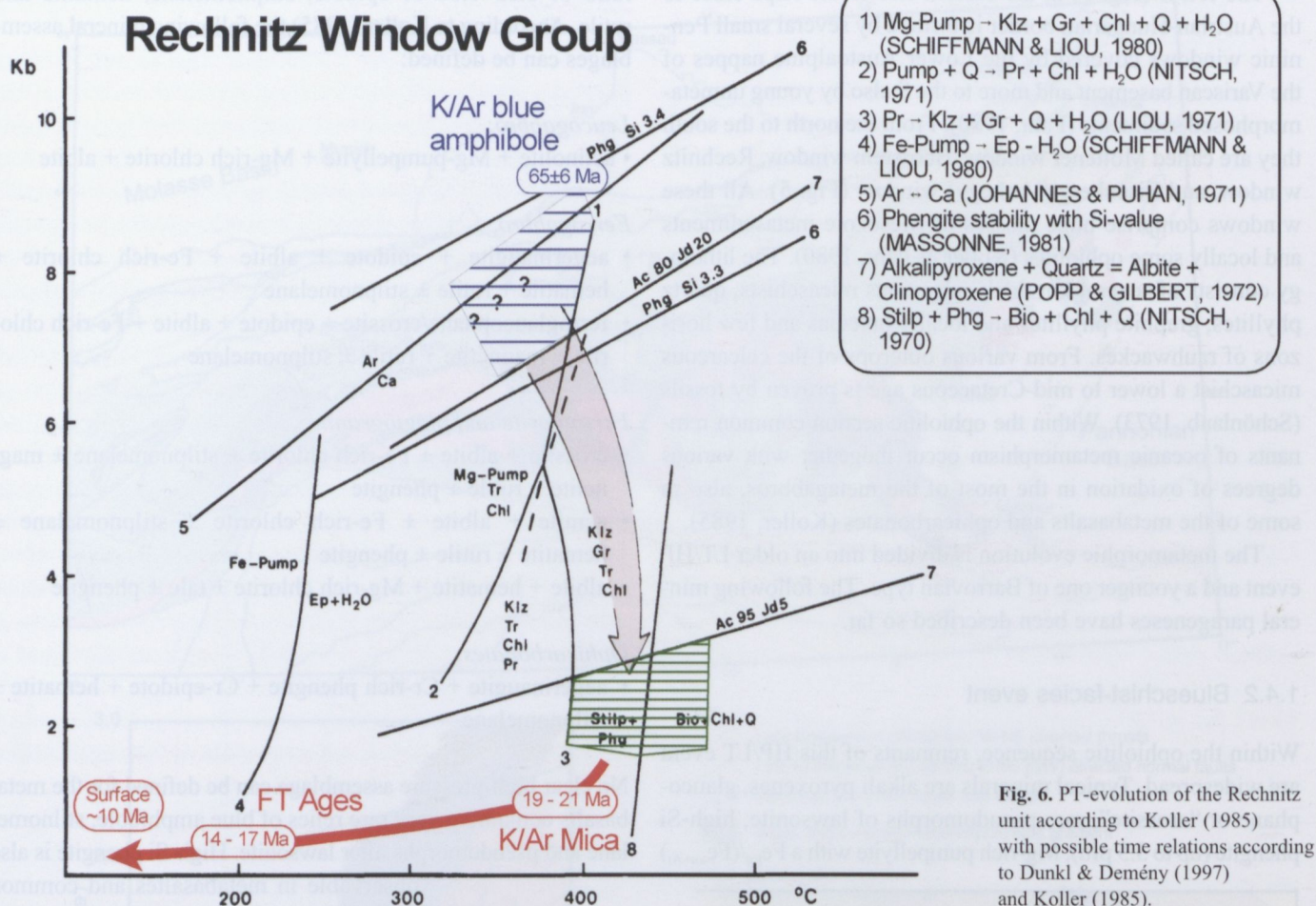


Fig. 6. PT-evolution of the Rechnitz unit according to Koller (1985) with possible time relations according to Dunkl & Demény (1997) and Koller (1985).

Classical prograde reactions cause the breakdown of pumpellyite to grossular + chlorite in rodingites and to clinozoisite + chlorite-actinolite (Czo + Chl + Act) in meta-leucogabbros. The Fe-rich Na-pyroxene is replaced by widespread low-pressure riebeckite/magnesioriebeckite, stilpnomelane is replaced by green biotite and lawsonite by epidote.

From the north to the south, there is a slight increase in temperature observable, which can be defined by following mineral isogrades: (1) Disappearance of metastable stilpnomelane and Mg-pumpellyite in the northern part of the Rechnitz window, (2) first appearance of green biotite in the northern part of the Bernstein window, and (3) the first appearance of garnet in metapelites (Bousquet *et al.*, 2008) is restricted to the southernmost outcrops of the Penninic units of the Eisenberg-Vashegy area (Fig. 5).

#### 1.4.4. Available radiometric age data and p-T path

Beside a single K/Ar age on blue amphibole with 65 ± 6 Ma no reliable age dating exists from the high-pressure event (Koller, 1985). The greenschist event is dated by K/Ar-ages of muscovite in the range of 22–19 Ma (Koller, 1985). Fission-track ages were reported by Dunkl & Demény (1997) for zircon from 21.9–13.4 Ma and for apatite from 7.3–9.7 Ma. Furthermore the Penninic rocks of the RWG is overlain by unmeta-

morphosed sediments of Miocene and Pliocene age (Pahr, 1980). The best available P-T path (Fig. 6) was described by Koller (1985) and in a more general view by Hoinkes *et al.* (1999) so far; further the exhumation history was also recently modelled by Dunkl *et al.* (1998).

### 1.5. Geology of the Koralpe – Saualpe region

The Koralpe and Saualpe region is known as the type locality of eclogite since the first naming of rocks we still call eclogite by Haüy (1822) using samples from this region. It is located in Styria and Carinthia, states of Austria (Figs. 7a,b). Geographically it is dominated by two approximately N–S oriented mountain ridges: (i) the westerly ridge of the Saualpe and Seetaler Alps and (ii) the Koralpe and Stubalpe ridge that continues north-eastwards into the Gleinalpe and south-eastwards into the Pohorje Mountains. These two ridges are separated by the Lavant valley. The terrain morphology is characterized by valleys and basins at altitudes between 500 and 700 m, and by gently sloping mountains up to 2150 m high. Outcrops are few and restricted to rocky cliffs (“Öfen”). The area is bordered to the east by the Styrian basin, to the north by the Knittelfeld basin, to the southwest by the Klagenfurt basin and to the west by the Gurktaler Alps.



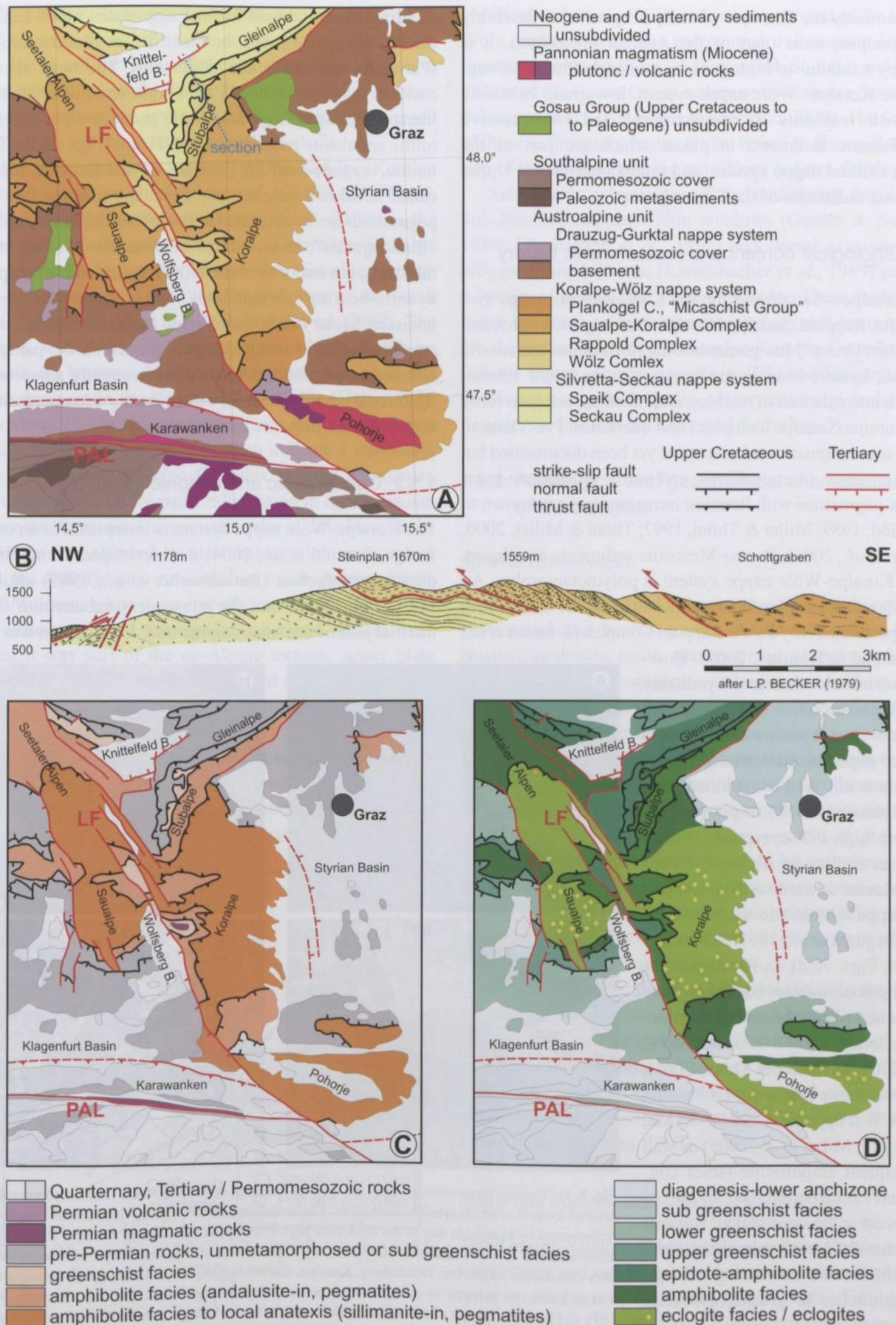


**Fig. 7.** a) Tectonic map of the Saualpe-Koralpe-Pohorje area and b) section in the northern part. c) and d) show maps with the distribution of the Permian and eo-Alpine metamorphic grades in the Saualpe-Koralpe-Pohorje area, respectively.



Tectonically the Koralpe – Saualpe region is an assembly of Austroalpine units (part of the Apulian microplate). It is formed by medium- to high-grade metamorphic units belonging to the Koralpe- Wölz nappe system, low-grade Paleozoic units with remnants of unmetamorphosed transgressive Permo-Triassic sediments in places which are part of the Drauzug-Gurktal nappe system, and unmetamorphosed Upper Cretaceous sediments of the Gosau Group.

### 1.5.1 Lithological content and metamorphic history

In the Koralpe – Saualpe region the Koralpe-Wölz nappe system (Wölz, Rappold, Saualpe-Koralpe, Plankogel Complex and “Micaschist Group”) has garnet-bearing micaschists and mostly mylonitic, kyanite-bearing paragneisses as its major lithologies, with intercalations of marbles, amphibolites, eclogites (only in the Koralpe-Saualpe Complex) and quartzites. Pre-Variscan and Variscan magmatic rocks have not yet been documented but granitic gneisses, (meta)gabbros, and partly spodumene-bearing meta-pegmatites with Permian intrusion ages are known to occur (Göd, 1989; Miller & Thöni, 1997; Thöni & Miller, 2000; Schuster *et al.*, 2001). Permo-Mesozoic sediments are absent.

The Koralpe-Wölz nappe system is polymetamorphic. An amphibolite-facies regional metamorphism related to the Variscan event is postulated only for the Rappold Complex (Schuster *et al.*, 2001; Faryad & Hoinkes, 2003). However, radiometric dating of probably Variscan garnet relics is still missing and it is not clear at present if the Rappold Complex experienced Variscan metamorphism at all. Well constrained are a Permo-Triassic low-P/T imprint and an eo-Alpine high-P/T overprint. Permo-Triassic as well as eo-Alpine P-T conditions increase upwards in the lower part of the nappe system and then decrease again (Gregurek *et al.*, 1997; Schuster *et al.*, 2004, Figs. 7c,d). In Permian times upper amphibolite-facies conditions have been reached within the central Koralpe-Saualpe Complex (0.38 GPa and 590 °C at 250–270 Ma; Habler & Thöni, 2001), whereas eclogite-facies (2.4 GPa and 650–730 °C at approximately 90–95 Ma; Miller, 1990; Miller *et al.*, 2005) as well as subsequent amphibolite-facies conditions have been determined for the eo-Alpine event in the same region. Towards the structurally deeper units in the north the conditions are decreasing via epidote-amphibolite to greenschist-facies conditions (Faryad & Hoinkes, 2003).

The polyphase evolution is visible in the metasedimentary rocks: Some types

of paragneisses contain kyanite aggregates which can, within the less deformed rocks, be identified as pseudomorphs after (Permian) andalusite and sillimanite. The most spectacular rocks of this type, called “Paramorphosenschiefer” in the local literature, exhibit large idioblastic pseudomorphs after chiascolitic andalusite measuring up to 50 cm (Figs. 8a,b). The mylonitic, kyanite-bearing gneisses of the Saualpe region are called “Disthenflasergneisses”. Permian and also a few Triassic pegmatoids are intercalated in the metasedimentary rocks. The “Plattengneiss”, an eo-Alpine blastomylonite of up to 700 m thickness, is a major element in the Koralpe and is composed of kyanite-bearing paragneisses and interlayered pegmatite gneisses. Meter to kilometre-sized lenses of eclogite, eclogite-amphibolite and (meta)gabbros occur within the paragneisses. Discordant pegmatoids formed preferentially adjacent to this rigid rock type (Neubauer, 1991) during decompression after the eo-Alpine pressure peak.

### 1.5.2 Geodynamic and tectonic evolution

The Koralpe-Wölz nappe system is interpreted as an extrusion wedge (Schmid *et al.*, 2004) that developed during the E–SE directed subduction (Ratschbacher *et al.*, 1989) until 90–95 Ma (Thöni, 2002) and the subsequent exhumation from the internal part of the Austroalpine unit. Exhumation was charac-

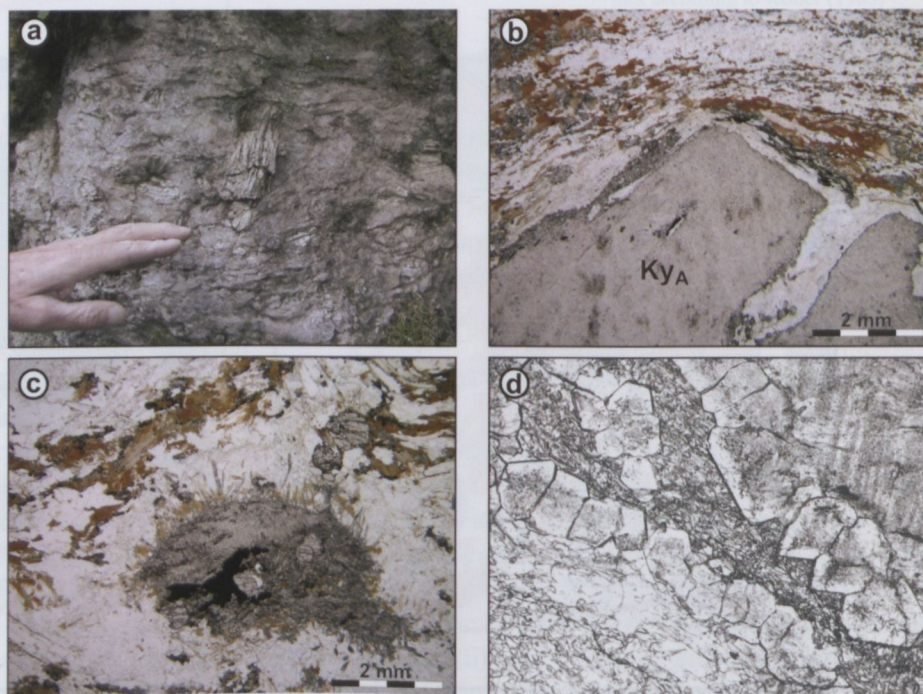


**Fig. 8.** a) “Paramorphosenschiefer” from the Koralpe complex with up to 40 cm long pseudomorphs of fine-grained kyanite after chiascolitic andalusite. The andalusite formed during the Permian low-P event, the replacement by kyanite is due to the eo-Alpine high-P overprint (Krakaberg, Koralpe, Carinthia, Österreichische Karte 1:50,000, hereafter ÖK 188). b) Thin section of a pseudomorph of fine-grained kyanite after chiascolitic andalusite. (Krakaberg, Koralpe, Carinthia, ÖK 188). c) Photograph showing the transition of gabbro to eclogite to eclogite-amphibolite within a single block (Bärofen, Koralpe, Styria, ÖK 189). d) Photomicrograph of coronitic Ky-rich eclogite where strings of inclusion-rich garnet separate former plagioclase and pyroxene domains. Igneous plagioclase has reacted to Ky + Zo + Qtz, pyroxenes have been replaced by omphacite or recrystallized to a granular aggregate of omphacite + magnesiohornblende + quartz (Bärofen, Koralpe, Styria, ÖK 189).



terised by penetrative deformation of the whole nappe system by NW-directed thrusting in the lower part of the wedge (Krohe, 1987) and SE–E directed extensional deformation in its upper part (Kurz *et al.*, 2002). These post-peak metamorphic tectonics caused an inversion of the metamorphic grade in the lower part of the nappe system (Figs. 4, 7).

Sm–Nd garnet ages on eclogites from the Saualpe, Koralpe and Pohorje areas are in the range of 108–87 Ma (Thöni, 2002). K–Ar and Ar–Ar muscovite ages are 85–90 Ma in the northern part of the nappe system (Gleinalpe–Stubalpe region), about 75 Ma in the central part (Saualpe–Koralpe region) and around 18 Ma in the Pohorje area to the south (Morauf, 1982; Schuster *et al.*, 1999; Fodor *et al.*, 2002). The same trend, with somewhat younger ages, is also shown by Rb–Sr data on biotites. Apatite fission track data from the Koralpe region are in the range of 35 to 40 Ma (Hejl, 1997), whereas about 11 Ma was measured from Pohorje (Fodor *et al.*, 2002). These geochronological data indicate a maximum burial of the Saualpe–Koralpe Complex in the Cenomanian and Turonian, followed by rapid exhumation in the Coniacian and Senonian. From the Campanian to the middle Eocene the Koralpe area was affected by slow exhumation and cooling whereas the Pohorje area remained at much greater depths until the Miocene, when it was rapidly exhumed.

The history of the Drauzug–Gurktal nappe system indicates that it was part of the eo-Alpine tectonic upper plate (Schmid *et al.*, 2004). It shows an upward decrease of the eo-Alpine metamorphic grade until reaching diagenetic conditions in the Permo-Mesozoic sediments at the top, indicating that it has not been buried since Permian times. It was affected by W-directed thrusting in the Lower Cretaceous (Fritz, 1988; Dallmeyer *et al.*, 1998), whereas in the Upper Cretaceous it was affected by ductile extensional deformation and normal fault-

ing (Neubauer *et al.*, 1995), as for the upper part of the Koralpe–Wölz nappe system. The extensional deformation led to the formation of basins (Kainach, Krappfeld, St. Paul) and the deposition of the Gosau Group sediments, which are Santonian to Paleogene in age (*e.g.* Ebner & Rantitsch, 2000). The formation of these sedimentary basins is also linked to the rapid exhumation of the eclogite bearing unit (Kurz & Fritz, 2003).

Subsequent exhumation of the underlying Penninic and Sub-Penninic nappes within windows (Genser & Neubauer, 1989; Fügenschuh *et al.*, 1997) and lateral extrusion of the orogene in the Miocene (Ratschbacher *et al.*, 1989) generated a system of normal and strike slip faults. These faults have a major influence on the recent morphology and are responsible for the exhumation of the Saualpe–Koralpe Complex in the Pohorje region. The Styrian, Knittelfeld and Klagenfurt basin developed along these faults. Major strike-slip faults are the Periadriatic line and the Lavanttal fault (Fig. 7).

### 1.5.3 Petrological and geochemical characteristics of the eclogites

#### Mineral assemblages:

The Koralpe, Saualpe and Pohorje eclogites are either quartz- or kyanite-rich and contain garnet, omphacite, quartz, kyanite, zoisite/clinozoisite, rutile, apatite, zircon, phengite, calcic-subcalcic amphiboles, paragonite, dolomite and sulfides (Miller, 1990; Miller & Thöni, 1997; Janák *et al.*, 2004; Sassi *et al.*, 2004). Amphiboles may be in textural equilibrium with omphacite and garnet, but more frequently form poikiloblasts overgrowing the foliation defined by omphacite  $\pm$  kyanite and zoisite. Retrogression is documented by (1) omphacite rimmed by symplectites of Na-poor clinopyroxene  $\pm$  calcic amphibole and sodic plagioclase, (2) kyanite mantled by complex symplectites of corundum + anorthite  $\pm$  spinel  $\pm$  sapphirine  $\pm$  Mg-staurolite, (3) symplectites of biotite + plagioclase after phengite, and (4) garnet replaced by a kelyphitic intergrowth of amphibole  $\pm$  plagioclase  $\pm$  epidote.

At the Bärenfen and Gressenberg localities in the Koralpe the transition from gabbro to eclogite can be studied *in situ*. The gabbros are generally isotropic and medium to coarse-grained, but modal layering on a cm-scale is locally present. They are mainly composed of calcic plagioclase and clinopyroxene  $\pm$  orthopyroxene  $\pm$  olivine (Heritsch, 1973; Thöni & Jagoutz, 1992; Miller & Thöni, 1997).

#### Major and trace element whole rock composition:

The Koralpe–Saualpe–Pohorje eclogites have a wide compositional range and can be subdivided into cumulate and basaltic types on the basis of the Pearce (1983)  $\text{Al}_2\text{O}_3$ – $\text{TiO}_2$  discrimination diagram (Fig. 9). The cumulate eclogite types are Mg-rich and characterized by low  $\text{TiO}_2$  (0.06–0.79 wt%), generally high  $\text{Al}_2\text{O}_3$  (up to 28.8 wt%), and Cr contents ranging from

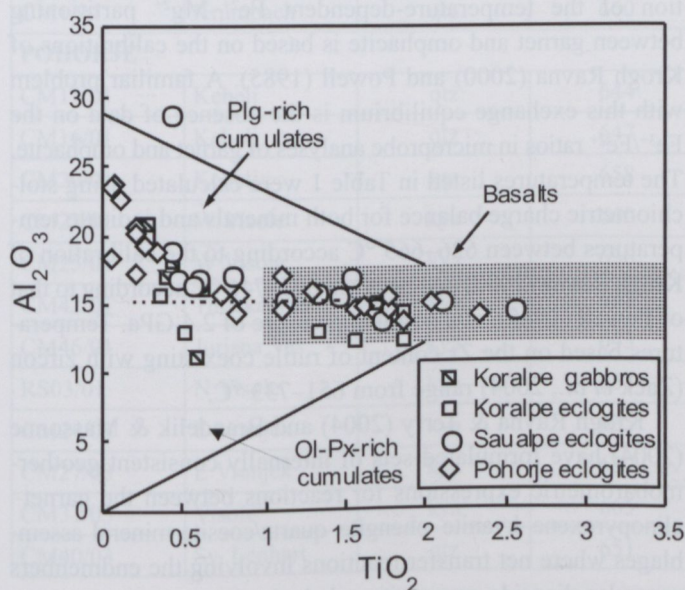
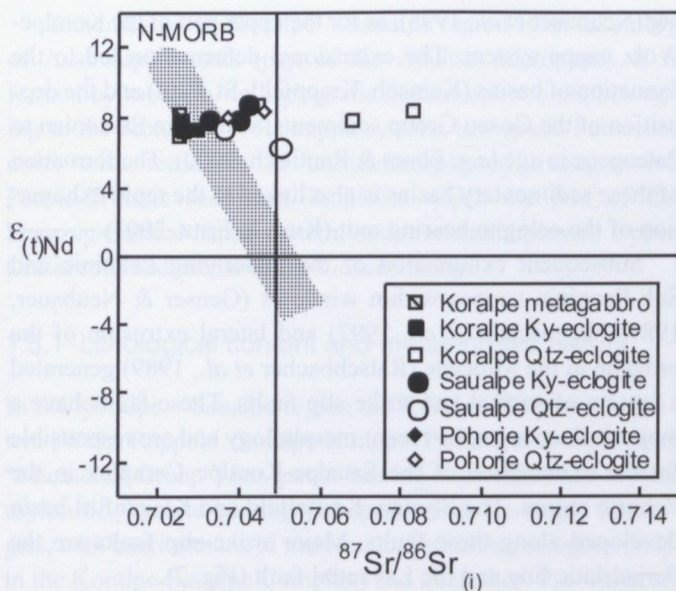


Fig. 9.  $\text{Al}_2\text{O}_3$ – $\text{TiO}_2$  variation of the Koralpe, Saualpe and Pohorje eclogites, plotted on the discrimination diagram of Pearce (1983). Dashed line separates kyanite-bearing and kyanite-free eclogites. Data are from Miller *et al.* (1988), Miller & Thöni (1997), Sassi *et al.* (2004) and unpublished data.





**Fig. 10.** Nd vs. Sr isotope correlation diagram of the Koralpe, Saualpe and Pohorje eclogites (data from Thöni & Jagoutz, 1992; Miller & Thöni, 1997; Sassi *et al.*, 2004). The gabbroic protoliths and most of the kyanite-rich eclogites plot on the Mantle array. The Sr isotopic composition of eclogites that plot to the right of the Mantle array could have been altered by reactions with seawater (e.g. Muehlenbachs, 1986).

400 to 1240 ppm, resulting in a low modal abundance of rutile and quartz in Mg-rich garnet and omphacite. The basaltic eclogite types, on the other hand, are quartz-rich and characterized by distinctly higher FeO and TiO<sub>2</sub> (1.10–2.70 wt%), but a lower Cr<sub>2</sub>O<sub>3</sub> content of 160–260 ppm. Kyanite is present in Al-rich compositions of both eclogite types, but modally much more abundant in the cumulate-type eclogites thought to be derived from plagioclase-rich cumulates (kyanite-rich eclogites). The low-K characteristics indicate a tholeiitic affinity for all investigated samples. Highly variable Cr and Ni contents and the wide range in Mg-ratios [Mg# = Mg/(Mg + ΣFe)] of 0.54–0.84 clearly point to igneous fractionation during protolith generation.

In terms of immobile trace element concentrations and Nd isotopic compositions, the Koralpe-Saualpe-Pohorje eclogites and their gabbroic protoliths are comparable to N-MORBs. Sr and oxygen isotope systematics (Miller *et al.*, 1988) are best explained by variable, but mostly minor, seawater alteration (Fig. 10). All samples are light rare earth element (LREE)-depleted (La<sub>N</sub>/Yb<sub>N</sub> = 0.35–0.69). Some of the analysed metagabbros and cumulate-type kyanite-rich eclogites have lower and more variable incompatible trace element contents compared to basaltic-type quartz-rich eclogites (Fig. 11) as well as positive Sr and Eu anomalies (Eu/Eu\* = 1.12–1.53).

As argued by Miller *et al.* (1988), Thöni & Jagoutz (1992), Miller & Thöni (1997), Sassi *et al.* (2004) and Miller *et al.* (2005), the eclogite precursor rocks represent a Permian (247–275 Ma) N-MORB-type gabbroic rock-suite evolving through fractional crystallization of olivine, clinopyroxene, orthopyroxene and plagioclase.

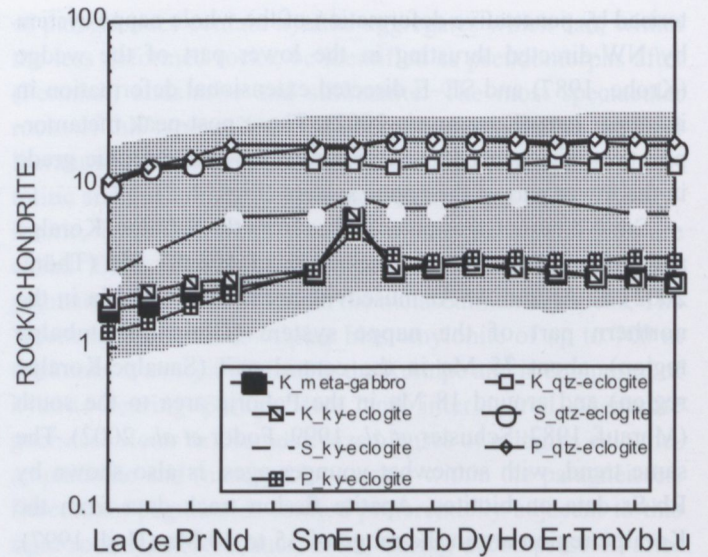


**Fig. 11.** Chondrite-normalized (Boynton, 1984) rare earth element plots showing representative patterns of a Koralpe metagabbro, kyanite- and quartz-rich eclogites form the Koralpe (K), Saualpe (S) and Pohorje (P). The shaded area represents the range of all compositions reported for these eclogites and their gabbroic protoliths by Miller *et al.* (1988), Miller & Thöni (1997), Sassi *et al.* (2004) and unpublished data.

#### 1.5.4 Geothermobarometry

Despite recent advances in high pressure/ultrahigh pressure (HP/UHP) geothermometry, the precise determination of eclogite peak metamorphic conditions remains difficult. Geothermobarometric calculations are critically dependent on thermodynamic data sets, activity models and the quality of mineral chemical data, and do not yet permit an unambiguous determination of pressure and temperature. The thermometric evaluation of the temperature-dependent Fe<sup>2+</sup>–Mg<sup>2+</sup> partitioning between garnet and omphacite is based on the calibrations of Krogh Ravna (2000) and Powell (1985). A familiar problem with this exchange equilibrium is the absence of data on the Fe<sup>3+</sup>/Fe<sup>2+</sup> ratios in microprobe analyses of garnet and omphacite. The temperatures listed in Table 1 were calculated using stoichiometric charge balance for both minerals and indicate temperatures between 626–665 °C according to the calibration of Krogh Ravna (2000) and between 695–746 °C according to that of Powell (1985), at a nominal pressure of 2.4 GPa. Temperatures based on the Zr content of rutile coexisting with zircon (Zack *et al.*, 2004) range from 651–733 °C.

Krogh Ravna & Terry (2004) and Brandelik & Massonne (2004) have formulated sets of internally consistent geothermobarometric expressions for reactions between the garnet–clinopyroxene–kyanite–phengite–quartz/coesite mineral assemblages where net transfer reactions involving the endmembers grossular, diopside, muscovite, celadonite, kyanite, quartz/coesite define equilibrium pressure and temperature for kyanite–phengite–quartz/coesite-bearing eclogites. The results listed in Table 1 show that these invariant points range from 2.2 to 2.4 GPa



**Table 1.** Estimated PT conditions of Saualpe, Koralpe and Pohorje eclogites

| sample  | locality      | type | T1 °C   | T2 °C   | T3 °C   | T4 °C    | T5 °C     |
|---------|---------------|------|---------|---------|---------|----------|-----------|
|         |               |      | 2.4 GPa | 2.4 GPa | Zr (Rt) | / P(GPa) | / P (GPa) |
| SAUALPE |               |      |         |         |         |          |           |
| GE2     | Gertrusk      | qtz  | 655     | 695     | 651     |          |           |
| SJ1     | Jurkikogel    | kya  | 635     | 716     |         | 693/2.25 | 724/2.49  |
| SJ4 TS  | Jurkikogel    | qtz  | 626     | 688     |         |          |           |
| SK20    | Kirchberg     | kya  | 664     | 744     |         |          |           |
| SK 30TS | Kirchberg     | kya  | 651     | 723     |         |          |           |
| SKP2    | Kupplerbrunn  | qtz  | 655     | 711     | 721     |          |           |
| CM06/03 | Kupplerbrunn  | kya  | 641     | 724     |         |          |           |
| 88T35   | Kupplerbrunn  | kya  | 654     | 731     |         | 721/2.23 | 744/2.52  |
| 04T30   | Kupplerbrunn  | qtz  | 659     | 740     |         |          |           |
| 04T31   | Kupplerbrunn  | kya  | 648     | 730     |         |          |           |
| SKP17   | Prickler Halt | qtz  | 648     | 713     |         |          |           |
| SKP23   | Prickler Halt | kya  | 639     | 717     |         | 705/2.22 | 729/2.47  |
| SKP26   | Prickler Halt | kya  | 639     | 719     |         |          |           |
| CM11/03 | Grünburg      | qtz  | 629     | 698     |         |          |           |
| CM12/03 | Grünburg      | qtz  | 647     | 717     |         |          |           |
| KORALPE |               |      |         |         |         |          |           |
| 94T44KH | Hohl          | kya  | 630     | 708     |         |          |           |
| H42     | Hohl          | qtz  | 657     | 704     |         |          |           |
| H8      | Hohl          | kya  | 665     | 732     |         |          |           |
| CM5/04  | Hohl          | kya  | 642     | 722     |         |          |           |
| KBE     | Bärofen       | kya  | 624     | 698     |         |          |           |
| KK3     | SE Kleinalpl  | qtz  | 639     | 688     |         |          |           |
| KM10    | Mauthner Eck  | qtz  | 661     | 700     | 681     |          |           |
| CM1/04  | Krumbach      | qtz  | 660     | 708     |         |          |           |
| POHORJE |               |      |         |         |         |          |           |
| CM15/01 | Kebelj        | qtz  | 644     | 703     | 701     | 696/2.21 | 707/2.47  |
| CM16/01 | Kebelj        | qtz  | 647     | 702     |         |          |           |
| CM20/01 | Kebelj        | qtz  | 658     | 722     | 697     | 666/2.19 | 696/2.38  |
| CM23/01 | W Visole      | kya  | 660     | 731     |         |          |           |
| CM25/01 | W Visole      | kya  | 636     | 747     |         |          |           |
| CM42/01 | Turiska Vas   | kya  | 648     | 741     |         |          |           |
| CM46/01 | Jurisna Vas   | kya  | 643     | 740     |         |          |           |
| RS03/01 | N Visole      | kya  | 653     | 746     |         |          |           |
| CM24/03 | E Vranjek     | kya  | 635     | 711     |         | 704/2.42 | 732/2.61  |
| CM27/03 | E Vranjek     | kya  | 637     | 721     | 733     | 745/2.41 | 773/2.67  |
| CM31/03 | Visole        | kya  | 665     | 758     |         | 760/2.43 | 785/2.80  |
| CM40/03 | Sv. Lenhart   | qtz  | 651     | 699     | 713     |          |           |

T1 = Krogh Ravna (2000); T2 = Powell (1985)

T3 = Zack *et al.* (2004); Zr in rutile determined by LA-ICP-MS

T4/P= Brandelik &amp; Massonne (2004)

T5/P= Krogh Ravna &amp; Terry (2004)



when calculated according to Brandelik & Massonne (2004), and from 2.4 to 2.8 when using the geothermometric expressions of Krogh Ravna & Terry (2004). The results also show that all samples plot within the stability field of quartz. The exhumation path is not well constrained with respect to P and T. The onset of lower-grade transformation is marked by the breakdown of omphacite to Ca-augite  $\pm$  Ca-amphibole-sodic plagioclase symplectites, by biotite-plagioclase symplectites that replace phengite and by plagioclase-corundum  $\pm$  spinel symplectites formed at the expense of kyanite. The only mineral reactions that can be attributed to the intervening stage are texturally late amphibole poikiloblasts that coexist with garnet and omphacite. Model calculations show that this could have happened as the pressure dropped to approximately 2 GPa.

### 1.5.5 Geochronology

The first protolith and metamorphism ages of metagabbros of this region were analysed by the Sm-Nd method by Thöni & Jagoutz, 1992 from the locality Bäröfen (N46°47'06" E15°05'13"; Österreichische Karte 1:50,000, sheet 189 Deutschlandsberg), which is not on the excursion route. Whole rock (wr), plagioclase (Pl), and clinopyroxene (Cpx) analyses of sample Bär1 define an isochron corresponding to an age of  $275 \pm 18$  Ma (MSWD = 0.12), resulting in an initial  $\epsilon_{\text{Nd}} = +8.4$  (Thöni & Jagoutz 1992). The Depleted Mantle model age for this rock is 253 Ma. Plagioclase-clinopyroxene two-point regression for another two gabbro samples (Miller & Thöni, 1997) yielded  $247.2 \pm 14.4$  Ma (sample Bär2) and  $254.4 \pm 8.7$  Ma (sample 92T11B). Within analytical uncertainties, these ages and the corresponding initial  $\epsilon_{\text{Nd}}$  values of +8.8 and +8.2 are identical with the results obtained on sample Bär1. Inclusion of all Bäröfen wr, Pl and Cpx fractions ( $n = 9$ ) in a single regression calculation results in:  $t = 257 \pm 21$  Ma;  $\epsilon_{\text{Nd}} = +8.4$ , MSWD = 4.1 (Fig. 12). The initial  $^{87}\text{Sr}/^{86}\text{Sr}$  ratios range between 0.70249 and 0.70278 when calculated for an age of 260 Ma, suggesting that the gabbro has more or less preserved its primary magmatic isotopic signature.

In addition, a coronitic eclogite (88T32) was analysed from this outcrop. This sample yields an  $\epsilon_{\text{Nd}}$  (260 Ma) of +8.4 and a corresponding  $^{87}\text{Sr}/^{86}\text{Sr}$  ratio of 0.70258. As discussed by Thöni & Jagoutz (1992), the Sm-Nd data of wr, garnet, clinopyroxene and amphibole show isotopic disequilibrium (Fig. 13), although wr and Grt yield a regression date of  $93 \pm 13$  Ma (or of  $88 \pm 9$  Ma if the data point for Zo is included; Thöni & Miller, 1997) that is close to new results obtained for well-equilibrated eclogites from the Saualpe and Pohorje (Miller *et al.*, 2005; Thöni *et al.*, in preparation).

A Ky-St-bearing Grt-mica schist sampled some 70 m away from the Bäröfen eclogite outcrop yielded a Grt-wr Sm-Nd age of  $88.7$  Ma (Miller & Thöni, 1997). Inclusion of an impure garnet fraction in the regression (Fig. 13) results in an age of  $89.5 \pm 2.7$  Ma (MSWD = 1.6;  $\epsilon_{\text{Nd}} = -10.1$ ).

At present, the age results for both protolith source and the subsequent evolution in time of the Koralpe-Saualpe type-

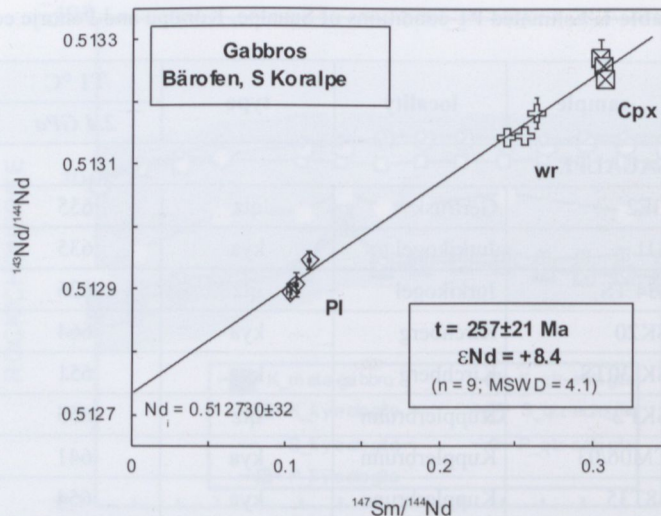


**Fig. 12.** Sm-Nd isochron plot showing results for handpicked plagioclase (Pl) and clinopyroxene (Cpx) fractions, and the whole rock (wr) for the three gabbro samples Bär1, Bär2 and 92T11B from Bäröfen locality, Koralpe. The mean regression age of  $257 \pm 21$  Ma (Upper Permian) is taken to indicate the time of crystallisation of the gabbro that was derived from a depleted N-MORB-type source (mean  $\epsilon_{\text{Nd}} = +8.4$ ).

locality eclogites can be summarized as follows: (1) The protoliths of the investigated eclogites were emplaced in Permian time within thinned continental crust, either as gabbros or basalts of MORB-type affinity; (2) Cretaceous HP conditions were effective in the Koralpe-Saualpe region up to 90–88 Ma B.P.; (3) fast exhumation, with exhumation rates in the range of 3–5 km/Ma, was operating in the time interval ~90–80 Ma B.P., with a clear decrease in cooling rates after that time.

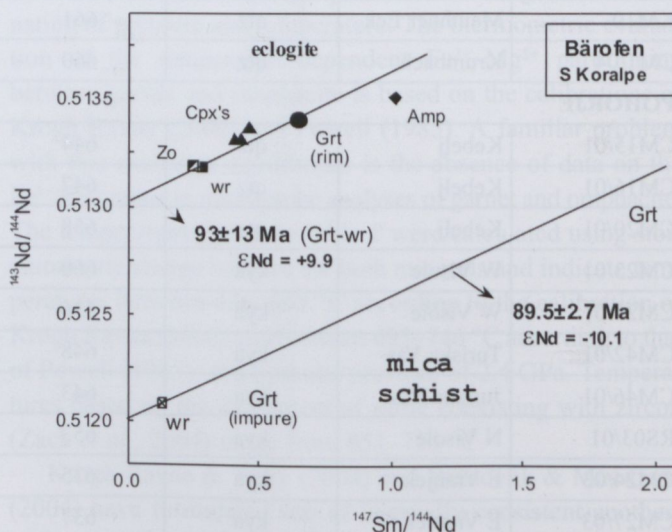


**Fig. 13.** Sm-Nd isochron plot showing mineral and whole rock data points for metagabbroic, coronitic eclogite 88T32 (upper part of the diagram; data from Thöni & Jagoutz, 1992) and metapelite 90T11B (lower part of the diagram; Miller & Thöni, 1997) from Bäröfen locality. Note the strong Nd isotope disequilibrium among the high-P minerals of the gabbro. The Grt fraction was handpicked from the largely inclusion-free rims only. The age result of  $89.5 \pm 2.7$  Ma for the metapelite garnet ( $n = 3$ ; MSWD = 1.6) is very similar to those of other metapelite garnets from the Saualpe-Koralpe-Pohorje crystalline.



### 1.5.6 Eclogite microstructures and crystallographic preferred orientations (CPOs)

The eclogites of the Koralm area form layers and lenses of 0.1 to 100 m thickness. Most eclogites show a strong schistosity and a mineral lineation at outcrop scale, due to a shape preferred orientation of omphacite, zoisite, kyanite, and amphibole, and a compositional layering at millimeter-scale. Coarse-grained eclogites without shape preferred orientation occur as boudins within schistose fine-grained eclogite mylonites. On a microscale, the eclogites show a clear succession of mineral parageneses related to several phases of their metamorphic evolution. The transformation of gabbroic parageneses into coarse-grained eclogitic assemblages occurred without penetrative deformation at a meso-scale. The coarse-grained boudinaged eclogites show a weak foliation. However, omphacite shows several features of plastic deformation. Coarse grains (omph1) are twinned, kinked and bent. Fine grains of recrystallized omphacite (omph2)

are arranged along twin lamellae, cleavage surfaces and the grain boundaries of the coarse omphacites; locally, core and mantle textures have been observed. Several stages from coarse-grained eclogites to the formation of fine-grained eclogite mylonites (due to dynamic recrystallisation and secondary grain size reduction) have been observed. These mylonites show a compositional layering with monomineralic layers of garnet, zoisite, and omphacite. The fine-grained garnets are interpreted to represent dynamically recrystallized grains (Kurz *et al.*, 2004).

Omphacite crystallographic preferred orientations (CPOs) from the Koralm-Saualm Complex may generally be described by S-type fabrics. Within coarse-grained samples WK17-98a, WK20-97, WK51-97 in Fig. 14 the  $\{001\}$  poles are distributed along a girdle parallel to the  $XY$  plane of the finite strain ellipsoid (foliation plane). These textures show  $\{001\}$  maxima near the  $Y$ -axis of the finite strain ellipsoid, *i.e.* perpendicular to the lineation, but parallel to the foliation plane. The  $\{010\}$  poles, oriented parallel to the  $b$   $[010]$  axes, show very well developed

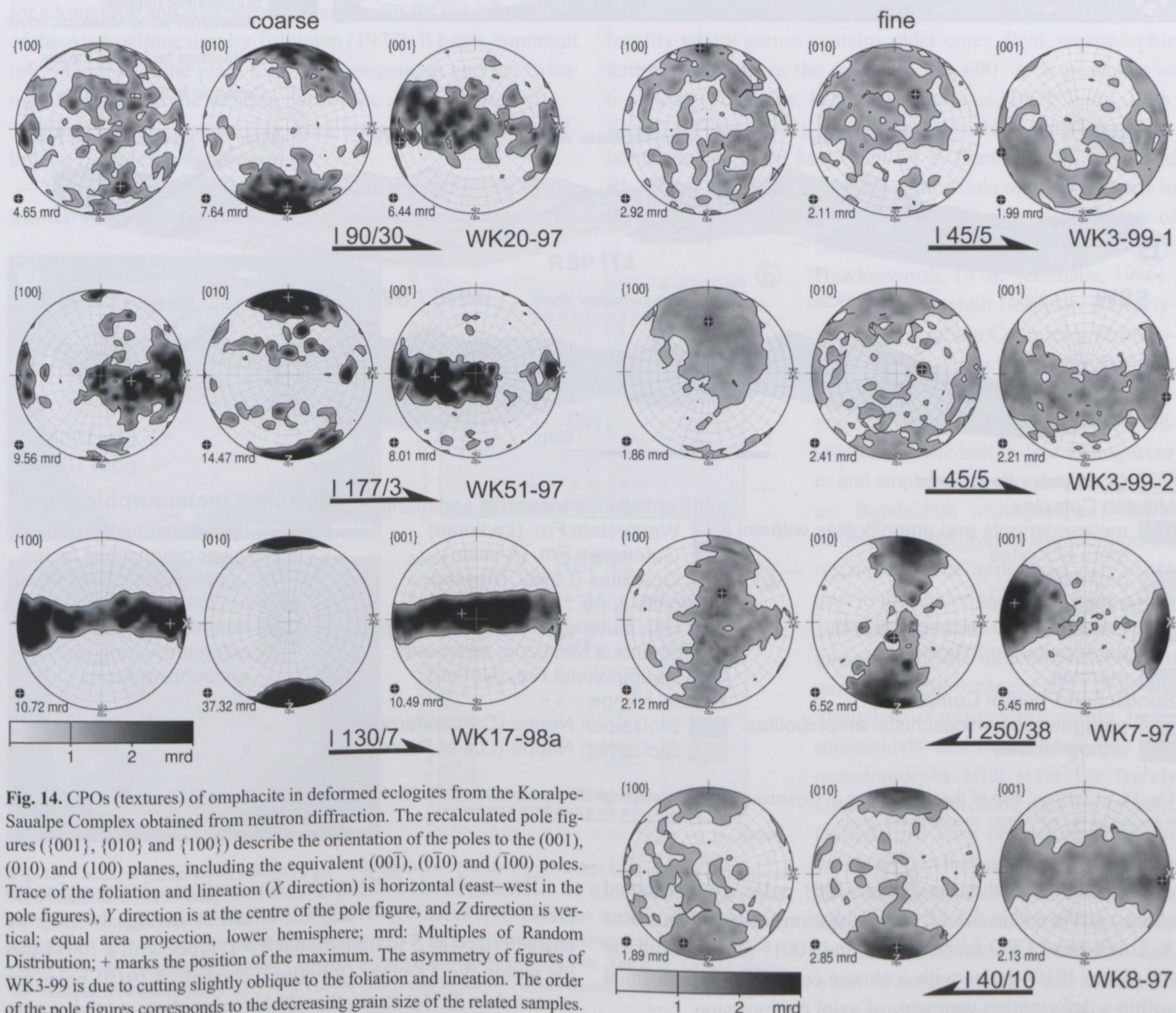


**Fig. 14.** CPOs (textures) of omphacite in deformed eclogites from the Koralpe-Saualpe Complex obtained from neutron diffraction. The recalculated pole figures ( $\{001\}$ ,  $\{010\}$  and  $\{100\}$ ) describe the orientation of the poles to the (001), (010) and (100) planes, including the equivalent ( $00\bar{1}$ ), ( $0\bar{1}0$ ) and ( $\bar{1}00$ ) poles. Trace of the foliation and lineation ( $X$  direction) is horizontal (east–west in the pole figures),  $Y$  direction is at the centre of the pole figure, and  $Z$  direction is vertical; equal area projection, lower hemisphere; mrd: Multiples of Random Distribution; + marks the position of the maximum. The asymmetry of figures of WK3-99 is due to cutting slightly oblique to the foliation and lineation. The order of the pole figures corresponds to the decreasing grain size of the related samples.



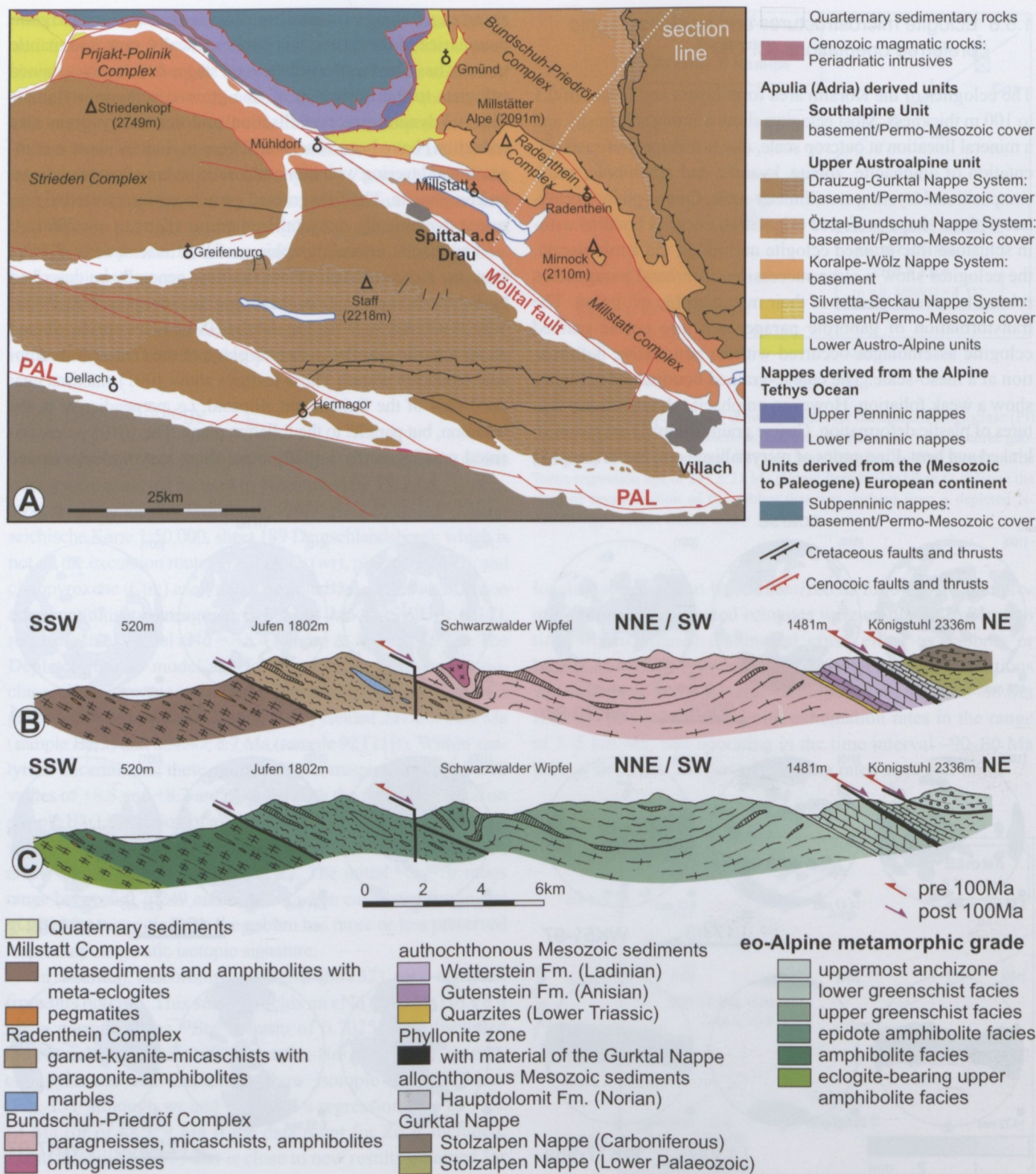


**Fig. 15.** a) Tectonic map of the western part of Carinthia. b-c) Section through the western part of the Nockberge area showing the geologic units and the distribution of the eo-Alpine metamorphic grade.

clusters centred within the Z; the {100} poles are distributed along a girdle within the XY plane (foliation), with maxima near X. This type of CPO fabric ({100} and {001} girdle within the XY plane, {010} poles with a cluster centred in Z) is formed within a deformation geometry of axial compression.

The omphacite CPOs within fine-grained eclogite mylonites (WK7-97, WK8-97, WK3-99, WKHF2) in Fig. 14 may be characterized as S to transitional S > L types with a {001} girdle within the XY plane (foliation); clusters of {010} poles are centered in Z. However, the {001} poles show a tendency to



form weak maxima centered in  $X$  (WK8-97, and especially WK7-97); accordingly, the  $\{010\}$  poles show a tendency to form a girdle within  $YZ$  (normal to the foliation plane).

We assume that the deformation geometry from the pressure peak onwards is directly related to the mechanism of exhumation. Therefore, the evolution of CPOs depends on the tectonometamorphic evolution of these units, in particular the mode of exhumation. Hence, S-type fabrics predominantly occur within eclogites exhumed by crustal extension. This is associated with a flattening strain geometry and subvertical axial compression.

## 1.6 Geology of the Nockberge area

In the section from Villach up to the Mur valley a complex eo-Alpine nappe pile composed of different crystalline units as well as Paleozoic and Mesozoic metasediments is preserved (Fig. 15). This section is a key area for the understanding of the eo-Alpine history of the Austroalpine unit. It is under discussion for a long time and was one major argument for the subdivision of the Austroalpine unit by Tollmann (1977). It bears important informations on the plate tectonic arrangement and the exhumation history in the western part of the Austroalpine unit.

From S to N, respectively from bottom to the top the following complexes are present:

The Millstatt Complex is bordered to the southwest by the Mölltal fault. The dominant lithologies are monotonous meta-

pelites and metapsammites, which are dipping to the north. Only in the lowermost part they sometimes contain two generations of staurolite, kyanite and garnet. Also calcsilicate rocks and massive marbles with intercalation of amphibolite lenses occur in this southern part (Teiml, 1996). Within the lowermost amphibolite layers, relict eclogite bodies are present (Strauss, 1990, Teiml *et al.*, 1995). Pegmatites of Permian age are common in the whole unit (Schuster *et al.*, 2001).

In the overlying, north dipping, Radenthein Complex the most abundant lithologies are white mica-rich, garnet-bearing micaschists. Garnets are up to several centimeters in size, kyanite and/or staurolite are present especially in biotite-bearing schists. Locally a very coarse grained, less deformed variety called "Radentheinit" occurs (Awerzger & Angel, 1948). It contains large, chemically continuously zoned garnet, kyanite, biotite, and chlorite and lacks muscovite. Frequent are amphibole-garnet-plagioclase schists, white mica-bearing amphibolites and marbles. A large magnesite body had been of economic interest. The microtextures and the chemical zoning indicate one prograde metamorphic imprint (Figs. 16a,b), except in one locality where garnet contains older cores. Peak metamorphic temperatures are in the range of 550–600 °C at pressures of 6–10 kbar (Schimana, 1986; Koroknai *et al.*, 1999; Teiml, 1996; Kaindl & Abart, 2002). Sm-Nd garnet isochron age of an amphibolite yielded ~100 Ma (Schuster & Frank, 1999), K-Ar and Rb-Sr ages determined on micas and whole rock samples are in the range of 78 to 125 Ma. These data prove an eo-Alpine age of

observed assemblages (Brewer, 1969; Hawkesworth, 1976; Schimana, 1986).

The Bundschuh Complex is overlying the Radenthein Complex with an eo-Alpine thrust contact (Schuster & Frank, 1999). Its lower part consists of fine-grained paragneisses with some intercalations of felsic biotite-free orthogneisses and amphibolites (Priedröf paragneisses, Bundschuh orthogneisses). micaschists and interlayered amphibolites are restricted to the uppermost part of the unit in the center of a large-scale gentle syncline structure. The Priedröf paragneisses contain a mineral assemblage of garnet + biotite + plagioclase (albite and oligoclase) + muscovite + quartz. In the micaschists additional staurolite and pseudomorphs after staurolite (rarely containing chloritoid) may be present. Garnets are very characteristic in the whole unit. In the paragneisses they have an average grain-size of less than 0.5 mm, whereas in the micaschists they are up to 2 cm in diameter. An inclusion-rich, often idiomorphic core can clearly be distinguished optically from an inclusion-

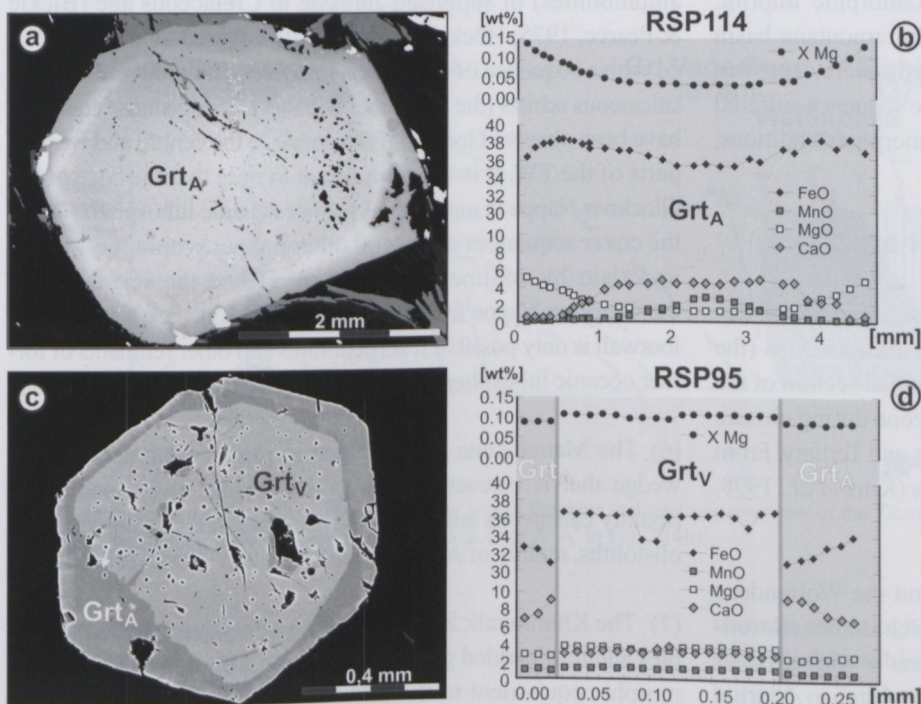


**Fig. 16.** Chemical garnet zoning pattern of the Radenthein and Bundschuh-Priedröf Complex. **a–b):** Typical back-scattered electron image and chemical profile through a garnet from the Radenthein Complex indicating a continuous growth of the porphyroblast (RSP81 and RSP 114 Schuster & Frank (2000), Predlitz, Styria, ÖK 158). **c–d):** Representative back-scattered electron image and chemical profile through a garnet from the Bundschuh-Priedröf Complex showing a distinct core and rim. The core formed during the Variscan tectonothermal event, whereas the rim is due to the eo-Alpine metamorphic imprint (RSP95 from Schuster & Frank (2000), Predlitz, Styria, ÖK 158).



free rim. The cores are compositionally homogeneous with low CaO contents of 3–5 wt%. Their age is presumed to be Variscan, because Variscan Rb–Sr ages (~350 Ma) have been measured on muscovites of orthogneisses from the uppermost part of the unit (Frimmel, 1986). In the rim the CaO content is much higher (6–8 wt%), FeO, MgO and also XMg is lower (Figs. 16c,d). Based on the regional metamorphic history, this garnet generation is eo-Alpine in age. Eo-Alpine metamorphic conditions reached up to 600 °C and 10 kbar in the lowermost parts in the south and greenschist-facies conditions below the transgressive Mesozoic unit.

The Mesozoic Stangalm Unit is unconformably transgressing onto the pre-Alpine syncline structure. The lowermost part consists of Permian to Early Triassic quartzites. Above Anisian carbonates and Carnian phyllitic schists are preserved (Tollmann, 1977). A phyllonite horizon, composed of highly sheared Paleozoic and Mesozoic rocks, marks the border to the overlying Pfannock Unit. The Pfannock orthogneiss, which is very similar to the Bundschuh orthogneisses (Frimmel, 1988) forms the stratigraphically deepest part. It is transgressed by Permo-Carboniferous clastic sediments. Continuing Mesozoic carbonates and schists reach up to the Rhaetian Kössen Formation. The sediments show a greenschist-facies metamorphic imprint.

The uppermost tectonic unit is the Gurktal Nappe. The latter comprises classic metasediments with some intercalations of carbonates and metatuffitic layers, which were deposited in Lower Palaeozoic times. During the Variscan tectonothermal event, they experienced a greenschist-facies metamorphic imprint. After that Carboniferous sediments of an intramontane basin (Krainer, 1993) and Permo-Mesozoic sediments were deposited on top. During the eo-Alpine event the whole sequence suffered anchizonal to lower greenschist-facies metamorphic conditions.

## 1.7. Geology of the Grossglockner area

The Tauern Window (TW) represents the largest exposed section of the lowest major tectonic unit in the Eastern Alps (the “Penninic” unit, Fig 1). It represents an exhumed section of the nappe stack that developed in a subduction zone during closure of the Penninic ocean in the Upper Cretaceous and Tertiary. From base to top, the Penninic nappe stack includes (Kurz *et al.*, 1998, 2001) (Fig 17).

(1) The Venediger Nappe (VN in VNC) and the Wolfendorn Nappe: these nappes comprise a pre-Variscan basement intruded by Variscan granitoids (the “Zentralgneis”) with a cover sequence of Jurassic metacarbonates (“Hochstegen Marble Formation”) and Cretaceous metapelites and metapsammities (“Kaserer Group”, sedimentation up to Eocene) (Frisch, 1980, 1984; Lammerer, 1988). The Wolfendorn Nappe is mainly a repeat of the Hochstegen Marble Formation and the Kaserer Group cover sequences, underlain by thin slices of former continental basement.

(2) The Storz and Riff Nappes comprise Variscan and Alpidic polymetamorphic basement rocks covered by metapelites and graphitic quartzites of the Murtörl Group, which was assumed to be of either late Paleozoic or, more likely, Cretaceous age (Kurz *et al.*, 1998, and references therein). The nature of the tectonic contact between the Venediger Nappe and the Riff Nappe has been highly debated and is interpreted by Frisch (1977, 1980) to be related to the Variscan orogeny.

(3) The Eclogite Zone (EZ) is restricted to the central southern TW and is characterized by a Mesozoic volcano-sedimentary sequence of a distal continental slope, which has experienced HP metamorphism. The Eclogite Zone is tectonically positioned above the Venediger Nappe Complex (VNC) and is overlain by the Rote Wand-Modereck Nappe. Where the Eclogite Zone is absent, however, the Rote Wand-Modereck Nappe is overthrust directly onto the Venediger Nappe.

(4) The Rote Wand-Modereck Nappe (RMN) is formed by basement rocks of the Rote Wand-Modereck Lamella that are covered by Permian to Triassic quartzites, Triassic metacarbonates, Jurassic breccias, calcareous micaschists and metatuffs as well as Cretaceous metapelites and metapsammities.

(5) The Glockner Nappe (GN) comprises an oceanic basement made up of an incomplete ophiolitic sequence of serpentinites, ultramafic rocks, MORB-type metabasites (greenschists and amphibolites) of supposed Jurassic to Cretaceous age (Bickle & Pearce, 1975; Höck & Miller, 1980), covered by or intercalated with a sequence of quartzites, micaceous calcitic marbles and calcareous schists (the “Bündner Schists”). Terrigenous sequences have been observed locally, for example in the central and western parts of the TW. It is very important to note that the base of the Glockner Nappe is made up of former oceanic lithosphere, while the cover sequences of several other nappes within the TW are underlain by continental basement. Hence the separation of the Glockner Nappe from the Rote Wand-Modereck Nappe in the footwall is only possible if serpentinites and other remnants of former oceanic lithosphere are intercalated between metasediments.

(6) The Matrei Zone is interpreted to represent an accretionary wedge that is characterized by metamorphic flysch sediments (mainly calcareous and carbonate-free micaschists), breccias and olistoliths, mainly of Austroalpine derivation (Frisch *et al.*, 1987).

(7) The Klammkalk Zone comprises calc-schists, massive marbles and thin-bedded green phyllites; it forms a low-grade metamorphic equivalent to the “Bündnerschiefer” of the Glockner Nappe.

(8) The Lower Austroalpine nappe stack, in the hanging wall of the Penninic nappe stack, comprises pre-Alpine continental basement units and Permian to Mesozoic cover sequences, predominantly derived from a rifted, passive continental margin.



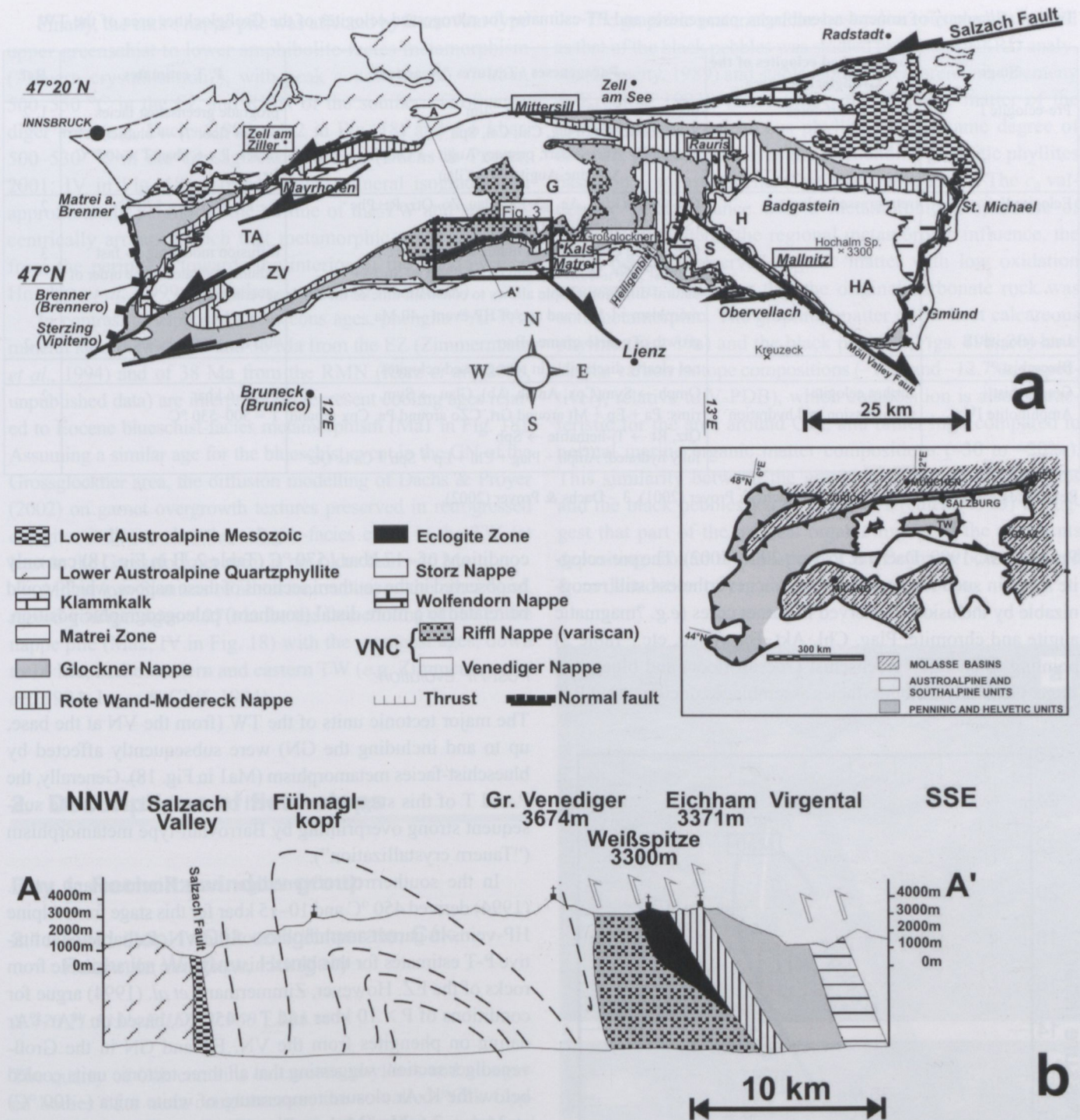


Fig. 17. a) Tectonic position of the Tauern Window within the Alps and geologic overview of the Tauern Window (according to Kurz *et al.*, 1998, 2001); b) Simplified geologic profile across the Tauern Window (line A-A' in Fig. T14b).

### 1.7.1 Tectonometamorphic evolution

#### HP evolution:

The rocks exposed within the EZ in the southern Großvenediger area were affected by a multiphase tectonometamorphic evolution. Inclusions in garnet from eclogites (Ep, Chl, Pa, Bt, Phe, Qtz, Ab) and metasediments (rhombic form-relics of Pa + Zo + Qtz interpreted as pseudomorphs after ?lawsonite) doc-

ument a pre-eclogite stage of prograde metamorphism of greenschist-to-blueschist facies. The eclogite-facies rocks were then buried to a depth of at least 65 km, as has been concluded from the HP parageneses of eclogites, associated metapelites and metacarbonates, which all yielded similar PT paths with peak conditions of ~20 kbar,  $\pm 600$  °C (Ma0 in Fig. 18).

In the tectonically higher RMN and GN eclogite-facies metamorphism is only locally recorded and former eclogites are much more affected by retrogression (Kurz *et al.*, 1996;



**Table 2.** Summary of mineral assemblages, parageneses and PT-estimates for retrogressed eclogites of the Großglockner area of the TW.

| Stage                        | Retrogressed eclogites of the Großglockner area | Parageneses / Textures / Reactions  | P, T estimates  | Ref.       |
|------------------------------|---|---|---|------------|
| Pre-eclogite I               | Relics in Grt cores                             | magmatic: Augite, Chromite, ?Ilm<br>greenschist: Act, Plag, Chl, Cal, Sph<br>blueschist: Act → Barr, primary Augit → Omph,<br>Aegirine-Augite, Win/Glau   | prograde greenschist facies<br>(ocean floor ?) → blueschist<br>facies: P ≈ 6 kbar, T ≈ 400 °C                               | 1, 2       |
| Eclogite II                  | retrogressed eclogites                          | Grt–Omph(Jd <sub>40-50</sub> Ae <sub>5-20</sub> )–Pa–Glau–Zo–Qtz–Rt±Phe<br>(Si = 3.3–3.43 apfu) ± Dol<br><br>Grt: strong compositional hiatus between core<br>(Alm <sub>36</sub> Py <sub>4</sub> Gr <sub>31</sub> Sp <sub>29</sub> ), and rim (Alm <sub>60</sub> Py <sub>18</sub> Gr <sub>21</sub> Sp <sub>1</sub> ) →<br>natural diffusion couple allows to constrain time of meta-<br>morphism ~1 Myr and age of HP-event ~40 Ma<br><br>growth of coarse-grained Barr | P ~17 kbar, T ≈ 570 °C<br><br>diffusion modelling → fast<br>exhumation rates in the order of<br>several cm yr <sup>-1</sup> | 2<br><br>3 |
| Late-eclogite III            |   |   | still in eclogite facies?   | 1, 2       |
| Blueschist                   |   | not clearly discernible in retrogressed eclogites   |   |            |
| Greenschist / Amphibolite IV | further eclogite<br>retrogression and hydration | Omph → Sym(Cpx, Amph, Ab), Glau → Sym,<br>rims: Pa + Ep + Mt around Grt, CZo around Pa, Cpx around<br>Qtz, Rt → Ti-hematite → Sph<br>fully hydrated: Amph + Plag + Chl + Ep + Sph ± Ca ± Qtz  | P = 5–6 kbar<br>T = 500–530 °C  | 2          |

References: 1 – Proyer *et al.* (1999), 2 – Dachs & Proyer (2001), 3 – Dachs & Proyer (2002).

Proyer *et al.*, 1999; Dachs & Proyer, 2001, 2002). The pre-eclogite stage in such retrogressed rocks is nevertheless still recognizable by inclusions preserved in garnet cores (*e.g.* ?magmatic augite and chromite, Plag, Chl, Akt, Barr/Glau, etc., Table 2) pointing to an early greenschist (?ocean-floor) and blueschist stage. Generally, eclogite-facies assemblages documenting P-T

conditions of ~17 kbar / 570 °C (Table 2, II in Fig. 18) can only be observed in the southern sections of these nappes, which would be related to a more distal (southern) paleogeographic position.

#### Post-HP evolution:

The major tectonic units of the TW (from the VN at the base, up to and including the GN) were subsequently affected by blueschist-facies metamorphism (Ma1 in Fig. 18). Generally, the P and T of this stage are not well constrained due to the subsequent strong overprinting by Barrovian-type metamorphism (“Tauern crystallization”).

In the southern Großvenediger area Zimmermann *et al.* (1994) derived 450 °C and 10–15 kbar for this stage from Alpine HP-veins in garnet amphibolites of the VN. Reliable quantitative P-T estimates for this blueschist stage are not available from rocks of the EZ. However, Zimmermann *et al.* (1994) argue for conditions of P > 10 kbar and T < 450 °C, based on <sup>40</sup>Ar–<sup>39</sup>Ar dating on phengites from the VN, EZ and GN in the Großvenediger section, suggesting that all three tectonic units cooled below the K-Ar closure temperature of white mica (~400 °C) at 34.4 ± 2.6 Ma (Ma1 in Fig. 18). From the occurrence of crossite and low-jadeitic pyroxene in metabasites from higher structural levels of the GN, Holland & Ray (1985) determined P > 8 kbar and T = 400–450 °C for this stage.

Within the VN and GN of the western and eastern TW, peak pressures of up to 10–12 kbar have been evaluated for the blueschist event (Selverstone *et al.*, 1984, 1992; Cliff *et al.*, 1985; Droop, 1985; Frank *et al.*, 1987; Selverstone, 1993).

Within the basal GN of the Grossglockner area this phase of metamorphic overprinting is not clearly discernible in retrogressed eclogites (Proyer *et al.*, 1999), but is evidenced by pseudomorphs after lawsonite and high-Si phengites in metabasites and calc-schists (Höck, 1974, 1980; Frank *et al.*, 1987).

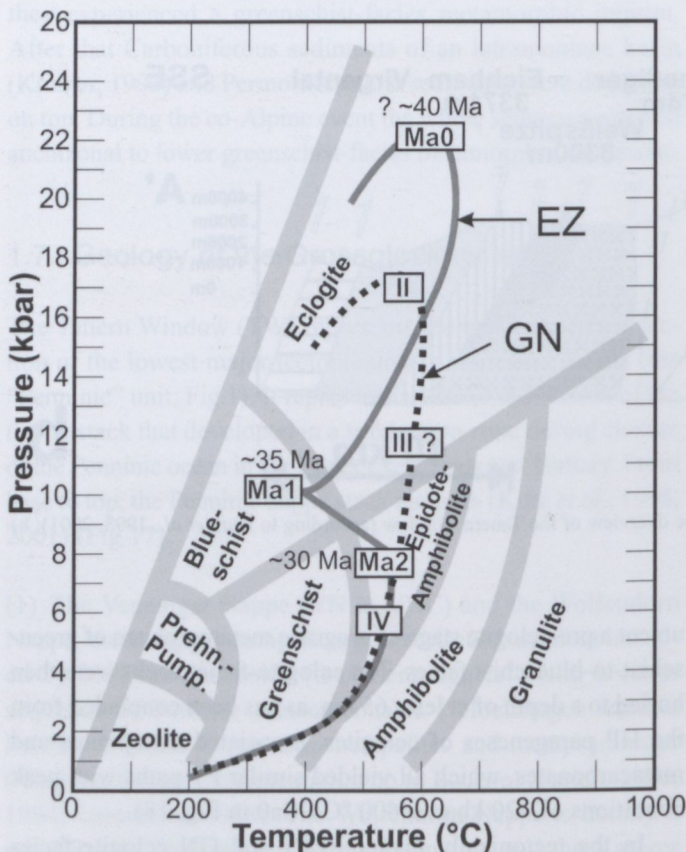


**Fig. 18.** P-T paths recorded from HP-rocks of the Eclogite Zone (EZ) and Glockner Nappe (GN).



Finally, the entire nappe pile was affected by Barrovian-type upper greenschist to lower amphibolite-facies metamorphism ("Tauern crystallisation"), with peak conditions of  $\sim 7$  kbar, 500–550 °C in the EZ and RMN of the southern Großvenediger area (e.g. Dachs, 1990; Ma2 in Fig. 18) and 5–6 kbar, 500–530 °C in the Grossglockner region (Dachs & Proyer, 2001; IV in Fig. 18). Corresponding mineral isogrades run approximately parallel to the outline of the TW and are concentrically arranged, such that metamorphic grade increases from the periphery towards the interior of the window (see Hoinkes *et al.*, 1999 for further details and references).

In contrast to supposed Cretaceous ages, phengite  $^{40}\text{Ar}$ - $^{39}\text{Ar}$  mineral ages between 32 and 36 Ma from the EZ (Zimmermann *et al.*, 1994) and of 38 Ma from the RMN (Kurz *et al.*, 2008, unpublished data) are interpreted to represent cooling ages related to Eocene blueschist-facies metamorphism (Ma1 in Fig. 18). Assuming a similar age for the blueschist event in the GN of the Grossglockner area, the diffusion modelling of Dachs & Proyer (2002) on garnet overgrowth textures preserved in retrogressed eclogites indicates that the eclogite-facies event in the TW (at least in the Grossglockner area) is not older than  $\sim 40$  Ma.

Alpine low-Si micas of all tectonic units, on the other hand, record younger ages  $< 27$  Ma for the late cooling of the entire nappe pile (Ma2, IV in Fig. 18) with the youngest ages, down to 14 Ma, in the western and eastern TW (e.g. Zimmermann *et al.*, 1994; Inger & Cliff, 1994).

## 2. Descriptions of field stops

### Day 1: Rechnitz window group

#### 2.1. Field stop 1: Cák conglomerate, Cák, Rechnitz Window, Hungary

*N 47° 21.535'; E 16° 30.960'; 321 m*

The quarry of Cák contains calcareous phyllites and elongated bodies of a meta-conglomerate, the so-called "Cák Conglomerate" (Figs. 19a,b). The calcareous phyllite is composed mainly of calcite, with smaller amounts of quartz and white mica. The accessory minerals are opaque minerals (including graphitic matter), tourmaline, zircon and rutile. The rock is strongly sheared beside conglomerate bodies resulting in elevated graphite content. The conglomerate forms folded bodies and contains predominantly black and grey dolomitic pebbles (Figs. 19b, 20) several cm in size (Juhász, 1965). Beside the dolomite pebbles, gneiss fragments have also been found in subordinate amounts (Juhász, 1965). Some of the black pebbles preserved primary sedimentary features, such as Triassic fossils (Mostler & Pahr, 1981) and algal mat-like structures (Demény & Kreulen, 1993).

The graphitic material of the host calcareous phyllite as well as that of the black pebbles was studied by means of XRD analyses (Demény, 1989) and stable isotope measurements (Demény & Kreulen, 1993). Interestingly, the graphitic matter of the strongly sheared calcareous phyllite has the same degree of ordering (graphitization) as the surrounding graphitic phyllites based on  $c_0$  measurements (Demény, 1989, 1990). The  $c_0$  values are in accordance with a metamorphic temperature of  $\sim 400$  °C. In spite of the regional metamorphic influence, the black pebbles preserved organic matter with low oxidation temperature, indicating that the original carbonate rock was non-metamorphic. The graphitic matter of the host calcareous phyllite (Fig. 19a) and the black pebbles (Figs. 19b, 20) have similar carbon isotope compositions ( $-13.5$  and  $-12.7\text{‰}$ , respectively, relative to V-PDB), which composition is also characteristic for the area around Cák, and rather high compared to normal marine organic matter compositions ( $-30$  to  $-20\text{‰}$ ). This similarity between the graphitic matter of the phyllites and the black pebbles led Demény & Kreulen (1993) to suggest that part of the original organic matter of the sediments depositing around the coastline of the Penninic ocean derived from denudation of organic-rich carbonate rocks.



**Fig. 19.** a) Strongly folded calcareous phyllite with beds of Cák conglomerate, quarry at Cák, Hungary. b) Detail from Fig. 19a with clear breccia material.





**Fig. 20.** Polished hand specimen of the Cák Conglomerat with a white carbonate matrix and dark components.

## 2.2 Field stop 2: View on Lockenhaus Castle, Burgenland

*N 47° 24.445'; E 16° 25.581'; 324 m*

The castle Lockenhaus (Fig. 21) was founded in the 13<sup>th</sup> century on a steep cliff above the meandering river Güns. Originally the castle was named Leuca. The oldest documents dates back to 1242. According to these documents the castle resisted the Mongolian attack in 1242. In an other document from 1671 the castle was referred as a meeting place of templars. During 1266-1337 the castle was owned by the counts of Güssing. After a period as royal castle in 1390 King Sigismund gave Lockenhaus to the Kanizsay family, followed in 1535 by Tamás Nádasdy and his clan. After 1676 the princes of Esterházy owned the castle. Famous is the gothic knight hall.

## 2.3 Field stop 3: Gabbro at Glashütten, community of Lockenhaus, Burgenland

*N 47° 22.735'; E 16° 22.934'; 427 m*

This gabbro outcrop is located in the NE part of the Rechnitz window in the village Glashütten in the community of Lockenhaus. The gabbro forms a rather large body with an extension of about 1200 m in SE direction with underlying talc schists and is mainly surrounded by phyllites. This gabbro complex is a typical isotropic and coarse-grained Mg-rich gabbro with a former primary mineral assemblage of Cpx + Plag ± Opx. During the high-pressure event the following paragenesis actinolite + Mg-pumpellyite + Mg rich chlorite + albite was formed in this gabbro type (Fig. 22).

Cpx is the only preserved phase of the magmatic assemblage. This Cpx is a diopside to an endiopside with a composition in the range of  $X_{Mg}$  of ~0.82 and an Al content varying between 4–2 wt%  $Al_2O_3$ . Beside the relict magmatic Cpx only



**Fig. 21.** View on the castle Lockenhaus from the east.

metamorphic phases can be found. Rather common is the assemblage actinolite–Mg-pumpellyite/clinozoisite–clinochlore–albite. Actinolite has a  $X_{Mg}$  of 0.85–0.90 and a Si of 7.75–7.95. The Mg-rich pumpellyite is low in Fe with a  $Fe_{tot}/(Fe_{tot}+Al)$  ratio of 0.03–0.06 and high in Al (Fig. 23). Within the fine-grained mass of pumpellyite, new-grown clinozoisite with abnormal blueish interference colour with a  $X_{Fe}$  in the range of 0.10–0.15. The chlorite is a Mg- and Al-rich clinochlore with a Si ranging from 5.65–6.10. The feldspar is pure albite (Koller, 1985).

This outcrop is the best example of a prograde breakdown of Mg-rich pumpellyite to “clinozoisite + actinolite + chlorite +  $H_2O$ ” (Fig. 23). This reaction is well documented by the experimental results of Schiffmann & Liou (1980). This type of reaction is typical for all Mg-rich gabbros and with normal Ca composition and restricted to gabbros not in close contact with any ultramafic rock. In all more Fe-rich gabbros the prograde breakdown of the Fe-rich pumpellyite to epidote was formed earlier and in this case epidote is related to the high-pressure mineral assemblage.

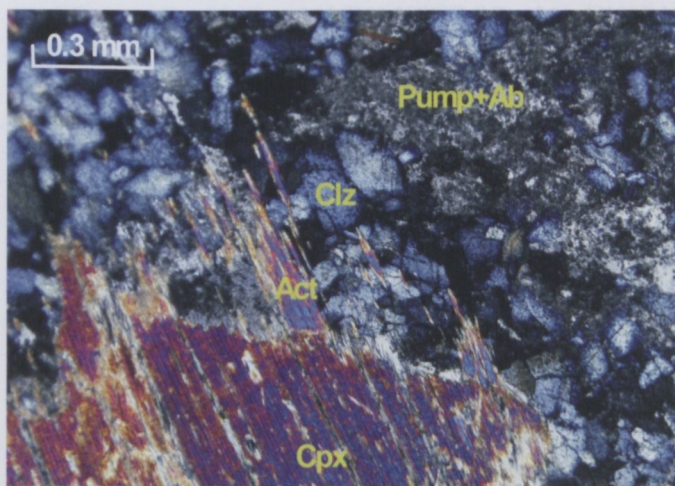


**Fig. 22.** Thin section picture with newly grown actinolite around old magmatic cpx in a matrix of fine-grained pumpellyite+albite ± chlorite with newly grown clinozoisite. Gabbro from Glashütten/Lockenhaus, crossed nicols.



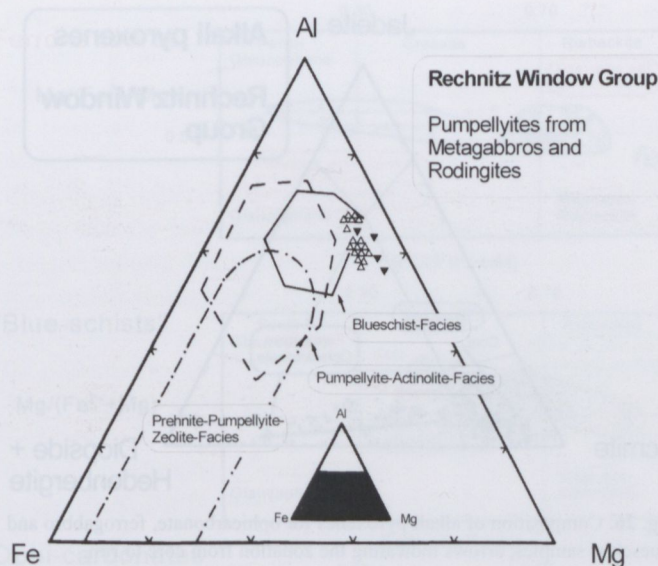


Fig. 23. Presentation of pumpellyite data in the triangle Fe–Al–Mg. Symbols: open triangle – Mg-rich gabbro, closed triangle – rodingitized gabbros. Fields for various pumpellyite compositions according to Barriga & Fyfe (1983)

## 2.4 Field stop 4: Quarry Bienenhütte, Bernstein, Bernstein window, Burgenland (FK)

N 47° 24.741'; E 16° 17.325'; 646 m

The quarry is located in the window of Bernstein close to the tectonic border of the overlying Lower Austroalpine with the Wechsel unit and consists of strongly tectonized serpentinites and rodingitized gabbroic (Fig. 24) dykes partly surrounded by pure chlorite schist. The latter are locally quarries for art crafts and named “Edelserpentin”.

The serpentinite contains mainly chrysotile and lizardite, no primary mineral phase has survived the serpentinisation. Bastites, as form relics after former orthopyroxene, are common only in non- or less deformed samples. The formation of tremolite, talc or fibrous asbestos minerals is related to the last metamorphic event. All serpentinites derive, according to their geochemistry from a harzburgitic source with low  $\text{Al}_2\text{O}_3$  contents (1.2–1.5 wt%), the REE data show a depletion of LREE (Melcher *et al.*, 2002). The Re-Os isotopic values are in good equilibrium with the other Mesozoic peridotites from the Penninic windows of the Eastern Alps (Meisel *et al.*, 1997).

The metamorphic recrystallization of the Mg-rich Cpx-gabbros can be characterized by the formation of chlorite, actinolite, albite, and Mg-pumpellyite during the high-pressure event (Fig. 23). During the thermal peak of the metamorphic event pumpellyite is replaced in gabbroic rocks close to the contact of the serpentinites or within ultramafic bodies by hydrogrossular. This is caused by Ca-metasomatism during rodingitization and is combined with depletion in Na. The following reaction has been reported by Koller (1985) based on the experimental results by Schiffmann & Liou (1980):

$$\text{Mg-Al-pumpellyite} + \text{Ca}^{2+} \rightarrow \text{grossular} + \text{chlorite} + \text{H}_2\text{O}$$

The rodingites exhibited in the quarry are boudinated dykes with a thickness up to 2 meter. They show a relative white colour and consist mainly of hydrogrossular with up to 1.5 wt%  $\text{H}_2\text{O}$  content. According to microprobe analyses the grossular content range between 75–92 mol%, the other components are andradite and spessartine (up to 3 mol%). Almandine and pyrope contents are generally low. The clinopyroxene, only locally preserved, is commonly Cr-rich (0.6–0.4 wt%  $\text{Cr}_2\text{O}_3$ ) and Ti poor. Cpx can be replaced by chlorite and grossular. Microprobe data define a diopside with Cr and Na contents typical for ophiolitic gabbros. The chlorite is a Fe-poor clinochlore.

The bulk geochemistry shows high Ca concentrations between 19–25 wt% CaO and a complete loss of Na. All immobile major and trace elements such as Al, Ti, Zr, Y, Cr, and the REE are at the same level as in an equivalent metagabbro without metasomatic effects. In contrast Ca and Eu are strongly enriched in the rodingites.

These dykes are surrounded by a metasomatic blackwall consisting of pure clinochlore. This reaction zone is equivalent to the monomineralic chlorite lenses common for the serpentinite bodies in this area. They are called “Edelserpentin” and used in local manufactures for art crafts. Koller (1985) has demonstrated by geochemical investigations, that chlorite lenses and blackwall zones around rodingite have a similar composition and origin. They derive from a former gabbro. Some type of these chlorite schists show idiomorphic magnetite crystals and resemble some more Fe-rich gabbro types. All of the pure chlorite schists are enriched in Mg and depleted by Ca and Eu, but the immobile elements show the gabbroic origin of this metasomatic rock.



Fig. 24. Folded rodingitized gabbro dyke in the serpentinitized harzburgite, Quarry Bienenhütte, Bernstein window. Size of the picture ~8m, situation before 1995.



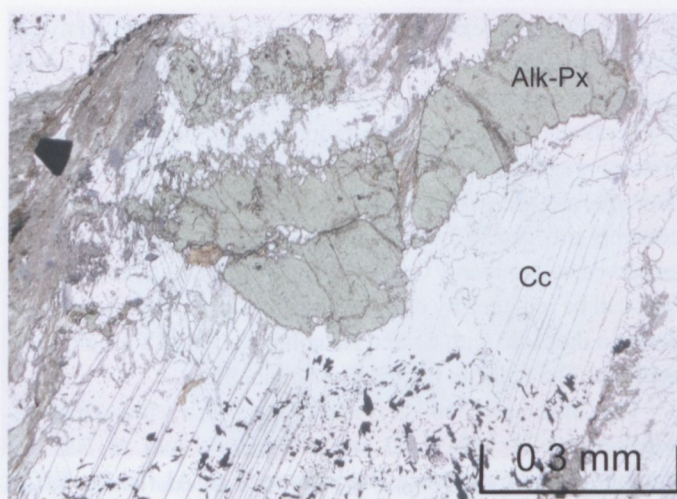


**Fig. 25.** Thin section picture of an ophicarbonate sample from Glashütten/Schlaining with green alkalipyroxene (Alk-Px), some small blue amphiboles, an idiomorphic magnetite in calcite (Cc) matrix, locally coated with fine hematite. || Nicols.

## 2.5 Field stop 5: Ophicalcite at Glashütten close to Schlaining, Rechnitz window, Burgenland

N 47° 21.233'; E 16° 19.144'; 560 m

The serpentinite complex south of the Glasbach valley is surrounded by ophicarbonate rocks containing alkali pyroxenes, blue amphiboles, chromian epidote, hematite and magnetite.

These rocks are characterized by coarse-grained calcite (ranging from 70–85 wt% carbonate) which is red coloured by a fine hematite pigmentation (Koller & Pahr, 1980). The following three main types can be distinguished:

- 1) *Ophicarbonate type 1*: This type is less common and shows dominant silicate phases such as epidote/clinozoisite, phengite, titanite and rare albite. The geochemistry is characterized by higher Al, Ti and lower Fe, Cr, and Ni contents compared with the other groups. According to Koller (1985, 1990) this type is interpreted as mechanical mixture of a gabbroic and sedimentary source rocks.
- 2) *Ophicarbonate type 2*: Besides calcite, the main mineral phases are alkali pyroxene, alkali amphibole, Cr-rich epidote, phengite, fine-grained and dispersely distributed hematite and idiomorphic magnetite. Chemically, this type is characterized with high Fe, Cr and Ni contents combined with low Al. Ti is almost missing. In the silicate portion the Cr values are as high as 1.2 wt% Cr<sub>2</sub>O<sub>3</sub>. The origin of this type is related to mechanical mixture of a chromite rich ultramafic source and the calcareous metasediment.
- 3) *Ophicarbonate type 3*: This lesser deformed type can be characterized by brecciated serpentinite fragments in a carbonate matrix. Typical mineral phases are serpentinite, tremolite and chlorite. According to Koller (1985), this type seems to be a tectonic breccia formed during the Alpine metamorphic event.

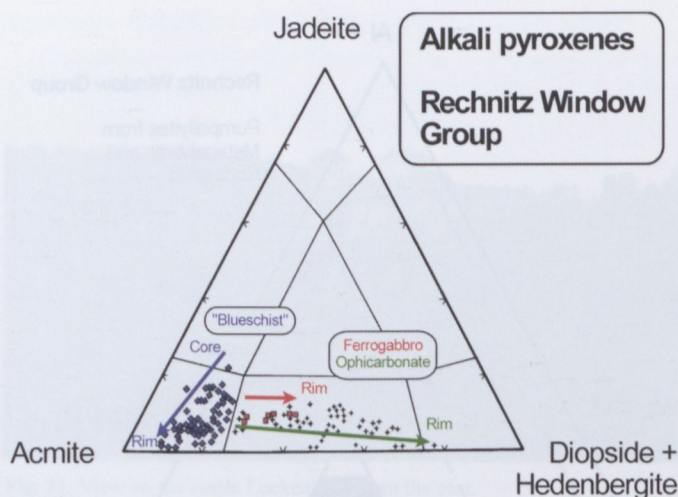


**Fig. 26.** Composition of alkali pyroxenes for ophicarbonate, ferrogabbro and blueschist samples, arrows indicating the zonation from core to rim.

Chromite has been found as the oldest mineral preserved in all ophicarbonate type 2 and 3 samples. Sometimes this chromite is surrounded by a yellow garnet with high andradite (88–60 mol%) and uvarovite (7–25 mol%) component combined with low grossular and spessartine. During the high-pressure event, the garnet was replaced by other minerals. These facts combined with the high grade of oxidation, documented by the hematite pigmentation, are the evidences for a transform fault related origin of this ophicarbonate rocks (Koller, 1985; Koller & Höck, 1990; Höck & Koller, 1989). Recent examples have been reported from oceanic fracture zones (White, 1991).

The high-pressure paragenesis consists of an alkali pyroxene (Figs. 25, 26), Cr-phengite und Cr-epidote and hematite, sometimes chlorite. The alkali pyroxene is replaced during the thermal peak by a blue amphibole (Fig. 27) with riebeckitic or magnesioriebeckitic composition (Fig. 28) coexisting with idiomorphic magnetite octaeders up to a size of 5 mm. The alkali pyroxene in the ophicarbonates is zoned with a core containing 12 mol% jadeite and 60 mol% aegirine (Fig. 26). The rim

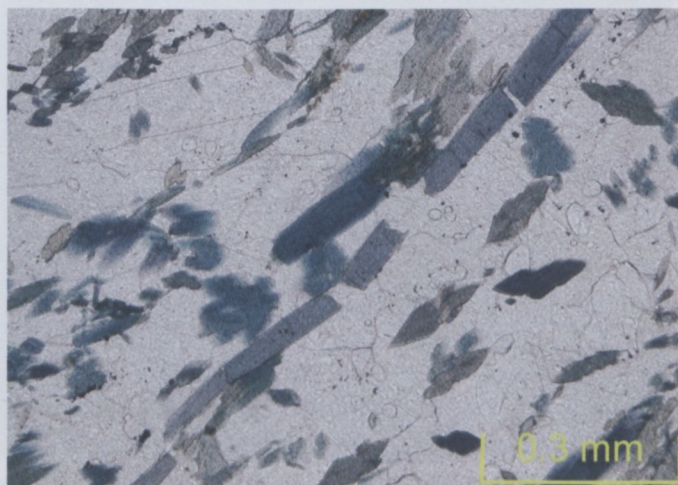


**Fig. 27.** Thin section picture with needles of blue amphiboles in an ophicarbonate sample from Glashütten/Schlaining in a calcite matrix. || Nicols.



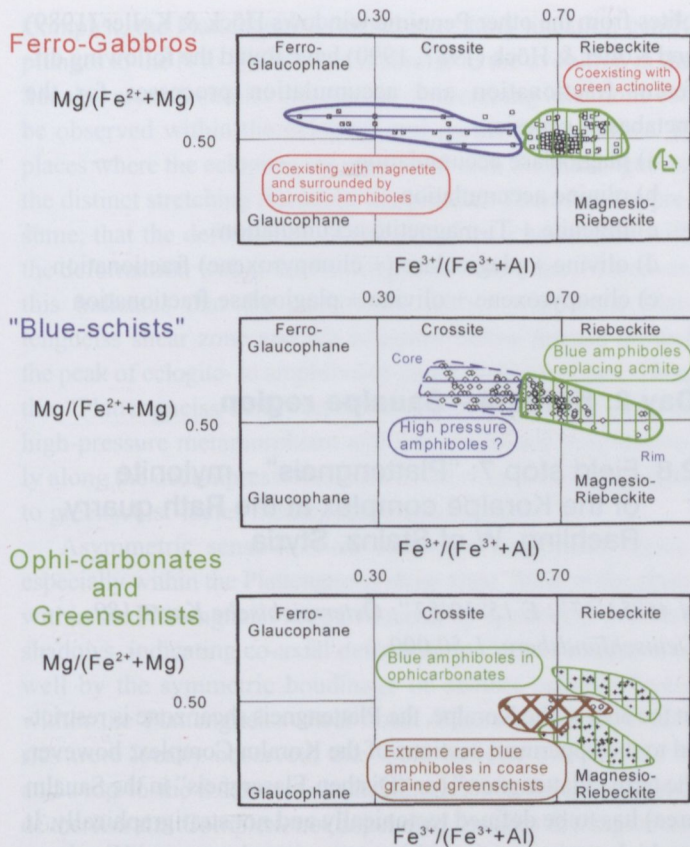


Fig. 28. Composition of blue amphiboles in ferro-gabbro, blue schists, ophi-carbonates and greenschists from the Rechnitz unit samples. Data according to Koller (1985).

shows a decrease of jadeite and aegirine components. The Si values of the phengite range around 3.4 with up to 7 wt%  $\text{Cr}_2\text{O}_3$  contents (Fig. 29). Stilpnomelane can be a minor phase in ophi-carbonate type 2.

In the ophi-carbonate samples the alkali pyroxenes have Cr contents up to 4 wt%  $\text{Cr}_2\text{O}_3$  and Ni contents up to 0.5 wt% NiO and are generally low in Ti. In contrast the Cr content in amphiboles is low. Both phengite and epidote contain high Cr contents up to 7 wt%  $\text{Cr}_2\text{O}_3$ .

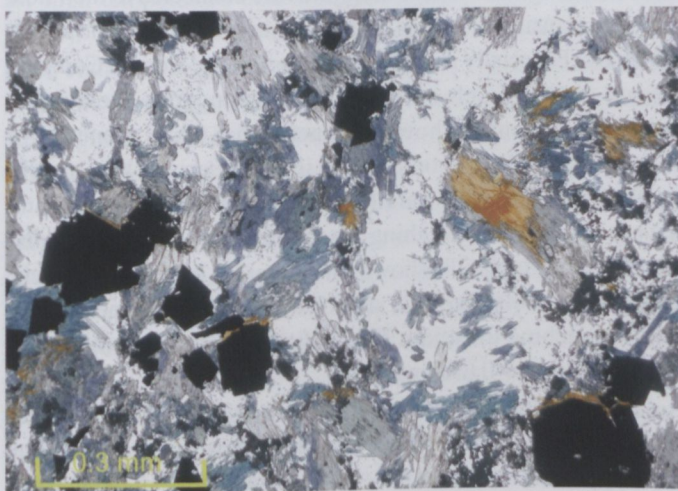


Fig. 30. Typical blueschist assemblage in basic rocks with blue amphiboles, brown stilpnomelane, idiomorphic magnetite, Glashütten/Schlaining.

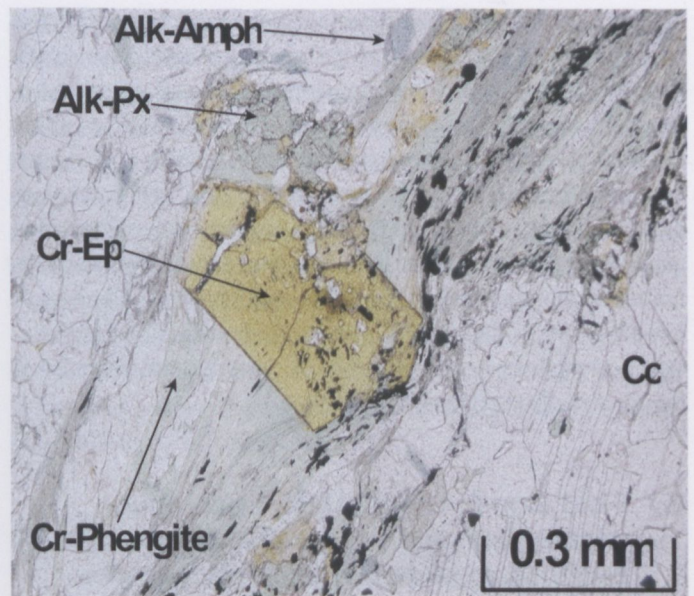


Fig. 29. Thin section picture with Cr-epidote (Cr-Epi), alkali pyroxene (Alk-Px), blue amphiboles (Alk-Amph), Cr-phengite and calcite (Cc) from an ophi-carbonate sample from Glashütten/Schlaining.

Similar to the ophi-carbonate rock with their high-pressure assemblage also ferro-gabbros and blueschists contain a wide variety of mineral assemblages with alkali pyroxenes (Fig. 26), blue amphiboles (Fig. 28) and stilpnomelane (Fig. 30).

## 2.6 Field stop 5a: Dark calcareous micaschist, close to Unterkohlstätten, Rechnitz Window, Burgenland

N 47° 22.172'; E 16° 18.686'; 444 m

This abandoned quarry is formed by massive calcareous phyllites, which shows nice folding features. The rock is practically made of calcite with subordinate amounts of quartz, white mica, chlorite, graphite and other opaque minerals (Fig. 31).

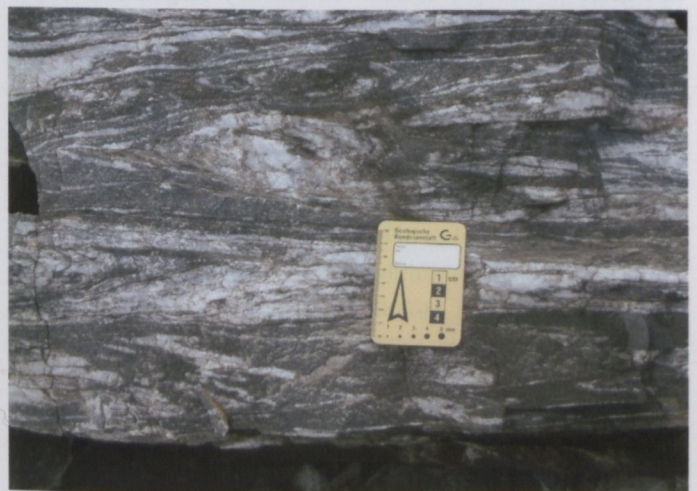


Fig. 31. Typical dark coloured, graphite-bearing calcareous micaschists from the abandoned quarry close to Unterkohlstätten (Rechnitz window).



Schönlaub (1973) has detected sponge spiculae from this rock, proving a middle to upper Cretaceous age of the series. Graphite in this area is well developed by means of crystallographic ordering. The carbon isotope composition of graphitic material is  $-14.1\text{‰}$ , the calcite matrix has carbon and oxygen isotope compositions of 0.3 and  $-8.0\text{‰}$  resp. (all values are expressed relative to V-PDB). The graphite composition is in accordance with the composition obtained for the carbonaceous matter of the black pebbles of Cák conglomerate (Demény & Kreulen, 1993), the calcite-graphite carbon isotope fractionation corresponds to the 400–450 °C metamorphism inferred by other methods (Demény, 1990).

## 2.7 Field stop 6: Greenschist, calcareous micaschists, quarry Freingruber, Rechnitz window, Burgenland

*N 47° 18.699'; E 16° 24.419'; 429 m*

In this quarry calcareous micaschists overlain by greenschists are exhibited, both dipping slightly towards the North below the serpentinite of Rumpersdorf and the "Kleine Plischa".

The calcareous micaschists are dark grey coloured by graphitic pigmentation and are veined by white recrystallized calcite. The total calcite content ranges from 70% up to more than 90%. Besides calcite, variable amounts of quartz, phengite, chlorite, albite, and epidote are present. 10–20% of the white mica may be paragonite. As accessory phases, tourmaline, pyrite and dispersely distributed graphite are present. High Sr and S contents are typical (Koller, 1985). Demény & Kreulen (1989) determined for calcite  $\delta^{18}\text{O}$  values ranging from  $-6.6$  to  $-9.7\text{‰}$  and for the graphites of the carbonate-rich samples a  $\delta^{13}\text{C}_{\text{Gr}} > -13.0\text{‰}$ . This is in accordance with the metamorphic conditions derived from the metabasic rocks and consistent with the Bündner schists of the Penninic Tauern window (Demény, 1987).

The greenschists are massive, sometimes laminated on a fine scale or strongly folded. All primary magmatic textures are completely extinct. Locally coarse-grained mobilisations of albite or calcite exist. Besides rare high-pressure relics, only the parageneses of the Tertiary event can be found in the coarse-grained mobilisations. The typical mineral assemblage is actinolite-chlorite-epidote-albite-titanite corresponding to greenschist facies.

Very rare older relics of brown or dark green coloured hornblende as uraltisation product of a former clinopyroxene can be mentioned. In few samples, complex zoned epidote occurs as a remnant of an older event. In the coarse-grained mobilisations, locally blueish amphiboles of riebeckitic or winchitic compositions are present (Fig. 28).

All geochemical investigations show a clear N-type MORB composition (Koller, 1985). The distribution of immobile elements including the REE's support this interpretation. Based on the data of Koller (1985) and in comparison with the ophi-

olites from the other Penninic windows Höck & Koller (1989) and Koller & Höck (1987, 1990) have found the following different fractionation and accumulation processes for the metabasalt genesis:

- a) plagioclase accumulation
- b) olivine accumulation
- c) ilmenite + Ti-magnetite accumulation
- d) olivine + plagioclase (+ clinopyroxene) fractionation
- e) clinopyroxene + olivine + plagioclase fractionation

## Day 2: Koralpe – Saualpe region

### 2.8 Field stop 7: "Plattengneis" – mylonite of the Koralpe complex at the Rath quarry, Rachling, W of Stainz, Styria

*N 46°54'37"; E 15°10'57"; Österreichische Karte 189, Deutschlandsberg, 1:50,000*

In the area of the Koralpe, the Plattengneis shear zone is restricted to the uppermost sections of the Koralm Complex; however, the term "Plattengneis" (or "Disthen-Flasergneis" in the Saualm area) has to be defined tectonically and not stratigraphically. It is a high-strain domain within paragneisses known as "Hirschegg Gneis" in the area of the Koralpe (part of the "Paragneisses and Paraschists with pegmatitic veins"). The thickness of the Plattengneis reaches up to five hundred meters; distinct shear zones with a thickness of a few cm to m locally occur. An essential part of the Plattengneis is derived from meta-pelitic protoliths (paragneisses). The dominant mineral assemblage is quartz – K-feldspar – plagioclase – muscovite – biotite – kyanite. The feldspar is completely recrystallized during deformation and the quartz displays monomineralic layers with grain shapes similar to those of granulites. From top to bottom, the Plattengneis shear zone develops continuously from an undeformed protolith to a protomylonite, and finally to the mylonites of the Plattengneis. These mylonites are connected to their host rocks by transitional zones with prevailing lenticular and augen structures. Especially in the northern parts of the Koralm Complex several distinct levels of high-strain Plattengneis shear zones exist. The mylonites show a distinct planar fabric (penetrative foliation  $S_2$ ). Macroscopically, it is characterized by a nearly perfect tabular fissility parallel to the penetrative foliation, and a very prominent stretching lineation ( $L_2$ ). Even though the Plattengneis typically shows this apparent lineation, the general fabric is oblate both in sections parallel and perpendicular to the stretching lineation. This indicates a strain geometry situated within the flattening field.

Eclogites and garnet amphibolites occur both below and above this shear zone. In several layers near its base, boudins of eclogite are incorporated into the Plattengneis shear zone. The boudins are elongated in N–S direction and range from 100 to 0.1 m in thickness. In the central parts of the Koralm



Complex, the Plattengneiss-related stretching lineation gently plunges to the N to NNW. This is similar to the evolution in the Saualpe area. A similar orientation of stretching lineations can be observed within the eclogites and garnet amphibolites. In places where the eclogites are associated with the plattengneiss, the distinct stretching lineations are parallel. Therefore we presume, that the deformation of the eclogites is associated with the deformation within the Plattengneiss shear zone. Moreover, this indicates that the penetrative fabrics within the Plattengneiss shear zone and the eclogites below formed around the peak of eclogite- to amphibolite-facies metamorphism. Thus, the "Plattengneiss-deformation" started close to the peak of high-pressure metamorphism and was continued progressively along the decompressional path down to lower amphibolite- to greenschist-facies metamorphic conditions.

Asymmetric sense-of-shear indicators are rather scarce, especially within the Plattengneiss shear zone. Most of the clasts within the Plattengneiss are surrounded by symmetric pressure shadows, indicating co-axial deformation. This is indicated as well by the symmetric boudinage of distinct eclogite layers within the Plattengneiss shear zone. Where asymmetric fabrics were locally observed, they both indicate a top-to-the N and a top-to-the S sense of shear, especially in the central parts of the Koralpe Complex, not depending on later folding of the penetrative foliation. Towards north, a top-to-the N to NE sense of shear dominates in the Koralpe area. This evolution is asserted by the evolution of the asymmetry of quartz lattice preferred orientations within the Plattengneiss shear zone as well. Generally, a continuous change from small circle distributions of quartz *c*-axes in the southernmost parts, to crossed girdles in the central parts, and single maxima centered in the *Y*-axis of the finite strain ellipsoid in the central and northern parts can be observed.

In the Plattengneiss, quartz typically forms layers and lenses. Within these lenses, the quartz grains are characterized by uniform size in the range from 0.1 to 0.2 mm. The grains are characterized by serrate and lobate grain boundaries typical for high temperature deformation (equigranular – interlobate fabric). The main mechanism of dynamic recrystallization is grain boundary migration recrystallisation. Subgrains commonly occur. Some domains are characterised by uniformly sized quartz grains bordered by straight grain boundaries. These fabrics may document partial annealing.

Feldspar clasts (K-feldspar and plagioclase) occur as single porphyroclasts within a fine-grained matrix of quartz, white mica, biotite and plagioclase. The porphyroclasts are characterized by undulatory extinction and the development of subgrains. Very often large grains with undulatory extinction are symmetrically surrounded by small, dynamically recrystallized grains forming core-and-mantle structures. The occurrence of subgrains and the development of core-and-mantle structures indicate medium- to high-grade deformation conditions (above 500 °C). The porphyroclasts are sometimes surrounded by symmetrically arranged strain shadows, probably related to co-

axial flow. The strain shadows are either filled with dynamically recrystallized feldspars, or with quartz grains. Garnets occurring in paragneisses are partly boudinaged, indicating strong extension in the *X*-direction of the finite strain ellipsoid. Similar to the macroscale deformation structures (see above), asymmetric sense-of-shear indicators are hardly observed at microscale, as well. Clasts of feldspar are usually surrounded by symmetric pressure shadows; mica-fish of muscovite are characterised by a symmetric shape in N–S direction.

Subsequently the penetrative foliation has been gently folded around subhorizontal, E–W oriented axes, which resulted in the development of km-scale syn- and anticlines, and a crenulation cleavage at macroscale.

## 2.9 Field stop 8: Kyanite eclogite of the Koralpe complex at Hohl, S of Schwanberg, Styria

*N 46°43'32" E 15°08'44"; Österreichische Karte 206, Eibiswald, 1:50,000*

Hidden in the forest is a residual hill consisting of coronitic kyanite-rich eclogite. The base of the hill is comprised of foliated quartz-rich eclogite with an intercalation of kyanite-garnet-phengite schist. Locally developed eclogite-facies shear zones show no evidence of large-scale displacements. Metamorphic textures and mineral compositions of the kyanite-rich eclogite are quite variable. Igneous relics have not been preserved, but the chemical composition and positive Eu anomalies clearly indicate a cumulate precursor rock (Fig 32: samples H8 and 94T44KH). In addition, igneous textures have been locally preserved, igneous clinopyroxene is frequently replaced by magnesiohornblende or by an aggregate of fine-grained

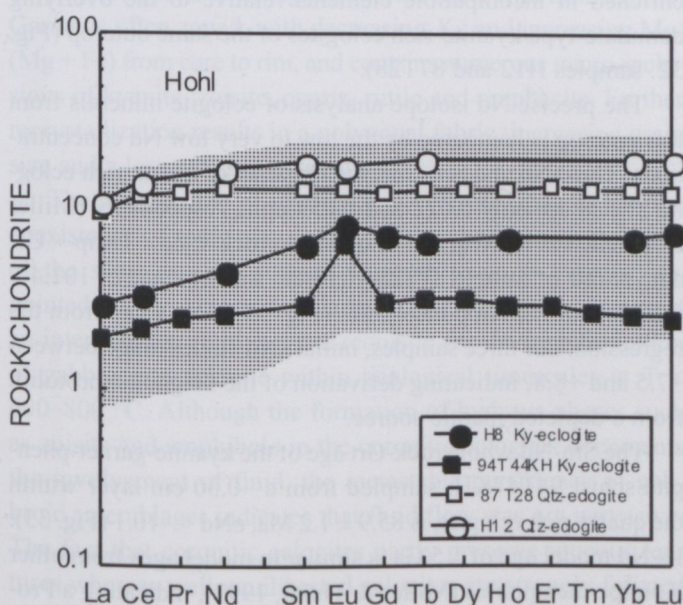
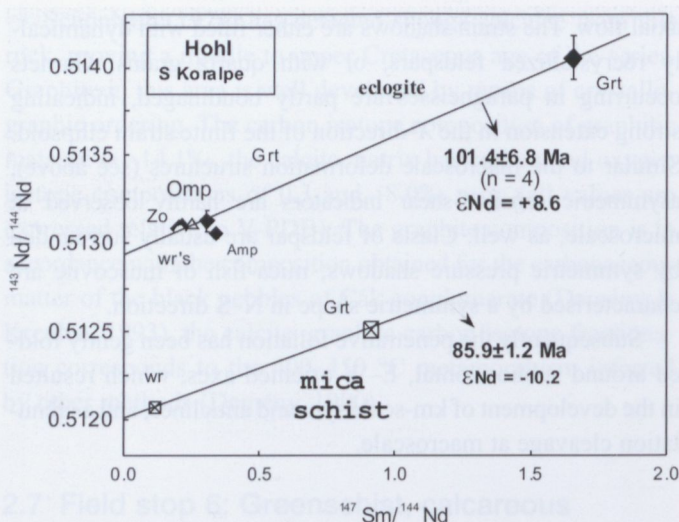


Fig. 32. Chondrite-normalized (Boynton, 1984) rare earth element plots showing representative patterns for Ky- and Qtz-rich eclogites from Hohl, Koralpe. Mineral abbreviations after Kretz (1983).





**Fig. 33.** Isochron plot of whole rock and mineral Sm-Nd data of three eclogite samples (upper part) and an intercalated Grt-Ky-Phe schist (lower part) from Hohl locality, southern Koralpe. Full symbols depict eclogite 87T28: wr, Zo, Omp and Grt of this sample define an age of  $101.4 \pm 6.8$  Ma ( $\epsilon_{\text{Nd}} = +8.6$ ; MSWD = 0.32), but overall uncertainties are high due to the extremely low Nd concentrations (Grt: 22 ppb Nd). Data from Miller & Thöni (1997).

omphacite ( $X_{\text{Jd}} = 0.32\text{--}0.39$ ). Inclusion-rich garnet ( $\text{Prp}_{40\text{--}48}\text{Alm}_{33\text{--}37}\text{Grs}_{14\text{--}24}\text{Sps}_{0.7\text{--}1.2}$ ) forms porphyroblasts or aggregates aligned along former clinopyroxene-plagioclase boundaries. Former plagioclase domains consist of kyanite + zoisite  $\pm$  quartz  $\pm$  garnet. Rutile, apatite and Fe sulfides are accessories.

The quartz-rich eclogite at the base of the hill is medium-grained, foliated and layered due to variable proportions of garnet ( $\text{Prp}_{22\text{--}29}\text{Alm}_{46\text{--}49}\text{Grs}_{22\text{--}28}\text{Sps}_{0.8\text{--}1.0}$ ), omphacite ( $X_{\text{Jd}} = 0.38\text{--}0.40$ ), Ca-amphibole (magnesiohornblende) and clinozoisite. These minerals coexist with quartz, minor phengite, rutile, apatite, zircon and pyrite. Bulk rock compositions are clearly enriched in incompatible elements relative to the overlying cumulate-type kyanite-rich eclogites of the same outcrop (Fig. 32: samples H12 and 87T28).

The precise Nd isotope analysis of eclogite minerals from this outcrop is hampered by the low to very low Nd concentrations. Thus, Nd and Sm contents in garnet of quartz-rich eclogite 87T28 are only 0.022 and 0.059 ppm, respectively (Miller & Thöni, 1997). Regression of whole rock + Zo + Omp + Grt data points of sample 87T28 yields an isochron age of  $101.4 \pm 6.8$  Ma, but the Amp data point (Fig. 33) plots away from the regression. For three samples, initial  $\epsilon_{\text{Nd}}$  values range between +7.5 and +8.8, indicating derivation of the magmatic protolith from a depleted mantle source.

The Sm-Nd whole rock-Grt age of the kyanite-garnet-phengite schist 94T47KH, sampled from a  $\sim 0.30$  cm layer within the quartz-rich eclogite, is  $85.9 \pm 1.2$  Ma,  $\epsilon_{\text{Nd}} = -10.1$  (Fig. 33). Its Nd model age of 1.5 Ga is similar to model ages from other Koralpe metapelites (Miller & Thöni, 1997), indicating a Proterozoic mean crustal residence age for this material.

At the locality Bäröfen (not on the excursion route) different stages of the gabbro to eclogite transition are well preserved

(see Fig. 8c) and allow detailed mineralogical studies of the transition stages. Fortunately, spectacular examples of polished gabbro-eclogite transitions are exhibited in the Geopark Glashütten (next stop) and can be examined there. Some microscopic and microchemical details are given below:

#### Mineral chemistry of precursor gabbros:

Plagioclase compositions range from  $\text{An}_{60}$  to  $\text{An}_{76}$  in unaltered domains of different samples. Incipient alteration results in cloudy areas consisting of extremely fine-grained kyanite, zoisite  $\pm$  Ca-rich garnet  $\pm$  sodic clinopyroxene. Clinopyroxene appears dark and cloudy due to exsolution of very fine-grained ilmenite in addition to exsolution of orthopyroxene (Fig. 34). The original composition prior to exsolution is not known; all analysed clinopyroxene grains are diopside ( $\text{Wo}_{46\text{--}49}\text{En}_{43\text{--}46}\text{Fs}_{6\text{--}10}$ ) containing 4.1–4.6 wt%  $\text{Al}_2\text{O}_3$ , 0.2–0.4 wt%  $\text{Cr}_2\text{O}_3$  and 0.7–0.9 wt%  $\text{Na}_2\text{O}$ . Orthopyroxene is relatively homogeneous bronzite ( $\text{En}_{71\text{--}76}$ ) with 2.2–2.9 wt%  $\text{Al}_2\text{O}_3$ . Olivine has been replaced in most samples by Opx and spinel, but when still present its composition ranges between  $\text{Fo}_{76}$  and  $\text{Fo}_{79}$ .

#### Coronitic stage of gabbro-eclogite transformation:

The breakdown of olivine to a complex aggregate of orthopyroxene ( $\text{En}_{82}$ ), green spinel (50–64 mol%  $\text{MgAl}_2\text{O}_4$ )  $\pm$  clinopyroxene  $\pm$  garnet ( $\text{Prp}_{43}\text{Alm}_{52}\text{Grs}_4\text{Sps}_1$ )  $\pm$  corundum (Figs. 35a,b) starts along grain boundaries. The  $\text{SiO}_2$ , CaO and  $\text{Al}_2\text{O}_3$  required for this reaction could have been released by the decomposition of plagioclase. Breakdown of plagioclase takes place along grain boundaries and at fractures and high-strain domains within the grains. Partly reacted plagioclase contains abundant kyanite and zoisite needles (Fig. 36), and small euhedral garnet or garnet aggregates strongly enriched in grossular

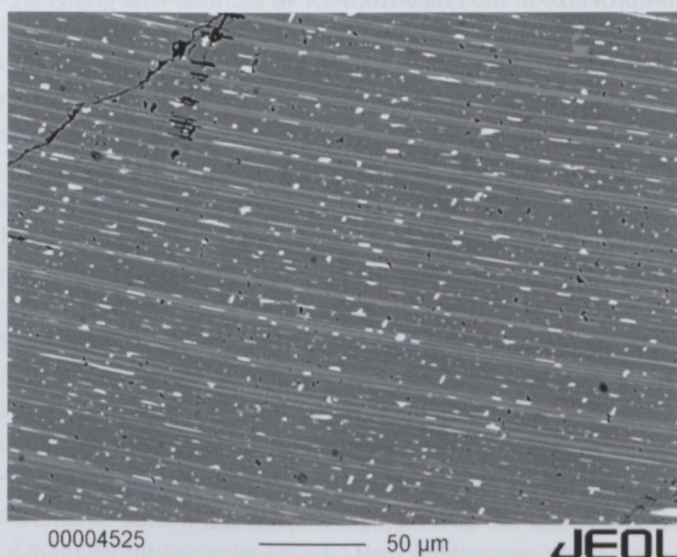


**Fig. 34.** BSE image of igneous clinopyroxene containing exsolution lamellae of orthopyroxene and ilmenite exsolutions. Bäröfen, Koralpe.



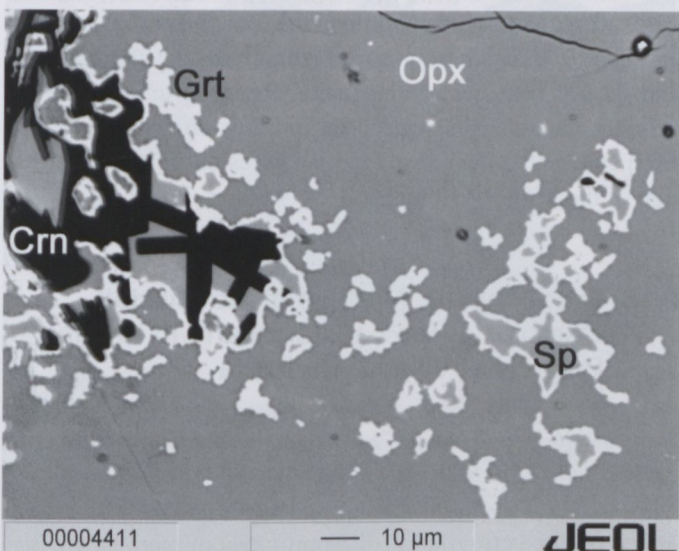
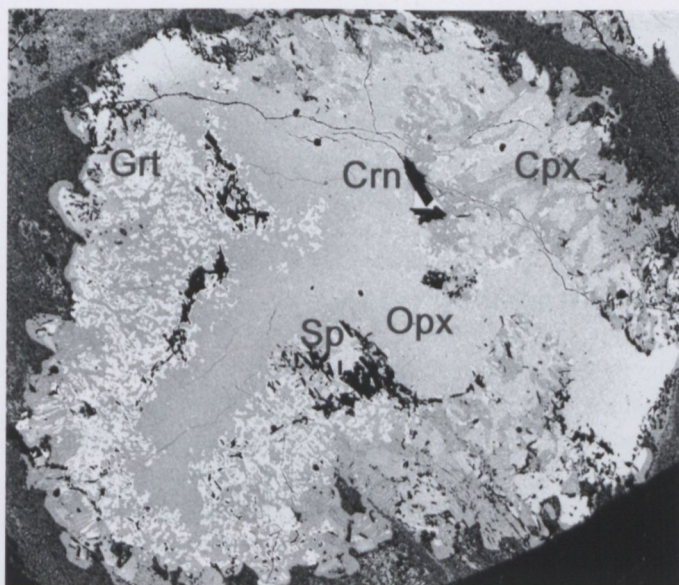


Fig. 35. BSE images of olivine pseudomorph in metagabbro sample Bär1, Bäröfen, Koralpe. Olivine is replaced by orthopyroxene (Opx), clinopyroxene (Cpx), spinel (Sp), garnet (Grt) and corundum (Crn).

(Grs = 53–91 mol%). In these altered domains, plagioclase composition becomes more sodic ( $An_{36-40}$ ) as reactions proceed. Igneous orthopyroxene has narrow coronas composed of sodic augite ( $X_{Jd} = 0.10-0.14$ ) when in contact with plagioclase. Igneous clinopyroxene has reacted with plagioclase forming garnet coronas along grain boundaries. Corona garnet is strongly zoned with higher values of grossular ( $Grs_{75-81}$ ) and  $Fe/(Fe + Mg)$  and abundant inclusions of kyanite  $\pm$  zoisite on the plagioclase side, and lower values of grossular ( $Grs_{35-38}$ ) and  $Fe/(Fe + Mg)$  and inclusions of rutile towards clinopyroxene. This texture suggests that kyanite and zoisite nucleated at an early stage of plagioclase decomposition, probably by the continuous reaction proposed by Goldsmith (1982).

$Pl + H_2O = Ky + Zo + Qtz + (NaSiCa_1Al_1)Pl$  which proceeds to the right with increasing pressure. Reactions responsible for the final breakdown of the igneous phases and the

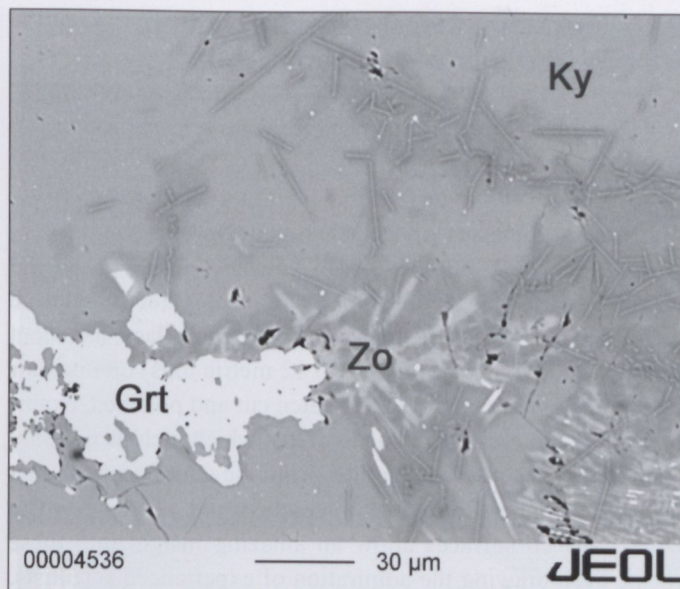


Fig. 36. BSE image of altered plagioclase domain in metagabbro sample Bär2, Bäröfen, Koralpe. Calcic plagioclase has partly reacted to grossular-rich garnet (Grt), kyanite (Ky), zoisite (Zo) and Na-rich plagioclase.

formation of eclogite involve recrystallization and extensive diffusion between different chemical domains through a set of complex continuous reactions.

#### *Eclogitic stage of gabbro-eclogite transformation:*

Eclogite samples that preserve igneous textures still show string-like clusters of euhedral garnet separating former plagioclase and mafic mineral domains (see Fig. 8d). Plagioclase has been replaced by kyanite + zoisite  $\pm$  garnet  $\pm$  quartz, pyroxene and olivine domains have been replaced by fine-grained polygonal omphacite, quartz and magnesiohornblende, with minor rutile. Garnet is often zoned, with decreasing  $X_{Ca}$  and increasing  $Mg/(Mg + Fe)$  from core to rim, and contains numerous micro-inclusions of kyanite, zoisite, quartz, rutile and omphacite. Further recrystallization results in a polygonal fabric, increasing grain size and a loss of igneous textures.

The preservation of igneous minerals and textures and the coexistence of sodic plagioclase and eclogite in a single block of the same outcrop suggest sluggish reaction kinetics. As pointed out by Ahrens & Schubert (1975a,b), the presence of an intergranular fluid is a pre-requisite for the transformation of gabbro into eclogite within geological timescales at  $T < 600-800^\circ C$ . Although the formation of hydrous phases such as zoisite and amphibole in the coronitic eclogites documents the involvement of fluid, the metastable persistence of gabbroic assemblages indicates that fluid flow was not pervasive. The fact that coronitic eclogites partly preserve igneous textures whereas well-equilibrated eclogites are strongly foliated suggests that deformation also enhanced reaction kinetics and aided recrystallization by dislocation creep, grain-size reduction and allowing ingress of catalytic fluid.



## 2.10 Field stop 9: Geopark, Glashütten, W of Deutschlandsberg, Styria

*N 46°49'26", E 15°03'33"; Österreichische Karte 188, Wolfsberg, 1:50,000*

The small, picturesque village of Glashütten, which was a booming centre for glass production ("Waldglas") in the 17<sup>th</sup> and 18<sup>th</sup> centuries, is today one of numerous tourist attractions in the area. The Geopark, situated in the centre of the village, has about 20 huge boulders (weighing up to 12 metric tons) on open-air display. These are hand-picked, often cut and polished, examples of typical rocks from the Koralpe, which include not only some rather spectacular eclogites from the main localities, but also "Plattengneis", marble, micaschist and pegmatite. The large polished surfaces allow an amazing insight into these rocks, even drawing the admiration of experienced scientists. A quartz-glass sculpture and a "geological mosaic" by artist Werner Schimpl add to the attraction and flair of the site.

## 2.11 Field stop 10: "Paramorphosen"-Schists with pseudomorphs of kyanite after andalusite of the Koralpe complex at Weinebene, W of Deutschlandsberg, Styria

*N 46°50'29" E 15°01'01"; Österreichische Karte 188, Wolfsberg, 1:50,000*

At this location paragneiss with pseudomorphs of kyanite after andalusite (known in the local literature as "Paramorphosen-schiefer") and Plattengneiss can be seen. Follow the road from Deutschlandsberg to the Weinebene, a saddle in the Koralpe.

From the stop follow the footpath to the south a few 100 metres towards Koralpe Speik, the summit of the Koralpe. Blocks of micaschists along the path contain pseudomorphs after andalusite, almost totally replaced by fine-grained kyanite (paramorphs) or in some cases replaced by composite sericite-kyanite-rich pseudomorphs (Figs. 8a,b). Sometimes rectangular outline of former andalusite can still be recognized and are interpreted as indications of Permian LP metamorphism which were overprinted by eo-Alpine HP metamorphism.

## 2.12 Field stop 11: Panorama view towards the Southalpine Karawanken mountains and cultural stop, Diex, N of Völkermarkt, Carinthia

*N 46°44'42", E 14°37'01"*

Diex, at the southern slope of the Saualpe, is known as the sunniest village in Austria and offers an excellent view over the Drau valley towards the south where the calcareous Karawanken

Mts. of the Southalpine tectonic unit mark a spectacular horizon. Diex is also well known for its fortified gothic church (Wehrkirche) founded in the 12<sup>th</sup> century and rebuilt in 1490 in gothic style. A special feature is the 5 m high defense wall surrounding the whole area around the church providing – at that time – a safe place of refuge from the invasion of the Turks.

## Day 3: Nockberge area

The pre-Alpine history of the Millstatt Complex is not well constrained. However, a Permian low-P event is indicated by the occurrence of Permian pegmatites and textures similar to those in units where a Permian low-P event is proved (Figs. 37a,b). For example there are kyanite aggregates which represent pseudomorphs after andalusite and sillimanite (Fig. 37c). The eo-Alpine metamorphic history was worked out by Teiml (1996), Teiml *et al.* (1995) and Teiml & Hoinkes (1996).

Peak metamorphic conditions reached  $\geq 13.8$  kbar and  $630 \pm 20^\circ$  C estimated from garnet-clinopyroxene thermometer and jadeite contents in omphacite. Reaction textures of the eclogite assemblages reflect decompression with a change from constant to decreasing temperatures during the exhumation of the Millstatt Complex.

## 2.13 Field stop 12: Marbles of the Millstatt Complex at the Lauster quarry in Krastal, Puch, N of Villach, Carinthia

*N 46°40'26", E 13°48'08"; Österreichische Karte 200, Arnoldstein, 1:50,000*

Based on the petrography, different types of marbles are distinguished in the Millstatt complex. The most dominant type is a coarse-grained (cm!) calcite marble with white to bluish colour caused by fluid inclusions soaking the marble. Reddish types of calcite marbles are due to contamination by Fe oxides or hydroxides. Others are rich in phlogopite (up to 5 mm) which are aligned parallel, forming dm-thick layers and marking a foliation. The petrologically most interesting type, although not beloved by the mining companies, is a siliceous dolomite-calcite marble with finely dispersed graphite of up to 10% responsible for a gradual change in colour from white to even black. They may contain diopside and tremolite, which are related by a retrograde reaction replacing the presumably pre-Alpine diopside by eo-Alpine tremolite.



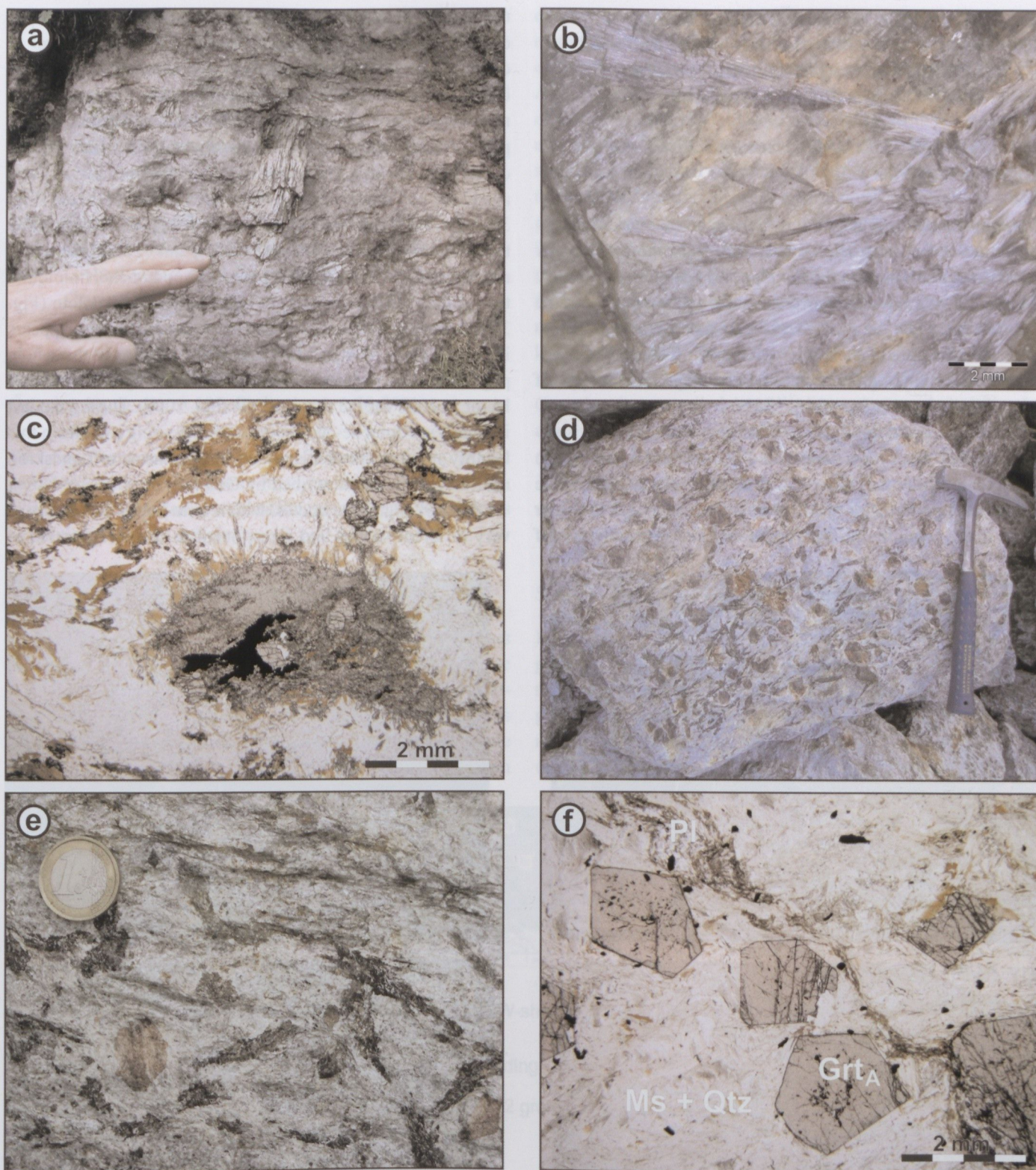


**Fig. 37.** Lithologies from the Nockberge area: a) Spodumene in pegmatite from the outcrop of Lug-ins-Land at the Millstätter lake ridge, Carinthia. b) Holmquistite in fractures and cleavage planes of spodumene from the pegmatite outcrop of Lug-ins-Land at the Millstätter lake ridge, Carinthia. c) Paragneiss of the Millstatt Complex with relict garnet surrounded by fine grained kyanite. The kyanite formed during the eo-Alpine event from pre-existing sillimanite. The sillimanite developed in Permian time during the breakdown of garnet by the reaction  $\text{Grt} + \text{Ms} = \text{Sil} + \text{Bt}$  (04R28, Puch, Carinthia, ÖK 200). d–e) Block of coarse-grained garnet-mica schist of the Radenthein Complex with biotite pseudomorphs after hornblende (Quarry at Nöringsattel, Carinthia, ÖK 183). f) Garnet-bearing micaschist of the Radenthein Complex with garnet porphyroblasts, which formed during the eo-Alpine event (RSP182, Predlitz, Styria, ÖK 158).



## 2.14 Field stop 13: Spodumene-bearing pegmatite and paragneisses of the Millstatt Complex at Lug-ins-Land, Baldersdorf, S of Spittal a.d. Drau, Carinthia

*N 46°46'55", E 13°33'36"; Österreichische Karte 182, Spittal an der Drau, 1:50,000.*

Spodumene-bearing pegmatites are dispersed over an extensive area of the Austroalpine basement from the Defferegger Mountains in the west to the Koralpe and Gleinalpe in the east. Most of them are small in size and show moderate to extreme deformation. Only the spodumene-bearing pegmatites at Weinbene (Koralpe) are of economic significance. Their mineral parageneses are ranking them with the albite-spodumene type of rare-element pegmatites (Göd, 1989).

The outcrop of the Lug-ins-Land pegmatite (775 m) is situated in the slope of a forest road about 200 m NW of the topographic peak Lug-ins-Land (816 m) at the Millstatt-lake ridge between the lake of Millstatt in the north and the river Drau in the south. In the outcrop, monotonous paragneisses of

the Millstatt Complex with an intrusion of a Permian spodumene-bearing pegmatite can be seen. The latter is fine- to coarse-grained and shows a primary mineral assemblage of muscovite + albite + quartz + spodumene ± alkali feldspar ± tourmaline (schorl) ± garnet ± beryl ± zircon. Greyish to greenish platy crystals of spodumene are conspicuous in a fine-grained quartz–albite matrix. Single crystals of spodumene have an average of about 4 cm in size and reach a maximum of 20 cm (Fig. 37a). The eo-Alpine metamorphic overprint is characterized by the formation of holmquistite and small grains of dark green chlorite. In fractures and cleavage planes of spodumene, holmquistite occurs in fibrous needles of light to dark violet colour (Fig. 37b). Nearly invisible with naked eye holmquistite also appears in the foliation of mica and dark green chlorite in the whole pegmatite. This pegmatite outcrop was found by a mineral collector in 2008 for the first time (Walter, 2009). During the last ice age a spodumene- and holmquistite-bearing rock from this locality was transported about 31 km southeast to Landskron near to Villach and described by Göd (1978).

A lot of pegmatite bodies, which form lenses and layers of very different shapes and sizes, occur in the paragneisses of

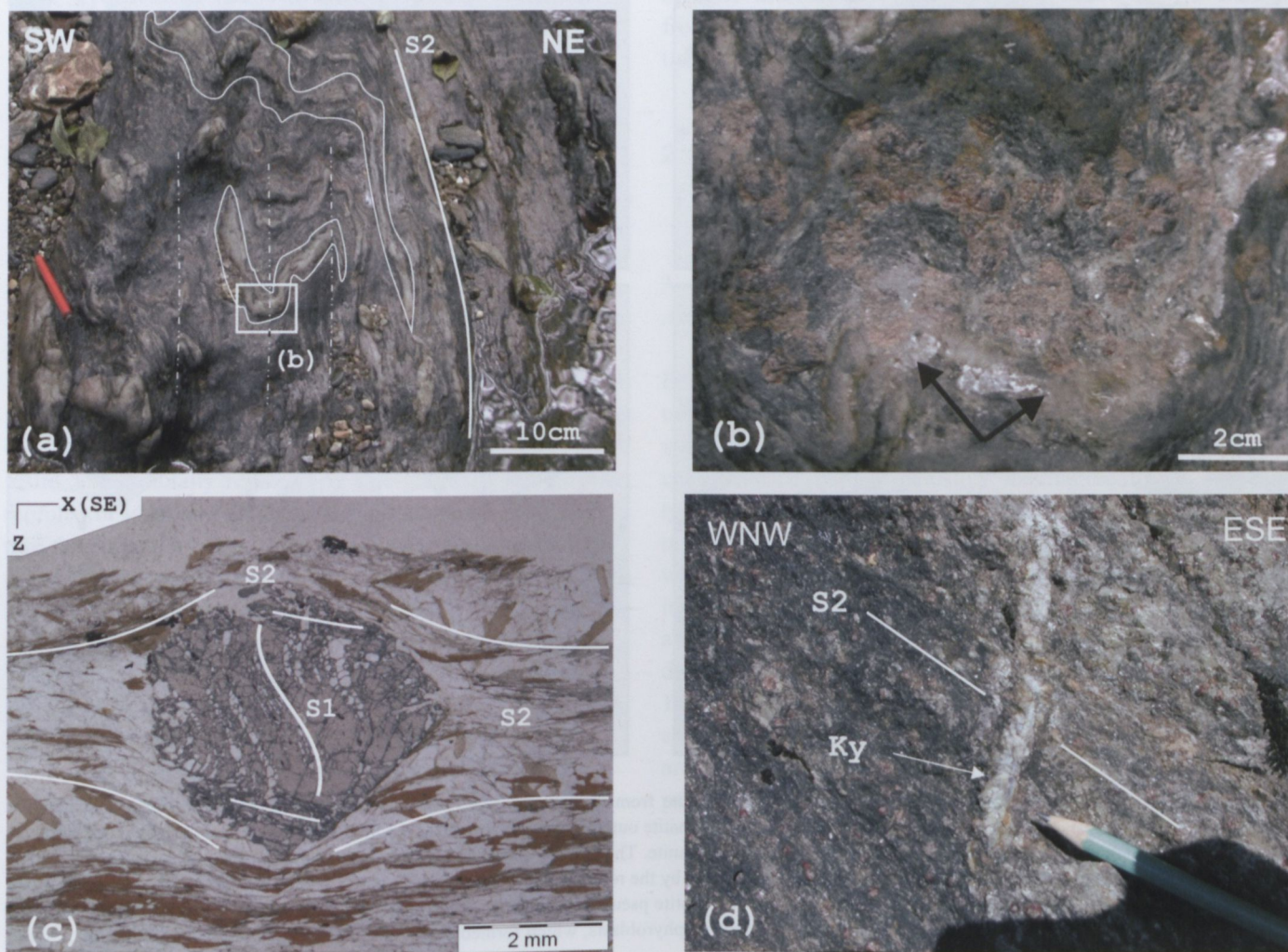


**Fig. 38** a) Intense folded quartz layers (Twengbachgraben). b) Post-kinematic growth of garnet rims in the fold hinge areas (arrows). c) Sigmoidal inclusion pattern in garnet poikiloblast of metapelites suggesting early synkinematic growth of the garnet core against direction of SE-stretching. Inclusion trails in the outer rim zone of the poikiloblast are parallel to the symmetric strain shadows. d) Kyanite-bearing extensional quartz vein cutting the main field foliation at high angles.



the Millstatt Complex. Some of the pegmatite bodies contain up to 1 million tons of rock material and were mined for pottery and glasswork until 1973 (Luecke & Ucik, 1986). From these pegmatites rare secondary phosphate minerals were reported e.g. brazilianite, childrenite, gormanite, wardite, whiteite- (CaFeMg), whitlockite, zanzaziite etc. (Walter, 1998).

## 2.15 Field stop 14: Coarse-grained garnet micaschists of the Radenthein complex, Untertweg and Granatium at Radenthein, Carinthia

a) Tweng-Klamm, N 46°47'33", E 13°44'04" and  
b) Granatium (N 46°48'09", E 13°42'14");  
Österreichische Karte 183, Radenthein, 1:50,000

The significant rock types of the Radenthein Complex are garnet-mica schists and garnet-mica-hornblende schists (Figs. 37d,e,f), which are interpreted as the metamorphic equivalents of pelitic and marly sediments.

### Stop 14a

A short walk along the outcrops at the Twengklamm shows typical rock types and the main deformation events of these metasediments. Fold interference dominates in garnet stability indicated by the post deformational growth of garnet rims (Figs 38a,b). Here, east of the Tauern Window, the observable folding stages are in their orientation comparable to the main

deformation stages west of the Tauern Window (Alpine mono-metamorphosed Schneeberg Complex) that developed during exhumation of the eo-Alpine high-pressure wedge of the Eastern Alps (Krenn *et al.*, in prep.). Garnet internal patterns consist of low-stress quartz grains and indicate top-to-the NW-directed shearing followed by coeval shortening perpendicular to shearing and coaxial stretching (Fig. 38c). When observable, the latter leads to dominant symmetric pressure shadows around porphyroblasts as well as to post-deformational growth of hornblende (hornblende-garben schists). Extension-related structures are mainly characterized by m- to dm-scale, almost undeformed quartz veins which crosscut the main foliation. In places, small crosscutting quartz veins bear a second generation of kyanite (Fig. 38d). On the basis of their orientation (NE–SW strike direction), late stage of exhumation of the Radenthein Complex is controlled by SW-directed normal faulting. In analogy to the rocks west of the Tauern Window which experienced cooling below 150 °C at ~60 Ma (Fügenshuh *et al.*, 2000) also here in Radenthein east of the Tauern Window, normal faulting may be related to Late Cretaceous extension in the Eastern Alps.

### Stop 14b

In the open air museum "Granatium", typical coarse-grained garnet-mica schists of the Radenthein Complex can be investigated and collected. Different mineral assemblages out of grt–wm–bt–chl–ky–st–hbl–pl–qtz may occur, the most dominant being simple garnet-mica schists with idioblastic garnets of mm- to cm size. Garnet is almandine-rich and shows either

slightly bell-shaped chemical zonation with Mn and Ca decreasing and Fe and Mg increasing from core to rim (see Figs. 16a,b) or are constant in composition due to discontinuous eo-Alpine metamorphic growth. The peak metamorphic AFM-assemblage is characterized by coexisting garnet, kyanite, staurolite and biotite. The prograde evolution is sometimes shown by chloritoid inclusions in garnet.

Primary fluid inclusions occur in kyanite and garnet and were investigated by Kaindl and Abart (2002). They belong to the systems CO<sub>2</sub>–N<sub>2</sub> and CO<sub>2</sub>–H<sub>2</sub>O and represent lower densities as expected for the P-peak conditions indicating post-entrapment density reequilibration of the primary fluid inclusions. The presence of chlorite aggregates within pri-

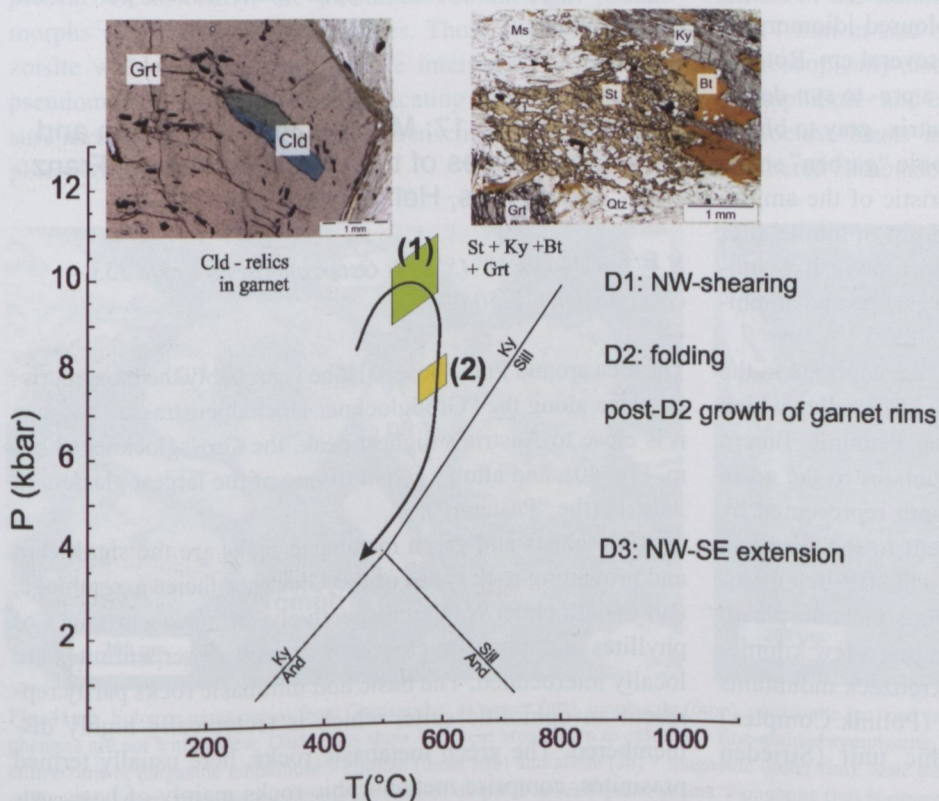


Fig. 39. Calculated PT conditions combined with deformation stages for metapelites of the Radenthein Complex.



mary inclusions indicate hydration reactions between the aqueous fluid and the garnet host as a possible mechanism leading to changes in composition and volume of the primary fluid.

PT data from metapelites of the central Radenthein Complex are about 9.5–11 kbar and ~550–600 °C (Koroknai *et al.*, 1999; Doppler, 2007; point 1 in Fig. 39). PT data from metapelites of the Twengklamm are about 7.5–8 kbar and 550–600 °C (Doppler, 2007; point 2 in Fig. 39). These data are indicative for early isothermal decompression after peak metamorphism.

## 2.16 Field stop 15: Coarse-grained micaschists and gneisses from the Radenthein Complex, Nöringsattel (Millstätter Alpe), N of Radenthein, Carinthia

*N 46°51'13", E 13°37'57", 1660 m; Oesterreichische Karte 183, Radenthein, 1:50,000.*

The outcrop is situated at the eastern margin of the magnesite mine (~1500 m a.s.l.) 6 km northwest of the village Radenthein. From Radenthein follow the road along the Kaningbach and the Globatschbach to the magnesite mine. Before reaching the mine, take the gravel road to Nöringsattel (1665 m). After approximately 1.5 km the road flattens and a barrier appears at the left-hand side. Stop at the barrier and walk towards the south across the terrace until you reach a block field, representing remnants of the former open pit mine.

The blocks consist of coarse-grained garnet-bearing micaschists and amphibole-garnet schists (Fig 37d). The diameter of the dark red to brownish coloured idiomorphic garnet porphyroblasts range from mm to several cm. Rotated internal structures of the garnets indicate a pre- to syn-deformational growth. Within the mica-rich matrix, gray to bluish kyanite crystals can be observed. Amphibole “garben” structures in the foliation planes are characteristic of the amphibole-garnet schists. Frequently pseudomorphs of biotite after amphibole occur (Fig. 37e). Yellowish to brownish weathered carbonates crosscut the blocks of the garnet- and amphibole-schists.

On the way to the last stop of this day we continue to the west over the Nöring Sattel and follow the Möll valley which marks the tectonic border between of the Penninic Tauern window represented by the Risseck mountains to the north and the Austroalpine basement to the south represented by the Kreuzeck mountains. Directly adjacent to the Penninic unit, the Austroalpine basement belongs to the HP-belt of eo-Alpine age. The southern limit of Alpine metamorphism (SAM) of the Austroalpine basement runs just a few kilometres further to the south and divides the Kreuzeck mountains into a northern Alpine metamorphic unit (Polinik Complex) and a southern pre-Alpine metamorphic unit (Strieden Complex, Fig. 15).

## 2.17 Field stop 16: Exhibition of minerals from the Hohe Tauern in the Mautturm at Winklern, Carinthia

*N 46°52'15"; E 12°52'37"; Österreichische Karte 180, Winklern, 1:50,000*

This exhibition is presented in the so-called Mautturm (toll tower), which is a historical building of unknown use in the village of Winklern, known since the 14<sup>th</sup> century. Due to its strategic position on a historic trade route crossing the Alps from south to north it probably had the function as watchtower or storehouse.

## Day 4: Großglockner toll road through the Tauern Window (Carinthia / Salzburg)

Topographically, this excursion traverses the Hohe Tauern between the Möll Valley in the south and the Salzach Valley in the north. The Hohe Tauern represent the main ridge of the Eastern Alps and contain a considerable number of summits exceeding an altitude of 3000 m, including the Großglockner (the highest point in Austria, 3798 m, which has been climbed for the first time in 1800). The pass section of the route is traversed by the Großglockner Hochalpenstraße, a road construction, which was begun in 1930 and completed in 1935, with the Hochtörl (2505 m) as one of the highest mountain passes crossed by a road in Europe.

Geologically, the excursion exhibits a section across the lower and upper Penninic nappes in the middle part of the Tauern Window.

## 2.18 Field stop 17: Metapelites, metamarls and metabasites of the Glockner Nappe, Franz Josef Haus, Heiligenblut, Carinthia

*N 47°04'21"; E 12°45'23"; Österreichische Karte 153, Großglockner, 1:50,000*

The area around Franz-Josefs-Höhe is probably the most touristic place along the “Großglockner Hochalpenstrasse” because it is close to Austria’s highest peak, the Grossglockner (3798 m, Fig. 40), and allows a visit of one of the largest glaciers in Austria (the “Pasterze”).

Calcschists and green metabasic rocks are the significant and prevailing rock types of the Glockner facies assemblage, and the Glockner Nappe, respectively. Minor occurrences of phyllites and garnet-mica schists as well as serpentinites are locally interbedded. The basic and ultrabasic rocks partly represent an ophiolitic suite, which is tectonically highly dismembered. The green metabasic rocks, here usually termed prasinites, comprise metamorphic rocks mainly of basic ori-





Fig. 40. View to the Großglockner and Franz Josef Höhe

gin, consisting of albite/oligoclase, epidote, actinolitic amphibole and chlorite. The metabasalts and leucocratic gabbros exhibit a chemical composition of tholeiites with normative hypersthene or sometimes even normative quartz. Analyses of trace elements Zr, Nb, Y, Ti confirm the assumption of ocean floor affinities for the metabasalts of Glockner facies assemblage. A major body of prasinites crops out in the area around the Franz Josefs Höhe. They consist of albite, with additional oligoclase and amphiboles, which are complex solid solutions between tremolite and a tschermakitic end member with some contributions of Na-amphibole end members as glaucophane or pargasite. The amphiboles are generally zoned with increasing Al and Fe towards the rims whereas in the zoned epidotes only Al increases from the core to the rim, while  $\text{Fe}^{3+}$  decreases. Chlorite and titanite are always present. Occasionally, the prasinites contain light pseudomorphs with rhombohedral outlines. These consist of clinozoisite with some chlorite and are interpreted to represent pseudomorphs after lawsonite, indicating an early high-pressure metamorphic event prior to greenschist-facies metamorphic overprint.

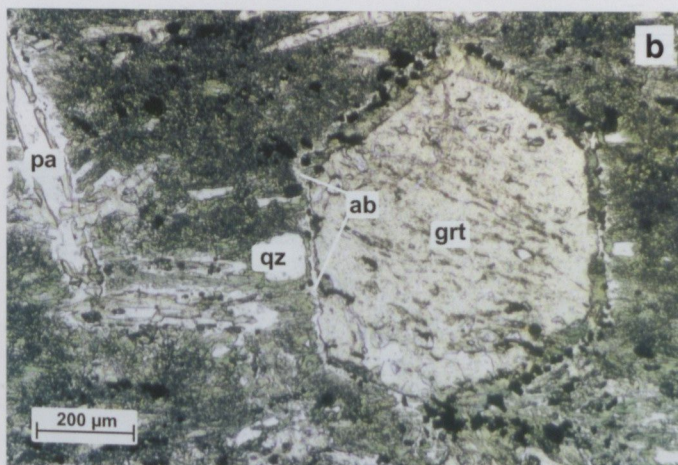
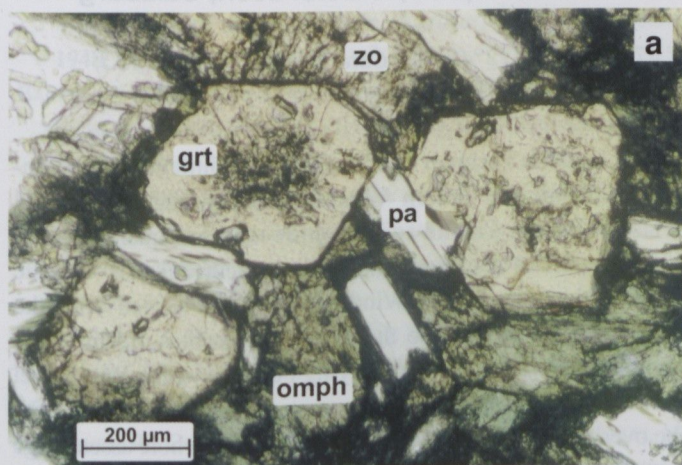


Fig. 41a,b. Eclogite parageneses from Gamsgrube: a) garnet (grt), omphacite (omp), paragonite (pa) and zoisite. Additional dolomite, glaucophane, quartz and phengite are not within view. Dark areas show incipient breakdown to extremely fine-grained symplectite. b) Replacement of idiomorphic garnet by polycrystalline rims of pargasitic amphibole + epidote (inner rim) and albite (ab) + magnetite (outer rim). Note the lack of corrosion of garnet along grain boundaries with matrix quartz (qz) and the light green rims of diopside around quartz grains. Paragonite (pa) is rimmed by clinozoisite and albite.

The greenschists alternate with micaceous marbles, and small interlayers of carbonate-bearing garnet-mica schists. Apart from calcite, quartz and dolomite the carbonaceous rocks consist of phengite, sometimes margarite, zoisite and chlorite. Pseudomorphs after lawsonite are also found as small dark dots.

## 2.19 Field stop 18: Retrogressed eclogite of the Glockner Nappe, Gamsgrube, Heiligenblut Carinthia

N 47°05'19"; E 12°44'07"; Österreichische Karte 153, Großglockner, 1:50,000

At the location "Gamsgrube" a band of eclogitic amphibolite with an average thickness of 20 m, running from the footpath north of the Pasterzenboden near Hoffmannshütte straight north towards the Fuscherkarkopf (from 2400 m to above 3000 m altitude), is exposed. This moderately to steeply southeast dipping band is underlain by graphitic garnet-mica schists and greenschists. The early workers in the Grossglockner area already recognized the eclogitic nature of these rocks and used the term "eclogitic prasinites" for them (Cornelius & Clar, 1939). Boulders of this rock type can be found directly above Hofmannshütte on the footpath from Hofmannshütte to Oberwalderhütte.

The retrogressed eclogite band consists of inconspicuous dark green massive to slightly banded and very fine-grained rocks. This band is underlain by graphitic garnet-mica schists and overlain by carbonaceous garnet-mica schists and greenschists of the Bündner Schist country rocks. Garnets of less than 1 mm in size or pseudomorphs of these are sometimes macroscopically discernible, some rocks show colour banding by amphibole- and epidote-rich layers. Small white specks of plagioclase blasts in peripheral samples and brown dots of weathered carbonate can also be recognized. Relict omphacite



is almost impossible to identify in the field and a large number of specimens, mostly garnet-bearing ones, were taken in order to find the relics of an earlier eclogite stage (Figs. 41a,b; Table 2). Most of the samples are retrogressed to a symplectitic amphibolite assemblage of amphibole + epidote + chlorite + plagioclase + quartz + garnet + paragonite + titanite, very often also containing calcite and biotite. Well preserved eclogite parageneses, however, consist of garnet + omphacite + dolomite + epidote + paragonite + rutile with some quartz and glaucophane and rare phengite.

The mineral assemblages of the retrogressed eclogites allow to postulate a metamorphic evolution from eclogite-facies conditions in the stability field of glaucophane + paragonite, related to the subduction of this unit. The eclogites were partially hydrated after the peak metamorphism, but still within the eclogite facies. The mineral assemblages in most of the hydrated eclogites, however, are equivalent to those observed in the metabasic country rocks, which is related to the main metamorphic overprint (Tauern Crystallization) of the Glockner Nappe.

Detailed petrographical study on these retrogressed eclogites, revealing a four-stage metamorphic evolution with peak pressures of ~17 kbar and temperatures of ~570 °C, followed by the main greenschist/amphibolite-facies event ("Tauern Crystallization") constrained at  $P = 5\text{--}6$  kbar,  $T = 500\text{--}530$  °C (Fig. 18).

## 2.20 Field stop 19: Serpentinities of the Glockner Nappe, Schönwand, Heiligenblut, Carinthia

$N 47^{\circ}03'21''$ ;  $E 12^{\circ}48'09''$ ;

Österreichische Karte 1:50,000, sheet 153 Großglockner

Well foliated serpentinites, intercalated with calcareous micaschists. The serpentinites form the bases of several thrust sheets within the Glockner Nappe.



**Fig. 42.** Thrust contact between the Rote Wand-Modereck Nappe (footwall) and the Glockner Nappe (hanging wall). Central Tauern Window, Großglockner Hochalpenstraße, Elendgrube, altitude 2420 m, Salzburg.

## 2.21 Field stop 20: Metaclastic rocks of the Brennkogel group, Hochtor Pass, Heiligenblut, Carinthia

$N 47^{\circ}04'58''$ ;  $E 12^{\circ}50'34''$ ; Österreichische Karte 154, Rauris, 1:50,000

The Brennkogel Group is characterized by abundant clastic rocks. The prevailing dark phyllites and (garnet-) mica schists are frequently interbedded with white to grey quartzites, carbonate quartzites, dolomite breccias, and meta-arkoses. Calc-schists and metabasic rocks are restricted to the uppermost sections of the Brennkogel Group.

## 2.22 Field stop 21: Thrust between Rote Wand – Modereck Nappe and Glockner Nappe, Elendgrube, Bruck/Fusch, Salzburg

$N 47^{\circ}05'51''$ ;  $E 12^{\circ}49'57''$ ; Österreichische Karte 153, Großglockner, 1:50,000

This location exposes Upper Triassic to Liassic Penninic quartzites and quartzitic schists in the footwall, and serpentinites in the hangingwall (Fig. 42). The serpentinites, representing metamorphosed oceanic lithospheric basement, form the base of the ophiolitic Glockner Nappe. Therefore, the thrust contact between a former passive margin sequence of the Rote Wand – Modereck Nappe in the footwall, and a former oceanic sequence represented by the Glockner Nappe can be observed.

## 2.23 Field stop 22: Chloritoid- and kyanite-bearing quartzitic schists, marbles and meta-evaporites of the Seidlwinkl Triassic Group, Fuschertörl – Edelweißspitze, Bruck/Fusch, Salzburg

$N 47^{\circ}07'05''$ ;  $E 12^{\circ}49'46''$  Österreichische Karte 153, Großglockner, 1:50,000

At this location Permian to Triassic metasediments of the Penninic units of the Tauern Window are exposed (Seidlwinkl Triassic Group). Calcite and dolomite marbles, quartzites and meta-evaporites represent the largest occurrence of Triassic rocks within the Tauern Window. They are named after the Seidlwinkl valley next to the east. The marbles are in stratigraphic contact with the underlying Permian Wustkogel Formation (metamorphic conglomerates and quartzites) and with the overlying Jurassic Brennkogel Group. The whole assemblage represents an individual thrust sheet (Rote Wand – Modereck Nappe) forming a sheath nappe with an amplitude of about 5 km.

This stop is located at the eastern side of the Glockner transverse. Isoclinal folding around N-trending  $b_1$  axes can be



observed. These folds are re-folded around N-trending b3 axes. In the carbonate rocks synclines of chloritoid schists and dark kyanite quartzites and quartzitic schists can be observed. The quartzites contain chlorite, chloritoid, magnetite and hematite. The trail from the Fuscher Törl to the Edelweißspitze is crossing middle Triassic dolomite marble. Immediately north of the Edelweißspitze black quartzites and quartzitic schists with black needles of kyanite ("Rhätizit") and dark chloritoid are exposed. The black colour of kyanite and chloritoid is caused by graphitic inclusions. Those quartzites represent parts of the Upper Triassic to Liassic cover of the Middle-Triassic dolomites and Limestones of the Seidlwinkl Group. At the northern side, meta-evaporites are exposed, especially bright white gypsum, metamorphosed at greenschist-facies conditions.

The panoramic view from the Edelweißspitze offers a magnificent insight to the tectonic structure of the Rote Wand – Modereck Nappe and the Glockner Nappe. To the east, both limbs of the recumbent fold of the Rote Wand – Modereck

Nappe are exposed on the west-flanking walls of the Seidlwinkl Valley. The central parts of this fold, consisting of Permo-skythian quartzites (Wustkogel Formation), are enveloped by the Seidlwinkl Triassic Group and the Brennkogel Group. The rocks of the Seidlwinkl Triassic Group can be traced to the south in the area of the Wustkogel, and to the north as far as to the ridge of the Hochtor. To the west, the main part of the Glockner nappe can be observed, comprising calcareous micaschists, greenschists and serpentinites.

### *Geology along the drive to Salzburg*

We follow the tollroad to the north down to the Salzach Valley, which represents the tectonic contact between the Penninic Tauern Window and Austroalpine Grauwacke Zone. We follow the Salzach valley towards the east and north and enter the Northern Calcareous Alps at Bischofshofen and remain in this tectonic unit until Salzburg, which is located at the tectonic contact to the Flysch Zone in the north.

## 3. References

- AHRENS, T.J. & SCHUBERT, G. (1975a): Rapid formation of eclogite in a slightly wet mantle. *Earth and Planetary Science Letters*, **27**: 90–94.
- AHRENS, T.J. & SCHUBERT, G. (1975b): Gabbro-eclogite reaction rate and its geophysical significance. *Reviews of Geophysics and Space Physics*, **13**: 383–400.
- AMATO, J.M., JOHNSON, C.M., BAUMGARTNER, L.P. & BEARD, B.L. (1999): Rapid exhumation of the Zermatt-Saas ophiolite deduced from high-precision Sm-Nd and Rb-Sr geochronology. *Earth and Planetary Science Letters*, **171**: 425–438.
- AWERZGER, A. & ANGEL, F. (1948): Die Magnesitlagerstätte auf der Millstätter Alpe bei Radenthein (Kärnten). *Radex-Rundschau*, **1948**: 91–95.
- BARRIGA, F. & FYFE, W.S. (1983): Development of rodingites in basaltic rocks in serpentinites, East Liguria, Italy. *Contributions to Mineralogy and Petrology*, **84**: 146–151.
- BECKER, H. (1993): Garnet peridotite and eclogite Sm-Nd mineral ages from the Lepontine dome (Swiss Alps): New evidence for Eocene high-pressure metamorphism in the central Alps. *Geology*, **21**: 599–602.
- BICKLE, M.J. & PEARCE, J.A. (1975): Oceanic mafic rocks in the Eastern Alps. *Contributions to Mineralogy and Petrology*, **49**: 177–189.
- BOUSQUET, R., GOFFÉ, B., VIDAL, O., OBERHÄNSLI, R. & PATRIAT, M. (2002): The tectono-metamorphic history of the Valaisan domain from the Western to the Central Alps: New constraints on the evolution of the Alps. *Geological Society of America Bulletin*, **114**: 207–225.
- BOUSQUET, R., OBERHÄNSLI, R., GOFFÉ, B., WIEDERKEHR, M., KOLLER, F., SCHMID, S.M., SCHUSTER, R., ENGI, M., BERGER, A. & MARTINOTTI, G. (2008): Metamorphism of metasediments at the scale of an orogen: a key to the Tertiary geodynamic evolution of the Alps. In Siegesmund, S., Fügenschuh, B. & Froitzheim, N. (eds): *Tectonic aspects of the Alpine-Dinaride-Carpathian system*. Geological Society London, Special Publication, **298**: 393–411.
- BRANDELIK, A. & MASSONNE, H.J. (2004): PTGIBBS – an EXCELTm Visual Basic program for computing and visualizing thermodynamic functions and equilibria of rock-forming minerals. *Computers & Geosciences*, **30**: 909–923.
- BREWER, M.S. (1969): Excess radiogenic argon in metamorphic micas from the Eastern Alps, Austria. *Earth and Planetary Science Letters*, **6**: 321–331.
- CHANNEL, J.E.T. & KOZUR, H.W. (1997): How many oceans? Meliata, Vardar, and Pindos oceans in Mesozoic Alpine paleogeography. *Geology*, **25**: 183–186.
- CHOPIN, C., HENRY, C. & MICHARD, A. (1991): Geology and petrology of the coesite-bearing terrain, Dora Maira massif, Western Alps. *European Journal of Mineralogy*, **3**: 263–291.
- CLIFF, R.A., DROOP, G.T.R. & REX, D.C. (1985): Alpine metamorphism in the south-east Tauern Window, Austria: II. Heating, cooling and uplift rates. *Journal of Metamorphic Geology*, **3**: 403–415.
- CLIFF, R.A., BARNICOAT, A.C. & INGER, S. (1998): Early Tertiary eclogite facies metamorphism in the Monviso Ophiolite. *Journal of Metamorphic Geology*, **16**: 447–455.
- CORNELIUS, H.P. & CLAR, E. (1939): *Geologie des Großglocknergebietes (I. Teil)*. Abhandlungen der Zweigstelle Wien der Reichsstelle für Bodenforschung [Geologische Bundesanstalt], **25**: 1–305.
- CSONTOS, L. & VÖRÖS, A. (2004): Mesozoic plate tectonic reconstruction of the Carpathian region. *Palaeogeography, Palaeoclimatology, Palaeoecology*, **210**: 1–56.



- DACHS, E. (1990): Geothermobarometry in metasediments of the southern Grossvenediger area (Tauern Window, Austria). *Journal of Metamorphic Geology*, **8**: 217–230.
- DACHS, E. & PROYER, A. (2001): Relics of high-pressure metamorphism from the Grossglockner region, Hohe Tauern, Austria: Paragenetic evolution and PT-paths of retrogressed eclogites. *European Journal of Mineralogy*, **13**: 67–86.
- DACHS, E. & PROYER, A. (2002): Constraints on the duration of high-pressure metamorphism in the Tauern Window from diffusion modelling of discontinuous growth zones in eclogite garnet. *Journal of Metamorphic Geology*, **20**: 769–780.
- DALLMEYER, R.D., HANDLER, R., NEUBAUER, F., & FRITZ, H. (1998): Sequence of thrusting within a thick-skinned tectonic wedge: Evidence from  $^{40}\text{Ar}/^{39}\text{Ar}$  and Rb-Sr ages from the Austroalpine nappe complex of the Eastern Alps. *Journal of Geology*, **106**: 71–96.
- DAL PIAZ, G.V., MARTIN, S., VILLA, I.M., GOSSO, G. & MARSHALCO, R. (1995): Late Jurassic blueschist facies pebbles from the Western Carpathian orogenic wedge and paleostructural implications for western Tethys evolution. *Tectonics*, **14**: 874–885.
- DAL PIAZ, G.V., CORTIANA, G., DEL MORA, A., MARTIN, S., PENNACHIONI, G. & TARTAROTTI, P. (2001): Tertiary age and paleostructural inferences of the eclogitic imprint in the Austroalpine outliers and Zermatt-Saas ophiolite, Western Alps. *International Journal of Earth Sciences*, **90**: 668–684.
- DAVIS, H.J. & VON BLANKENBURG, F. (1995): Slab breakoff: A model of lithospheric detachment and its test in the magmatism and deformation of collisional orogens. *Earth and Planetary Science Letters*, **129**: 85–102.
- DECKER, K. (1990): Plate tectonics and pelagic facies: Late Jurassic to Early Cretaceous deep-sea sediments of the Ybbsitz ophiolite unit (Eastern Alps, Austria). *Sedimentary Geology*, **67**: 85–99.
- DEMÉNY, A. (1987): Geochemical investigation of tourmaline grains. *Földtani Közlöny*, **117**: 131–140 (in Hungarian with English and Russian abstract).
- DEMÉNY, A. (1989): Structural ordering of carbonaceous matter in Penninic terranes. *Acta Mineralogica-Petrographica* (Szeged), **30**: 103–113.
- DEMÉNY, A. (1990): Mineralogical, geochemical and stable isotope investigations in the Penninic rocks of Hungary: A comparison of the Kőszeg-Rechnitz Series and the Tauern Window. Unpublished doctoral (Dr. univ.) thesis, Eötvös Loránd University, Budapest, Hungary, 100 p (in Hungarian).
- DEMÉNY, A., & DUNKL, I. (1991): Preliminary fission track results in the Kőszeg Penninic unit. *Acta Mineralogica-Petrographica* (Szeged), **32**: 43–47.
- DEMÉNY, A. & KREULEN, R. (1989): Carbon isotope compositions of graphites in the Penninic windows of Eastern Austria and Western Hungary and the Tauern Window. *Terra Abstracts*, **1**: 332.
- DEMÉNY, A. & KREULEN, R. (1993): Carbon isotope ratios of graphites in the Bündnerschiefer series of the Tauern Window and the Kőszeg-Rechnitz windows (Austria and Western Hungary): Origin of organic matter and sedimentary facies correlation. *Geologica Carpathica*, **44** (1): 3–9.
- DEMÉNY, A., VENNEMANN, T.W. & KOLLER, F. (2007): Stable isotope compositions of the Penninic ophiolites of the Kőszeg-Rechnitz series. *Central European Geology*, **50**: 29–46.
- DINGELDEY, CH., DALLMEYER, R.D., KOLLER, F. & MASSONNE, H.-J. (1997): P-T-t history of the Lower Austroalpine Nappe Complex in the “Tarntaler Berge”, NW of the Tauern Window: implications for the geotectonic evolution of the central Eastern Alps. *Contributions to Mineralogy and Petrology*, **129**: 1–19.
- DROOP, G.T.R. (1985): Alpine metamorphism in the south-east Tauern Window, Austria: I. P-T variations in space and time. *Journal of Metamorphic Geology*, **3**: 371–402.
- DROOP, G.T.R., LOMBARDO, B. & POGNATE, U. (1990): Formation and distribution of eclogite facies rocks in the Alps. In Carswell, D.A. (ed.): *Eclogite facies rocks*. Glasgow: Blackie, 225–259.
- DUCHENÉ, S., BLICHERT-TOFT, J., LUIS, B., TELOUK, P., LARDEAUX, J.-M. & ALABAREDE, F. (1997): The Lu-Hf dating of garnets and the ages of Alpine high-pressure metamorphism, *Nature*, **387**: 586–589.
- DUNKL, I. & DEMÉNY, A. (1997): Exhumation of the Rechnitz Window at the border of the Eastern Alps and Pannonian Basin during Neogene extension. *Tectonophysics*, **272**: 197–211.
- DUNKL, I., GRASEMANN, B. & FRISCH, W. (1998): Thermal effects of exhumation of a metamorphic core complex on hanging wall syn-rift sediments: an example from the Rechnitz Window, Eastern Alps. *Tectonophysics*, **297**: 31–50.
- EBNER, F. & RANTITSCH, G. (2000): Das Gosaubecken von Kainach: Ein Überblick. *Mitteilungen der Gesellschaft der Geologie und Bergbaustudenten Österreichs*, **44**: 157–172.
- ENGI, M., BERGER, A. & ROSELLE, G.T. (2001): Role of the tectonic accretion channel in collisional orogeny. *Geology*, **29**: 1143–1146.
- FARYAD, S.W. & HOINKES, G. (2003): P-T gradient of Eo-Alpine metamorphism within the Austroalpine basement units east of the Tauern Window (Austria). *Mineralogy and Petrology*, **77**: 129–159.
- FARYAD, S.W., MELCHER, F., HOINKES, G., PUHL, J., MEISEL, T. & FRANK, W. (2002): Relics of eclogite facies metamorphism in the Austroalpine basement, Hochgrössen (Speik Complex), Austria. *Mineralogy and Petrology*, **74**: 49–73.
- FAUPL, P. & WAGREICH, M. (1992): Cretaceous flysch and pelagic sequences of the Eastern Alps: correlations, heavy minerals, and paleogeographic implications. *Cretaceous Research*, **13**: 387–403.
- FAUPL, P. & WAGREICH, M. (2000): Late Jurassic to Eocene palaeogeography and geodynamic evolution of the Eastern Alps. *Mitteilungen der Österreichischen Geologischen Gesellschaft*, **92**: 79–94.
- FLÜGEL, H.W. & FAUPL, P. (eds) (1987): *Geodynamics of the Eastern Alps*. Wien: Deuticke, 418 p.
- FLÜGEL, H.W. & NEUBAUER, F. (1984): *Erläuterungen zur geologischen Karte der Steiermark*. Wien: Geologische Bundesanstalt, 127 p.
- FODOR, L., JELEN, B., MÁRTON, E., ZUPANČIČ, N., TRAJANOVA, M., RIFELJ, H., PÉCSKAY, Z., BALOGH, K., KOROKNAI, B., DUNKL, I., HORVÁTH, P., HORVAT, A., VRABEC, M., KRALJIČ, M. & KEVRIČ, R. (2002): Connection of Neogene basin formation, magmatism and cooling of metamorphics in NE Slovenia. *Geologica Carpathica*, **53** (Special issue): 199–201.



- FODOR, L.I., GERDES, A., DUNKL, I., KOROKNAI, B., PÉCSKAY, Z., TRAJANOVA, M., HORWÁTH, P., VRABEC, M., JELEN, B., BALOGH, K. & FRISCH, W. (2008): Miocene emplacement and rapid cooling of the Pohorje pluton at the Alpine-Pannonian-Dinaric junction, Slovenia, *Swiss Journal of Geoscience*, **101**: 255–271.
- FRANK, W. (1987): Evolution of the Austroalpine elements in the Cretaceous. In Flügel, H.W. & Faupl, P. (eds): *Geodynamics of the Eastern Alps*. Wien: Deuticke, 379–406.
- FRANK, W., HÖCK, V., & MILLER, CH. (1987): Metamorphic and tectonic history of the central Tauern Window. In Flügel, H. W. & Faupl, P. (eds): *Geodynamics of the Eastern Alps*. Wien: Deuticke, 34–54.
- FREY, M., DESMONS, J. & NEUBAUER, F. (1999): The new metamorphic map of the Alps: Introduction. *Schweizerische Mineralogische und Petrographische Mitteilungen*, **79**: 1–4.
- FRIMMEL, H. (1986): Isotopengeologische Hinweise für eine paläogeographische Nachbarschaft von Gurktaler Decke (Oberostalpin) und dem Altkristallin östlich der Hohen Tauern (Österreich). *Schweizerische Mineralogische und Petrographische Mitteilungen*, **66**: 193–208.
- FRIMMEL, H. (1988): Metagranitoide am Westrand der Gurktaler Decke (Oberostalpin): Genese und paläotektonische Implikationen. *Jahrbuch der Geologischen Bundesanstalt*, **131** (4): 575–592.
- FRISCH, W. (1977): Die Alpen im westmediterranen Orogen – eine plattentektonische Rekonstruktion. *Mitteilungen der Gesellschaft der Geologie und Bergbaustudenten Österreichs*, **24**: 263–275.
- FRISCH, W. (1979): Tectonic progradation and plate tectonic evolution of the Alps. *Tectonophysics*, **60**: 121–139.
- FRISCH, W. (1980): Post-Hercynian formations of the western Tauern window: sedimentological features, depositional environment and age. *Mitteilungen der Österreichischen Geologischen Gesellschaft*, **71/72**: 49–63.
- FRISCH, W. (1984): Metamorphic history and geochemistry of a low-grade amphibolite in the Kaserer Formation (Marginal Bündner Schiefer of the Western Tauern Window, the Eastern Alps). *Schweizerische Mineralogische und Petrographische Mitteilungen*, **64**: 193–214.
- FRISCH, W., GOMMERINGER, K., KELM, U. & POPP, F. (1987): The Upper Bündner Schiefer of the Tauern Window – A key to understanding Eoalpine orogenic processes in the Eastern Alps. Flügel, H.W. & Faupl, P. (eds): *Geodynamics of the Eastern Alps*. Wien: Deuticke, 55–69.
- FRITZ, H. (1988): Kinematics and geochronology of Early Cretaceous thrusting in the northwestern Paleozoic of Graz (Eastern Alps). *Geodinamica Acta*, **2**: 53–62.
- FROITZHEIM, N. & MANATSCHAL, G. (1996): Kinematics of Jurassic rifting, mantle exhumation, and passive margin formation in the Austroalpine and Penninic nappes (eastern Switzerland). *Geological Society of America Bulletin*, **108**: 1120–1133.
- FROITZHEIM, N., SCHMID, S.M. & FREY, M. (1996): Mesozoic paleogeography and the timing of eclogite facies metamorphism in the Alps: A working hypothesis. *Eclogae Geologicae Helveticae*, **89**: 81–110.
- FÜGENSCHUH, B., SEWARD, D. & MANCKTELOW, N. (1997): Exhumation in a convergent orogen: the western Tauern window. *Terra Nova*, **9**: 213–217.
- FÜGENSCHUH, B., MANCKTELOW, N.S. & SEWARD, D. (2000): Cretaceous to Neogene cooling and exhumation history of the Ötztal-Stubai basement complex, Eastern Alps; a structural and fission track study. *Tectonics*, **19**: 905–918.
- GAIDIES, F., ABART, R., DE CAPITANI, C., SCHUSTER R., CONNOLLY, J.A.D. & REUSSER, E. (2006): Characterization of polymetamorphism in the Austroalpine basement east of the Tauern Window using garnet isopleths thermobarometry. *Journal of Metamorphic Geology*, **24**: 451–475.
- GAWLIK, H.-J., FRISCH, W., VECSEI, A., STEIGER, T. & BÖHM, F. (1999): The change from rifting to thrusting in the northern Calcareous Alps as recorded in Jurassic sediments. *Geologische Rundschau*, **87**: 644–657.
- GEBAUER, D. (1999): Alpine geochronology of the Central and Western Alps: new constraints for a complex geodynamic evolution. *Schweizerische Mineralogische und Petrographische Mitteilungen*, **79**: 191–208.
- GEBAUER, D., SCHERTL, H.-P., BRIX, M. & SCHREYER, W. (1997): 35 Ma old ultrahigh-pressure metamorphism and evidence for rapid exhumation in the Dora Maira Massif, Western Alps. *Lithos*, **41**: 5–24.
- GENSER, J. & NEUBAUER, F. (1989): Low angle normal faults at the eastern margin of the Tauern window (Eastern Alps). *Mitteilungen der Österreichischen Geologischen Gesellschaft*, **81**: 233–243.
- GÖD, R. (1978): Vorläufige Mitteilung über einen Spodumen-Holmquistit führenden Pegmatit aus Kärnten. *Anzeiger der Österreichischen Akademie der Wissenschaften. Mathematisch-naturwissenschaftliche Klasse*, **7**: 1–5.
- GÖD, R. (1989): The spodumene deposit at “Weinebene”, Koralpe, Austria. *Mineralium Deposita*, **24**: 270–278.
- GOLDSMITH, J.R. (1982): Plagioclase stability at elevated pressures and temperatures. *American Mineralogist*, **66**: 1183–1188.
- GREGUREK, D., ABART, R., & HOINKES, G. (1997): Contrasting Eoalpine P-T evolution in the southern Koralpe, Eastern Alps. *Mineralogy and Petrology*, **60**: 61–80.
- HABLER, G. & THÖNI, M. (2001): Preservation of Permo-Triassic low-pressure assemblages in the Cretaceous high-pressure metamorphic Saualpe crystalline basement (Eastern Alps, Austria). *Journal of Metamorphic Geology*, **19**: 679–697.
- HANDLER, R., DALLMEYER, R.D. & NEUBAUER, F. (1997):  $^{40}\text{Ar}/^{39}\text{Ar}$  ages of detrital white mica from Upper Austroalpine units in the Eastern Alps, Austria: Evidence for Cadomian and contrasting Variscan sources. *Geologische Rundschau*, **86**: 69–80.
- HANDY, R.M. & OBERHÄNSLI, R. (2004): Explanatory notes to the map: Metamorphic structure of the Alps. Age map of the metamorphic structure of the Alps – Tectonic interpretation and outstanding problems. *Mitteilungen der Österreichischen Mineralogischen Gesellschaft*, **149**: 201–226.
- HAÜY, R.-J. (1822): *Traité de mineralogy*. 2<sup>nd</sup> ed. Paris: Bachelier et Huizard.
- HAWKESWORTH, C.J. (1976): Rb/Sr geochronology in the eastern Alps. *Contributions to Mineralogy and Petrology*, **54**: 225–244.
- HEIDRON, R., NEUBAUER, F., GENSER, J. & HANDLER, R. (2002):  $^{40}\text{Ar}/^{39}\text{Ar}$  mica age constraints for the tectonic evolution of the Lower Aus-



- troalpine to Penninic boundary, Austria. *Memorie di Scienze Geologiche*, **54**: 217–220.
- HERITSCH, H. (1973): Die Bildungsbedingungen von alpinotypem Eklogitamphibolit und Metagabbro, erläutert an Gesteinen der Koralpe, Steiermark. *Tschermaks Mineralogische und Petrographische Mitteilungen*, **19**: 213–271.
- HÖCK, V. (1974): Zur Metamorphose mesozoischer Metasedimente in den mittleren Hohen Tauern (Österreich). *Schweizerische Mineralogische und Petrographische Mitteilungen*, **54**: 567–593.
- HÖCK, V. (1980): Distribution maps of minerals of the Alpine metamorphism in the penninic Tauern Window, Austria. *Mitteilungen der Österreichischen Geologischen Gesellschaft*, **71/72**: 119–127.
- HÖCK, V. & KOLLER, F. (1987): The Idalp ophiolite (Lower Engadine Window, Eastern Alps) its petrology and geochemistry. *Ofioliti*, **12** (1): 179–192.
- HÖCK, V. & KOLLER, F. (1989): Magmatic evolution of the Mesozoic ophiolites in Austria. *Chemical Geology*, **77**: 209–227.
- HÖCK, V. & MILLER, CH. (1980): Chemistry of mesozoic metabasites in the middle and eastern part of the Hohe Tauern. *Mitteilungen der Österreichischen Geologischen Gesellschaft*, **71/72**: 81–88.
- HOINKES, G., KOSTNER, A. & THÖNI, M. (1991): Petrologic constraints for Eoalpine eclogite facies metamorphism in the Austroalpine Ötztal Basement. *Mineralogy and Petrology*, **43**: 237–254.
- HOINKES, G., KOLLER, F., RANTITSCH, G., DACHS, E., HÖCK, V., NEUBAUER, F. & SCHUSTER, R. (1999): Alpine metamorphism of the Eastern Alps. *Schweizerische Mineralogische und Petrographische Mitteilungen*, **79**: 155–181.
- HOKE, L. (1990): The Altkristallin of the Kreuzeck Mountains, SE Tauern Window, Eastern Alps – Basement crust in a convergent plate boundary zone. *Jahrbuch der Geologischen Bundesanstalt*, **133**: 5–87.
- HOLLAND, T.J.B. (1979): High water activities in the generation of high pressure kyanite eclogites in the Tauern Window, Austria. *Journal of Geology*, **87**: 1–27.
- HOLLAND, T. J. B. & RAY, N. J. (1985): Glaucophane and pyroxene breakdown reactions in the Pennine units of the Eastern Alps. *Journal of Metamorphic Geology*, **3**: 417–438.
- HOSCHEK, G. (2001): Thermobarometry of metasediments and metabasites from the Eclogite zone of the Hohe Tauern, Eastern Alps, Austria. *Lithos*, **59**: 127–150.
- INGER, S. & CLIFF, R.A. (1994): Timing of metamorphism in the Tauern Window, Eastern Alps: Rb-Sr ages and fabric formation. *Journal of Metamorphic Geology*, **12**: 695–707.
- JANÁK, M., FROITZHEIM, N., LUPTÁK, B., VRABEC, M. & KROGH RAVNA, E.J. (2004): First evidence for ultrahigh-pressure metamorphism in Pohorje, Slovenia: Tracing deep continental subduction in the Eastern Alps. *Tectonics*, **23**: TC5014.
- JANÁK, M., FROITZHEIM, N., VRABEC, M., KROGH RAVNA, E.J. & HOOG, J.C.M. (2006): Ultrahighpressure metamorphism and exhumation of garnet peridotite in Pohorje, Eastern Alps. *Journal of Metamorphic Geology*, **24**: 19–31.
- JOHANNES, W. & PUHAN, D. (1972): The calcite-aragonite transition, reinvestigated. *Contributions to Mineralogy and Petrology*, **31**: 28–38.
- JUHÁSZ, Á. (1965): Petrographic investigations on the “Cák conglomerate”. *Földtani Közlemény*, **95**: 313–319 (in Hungarian with German abstract).
- KAINDL, R. & ABART, R. (2002): Reequilibration of fluid inclusions in garnet and kyanite from metapelites of the Radenthein Complex, Austroalpine Basement, Austria. *Schweizerische Mineralogische und Petrographische Mitteilungen*, **82**: 467–486.
- KLÖTZLI-CHOWANETZ, E., KLÖTZLI, U. & KOLLER, F. (1997): Lower Ordovician migmatization in the Ötztal crystalline basement (Eastern Alps, Austria): Linking U-Pb and Pb-Pb dating with zircon morphology. *Schweizerische Mineralogische und Petrographische Mitteilungen*, **77**: 315–324.
- KOLLER, F. (1985): Petrologie und Geochemie der Ophiolithe des Penninikums am Alpenostrand. *Jahrbuch der Geologischen Bundesanstalt*, **128** (1): 85–150.
- KOLLER, F. (1990): Die Entwicklung der penninischen ozeanischen Kruste im Bereich der Rechnitzer Fenstergruppe. In Koller, F. (ed.): *Exkursionsführer 13*, Wien: Österreichische Geologische Gesellschaft, 11–27.
- KOLLER, F. & HÖCK, V. (1987): Die mesozoischen Ophiolite der Ostalpen. *Mitteilungen der Österreichischen Geologischen Gesellschaft*, **132**: 61–77.
- KOLLER, F. & HÖCK, V. (1990): Mesozoic ophiolites in the Eastern Alps. In Malpas, J., Moores, E.M., Panayiotou, A. & Xenophontos, C. (eds): *Ophiolites, oceanic crustal analogues. Proceedings of the Symposium “Troodos 1987”*. Nicosia: Geological Survey Dept., 253–263.
- KOLLER, F. & PAHR, A. (1980): The Penninic ophiolites on the eastern end of the Alps. *Ofioliti*, **5**: 65–72.
- KOROKNAI, B., NEUBAUER, F., GENSER, J. & TOPA, D. (1999): Metamorphic and tectonic evolution of Austroalpine units at the western margin of the Gurktal nappe complex, Eastern Alps. *Schweizerische Mineralogische und Petrographische Mitteilungen*, **79**: 277–295.
- KOZUR, H. (1992): The evolution of the Meliata-Hallstatt ocean and its significance for the early evolution of the Eastern Alps and Western Carpathians. *Paleogeography, Paleoclimatology, Paleogeology*, **87**: 109–135.
- KROGH RAVNA, E.J. (2000) The garnet-clinopyroxene Fe<sup>2+</sup>-Mg geothermometer: an updated calibration. *Journal of Metamorphic Geology*, **18**: 211–219.
- KROGH RAVNA E.J. & TERRY P. (2004) Geothermobarometry of UHP and HP eclogites and schists – an evaluation of equilibria among garnet-clinopyroxene-kyanite-phengite-coesite/quartz. *Journal of Metamorphic Geology*, **22**: 579–592.
- KROHE, A. (1987): Kinematics of Cretaceous nappe tectonics in the Austroalpine basement of the Koralpe region (Eastern Austria). *Tectonophysics*, **136**: 171–196.
- KRONER, U., MANSKY, J.-L., MAZUR, S., ALEKSANDROWSKI, P., HANN, H.P., HUCKRIDE, H., LACQUEMENT, F., LAMARCHE, J., LEDRU, P., PHARAOH, T.C., ZEDLER, H., ZEH, A. & ZULAUF, G. (2008): Variscan tectonics. In McCann, T. (ed.): *The geology of Central Europe. Volume 1: Precambrian and Palaeozoic*. Geological Society of London, 599–664.



- KURZ, W. & FRITZ, H. (2003): Tectonometamorphic evolution of the Austroalpine Nappe Complex in the central Eastern Alps – consequences for the Eo-Alpine evolution of the Eastern Alps. *International Geology Review*, **45**: 1110–1127.
- KURZ, W. & FROITZHEIM, N. (2002): The exhumation of eclogite-facies metamorphic rocks – a review of models confronted with examples from the Alps. *International Geology Review*, **44**: 702–743.
- KURZ, W., NEUBAUER, F. & GENSER, J. (1996): Kinematics of Penninic nappes (Glockner Nappe and basement-cover nappes) in the Tauern Window (Eastern Alps, Austria) during subduction and Penninic-Austroalpine collision. *Eclogae Geologicae Helvetiae*, **89**: 573–605.
- KURZ, W., NEUBAUER, F., GENSER, J. & DACHS, E. (1998): Alpine geodynamic evolution of passive and active continental margin sequences in the Tauern Window (Eastern Alps, Austria, Italy): a review. *Geologische Rundschau*, **87**: 225–242.
- KURZ, W., NEUBAUER, F., GENSER, J., UNZOG, W. & DACHS, E. (2001): Tectonic evolution of Penninic Units in the Tauern Window during the Paleogene: Constraints from structural and metamorphic geology. In Piller, W.E. & Rasser, M.W. (eds): *Paleogene of the Eastern Alps*. Österreichische Akademie der Wissenschaften, Schriftenreihe der Erdwissenschaftlichen Kommission, **14**: 347–375.
- KURZ, W., FRITZ, H., TENCZER, V. & UNZOG, W. (2002): Tectonometamorphic evolution of the Koralm Complex (Eastern Alps): Constraints from microstructures and textures of the “Plattengneis” shear zone. *Journal of Structural Geology*, **24**: 1957–1970.
- KURZ, W., JANSEN, E., HUNDENBORN, R., PLEUGER, J., SCHÄFER, W. & UNZOG, W. (2004): Microstructures and Crystallographic Preferred Orientations of omphacite in Alpine eclogites: implications for the exhumation of (ultra-) high-pressure units. *Journal of Geodynamics*, **37**: 1–55.
- KURZ, W., HANDLER, R. & BERTHOLDI, C. (2008): Tracing the exhumation of the Eclogite Zone (Tauern Window, Eastern Alps) by  $^{40}\text{Ar}/^{39}\text{Ar}$  dating of white mica in eclogites. *Swiss Journal of Geosciences*, **101** (Supplement 1): S191–S206.
- LAMMERER, B. (1988): Thrust-regime and transpression-regime tectonics in the Tauern Window (Eastern Alps). *Geologische Rundschau*, **77**: 143–156.
- LINNER, M. (1995): Das ostalpine Kristallin der südwestlichen Schober-Gruppe mit den frühalpidischen Eklogiten im Bereich der Prijakte–Alkuser See–Schleinitz. *Geologische Bundesanstalt, Arbeitstagung 1995*: 15–21.
- LIU, J.G. (1979): Synthesis and stability relations of prehnite  $\text{Ca}_2\text{Al}_2\text{Si}_3\text{O}_{10}(\text{OH})_2$ . *American Mineralogist*, **56**: 507–531.
- LUECKE, W. & UCIK, F.H. (1986): Die Zusammensetzung der Pegmatite von Edling und Wolfsberg bei Spittal/Drau (Kärnten) im Rahmen der Pegmatitvorkommen des Millstätter Seerückens. *Archiv für Lagerstättenforschung, Geologische Bundesanstalt*, **7**: 173–187.
- LUTH, S.W. & WILLINGSHOFER, E. (2008): Mapping of the post-collisional cooling history of the Eastern Alps. *Swiss Journal of Geosciences*, **101**: 207–223.
- MANDL, G.W. (2000): The Alpine sector of the Tethyan shelf – Examplex of Triassic to Jurassic sedimentation and deformation from the Northern Calcareous Alps. *Mitteilungen der österreichischen geologischen Gesellschaft*, **92**: 61–78.
- MANDL, G. & ONDREJICKOVA, A. (1993): Radiolarien und Conodonten aus dem Meliatikum im Ostabschnitt der NKA (A). *Jahrbuch der Geologischen Bundesanstalt*, **136** (4): 841–871, Wien.
- MASSONNE, H.-J. (1981): Phengite: Eine experimentelle Untersuchung ihres Druck-Temperatur-Verhaltens im System  $\text{K}_2\text{O}-\text{MgO}-\text{Al}_2\text{O}_3-\text{SiO}_2-\text{H}_2\text{O}$ . Thesis, Faculty of Natural Sciences, Ruhr-Universität, Bochum, Germany.
- MEISEL, TH., MELCHER, F., TOMASCAK, P., DINGELDEY, CH. & KOLLER, F. (1997): Re-Os isotopes in orogenic peridotite massifs in the Eastern Alps, Austria. *Chemical Geology*, **143**: 217–229.
- MELCHER, F., MEISEL, T., PUHL, J. & KOLLER, F. (2002): Petrogenesis and geotectonic setting of ultramafic rocks in the Eastern Alps: constraints from geochemistry. *Lithos*, **65**: 69–112.
- MEYER, J. (1977): *Geologie des mittleren Liesertales mit Gmeineck und Tschirnock (Kärnten)*. Unpublished thesis, Formal- und Naturwissenschaftlichen Fakultät der Universität Wien, Austria, 138 p.
- MILLER, CH. (1990): Petrology of the type locality eclogites from the Koralpe and Saualpe (Eastern Alps), Austria. *Schweizerische Mineralogische und Petrographische Mitteilungen*, **70**: 287–300.
- MILLER, CH. & THÖNI, M. (1997): Eo-Alpine eclogitization of Permian MORB-type gabbros in the Koralpe (Eastern Alps, Austria): new geochronological, geochemical and petrological data. *Chemical Geology*, **137**: 283–310.
- MILLER, CH., STOSCH, H.G. & HOERNES, S. (1988): Geochemistry and origin of eclogites from the type locality Koralpe and Saualpe, Eastern Alps, Austria. *Chemical Geology*, **67**: 103–118.
- MILLER, CH., MUNDIL, R., THÖNI, M. & KONZETT, J. (2005): Refining the timing of eclogite metamorphism: a geochemical, petrological, Sm-Nd and U-Pb case study from the Pohorje Mountains, Slovenia (Eastern Alps). *Contributions to Mineralogy and Petrology*, **150**: 70–84.
- MORAU, W. (1982): Rb-Sr und K-Ar Evidenz für eine intensive alpidische Beeinflussung der Paragesteine der Kor- und Saualpe. *Tschermaks Mineralogische und Petrographische Mitteilungen*, **29**: 255–282.
- MOSTLER, H. & PAHR, A. (1981): Triasfossilien im “Caker Konglomerat” von Goberling. *Verhandlungen der Geologischen Bundesanstalt*, **1981** (2): 83–91.
- NEUBAUER, F. (1991): Kinematic indicators in the Koralm and Saualpe eclogites (Eastern Alps). *Zentralblatt für Geologie und Paläontologie Teil I*, (1): 139–155.
- NEUBAUER, F. (2002): Evolution of late Neoproterozoic to early Palaeozoic tectonic elements in Central and Southeast European Alpine mountain belts: review and synthesis. *Tectonophysics*, **352**: 87–103.
- NEUBAUER, F., DALLMEYER, R.D., DUNKL, I. & SCHIRNIK, D. (1995): Late cretaceous exhumation of the metamorphic Gleinalpe dome, Eastern Alps: kinematics, cooling history and sedimentary response in a sinistral wrench corridor. *Tectonophysics*, **242**: 79–89.



- NEUBAUER, F., DALLMEYER, R.D. & TAKASU, A. (1999): Conditions of eclogite formation and age of retrogression within the Siegraben unit, Eastern Alps: Implications for Alpine-Carpathian tectonics. *Schweizerische Mineralogische und Petrographische Mitteilungen*, **79**: 297–307.
- NEUBAUER, F., GENSER, J. & HANDLER, R. (2000): The Eastern Alps: Result of a two-stage collision process. *Mitteilungen der Österreichischen Geologischen Gesellschaft*, **92** (for 1999): 117–134.
- NIMIS, P. & TROMMSDORFF, V. (2001): Revised Thermobarometry of Alpe Arami and other garnet peridotites from the Central Alps. *Journal of Petrology*, **42**: 103–115.
- NITSCH, K.H. (1970): Experimentelle Bestimmung der oberen Stabilitätsgrenze von Stilpnomelan. *Fortschritte der Mineralogie*, **47** (Beiheft 1): 48–49.
- OBERHÄNSLI, R. (ed.) (2004): Metamorphic structure of the Alps. *Mitteilungen der Österreichischen Mineralogischen Gesellschaft*, **149**: 115–226.
- PAHR, A. (1980): Die Fenster von Rechnitz, Bernstein und Möltern. In Oberhauser, R. (ed.): *Der geologische Aufbau Österreichs*. Wien-New York: Springer-Verlag, 320–326.
- PEARCE, J.A. (1983): A “user’s guide” to basalt discrimination diagrams. Unpublished report, Milton Keynes: The Open University, 37 p.
- POPP, R.K. & GILBERT, M.C. (1972): Stability of acmite-jadeite pyroxenes at low pressure. *American Mineralogist*, **57**: 1210–1231.
- POWELL, R. (1985) Regression diagnostics and robust regression in geothermometer/geobarometer calibration: the garnet-clinopyroxene geothermometer revisited. *Journal of Metamorphic Geology*, **3**: 231–243.
- PROYER, A., DACHS, E. & KURZ, W. (1999): Relics of high-pressure metamorphism from the Großglockner region, Hohe Tauern, Austria: Textures and mineral chemistry of retrogressed eclogites. *Mitteilungen der österreichischen geologischen Gesellschaft*, **90**: 43–56.
- PUTIS, M., KORIKOVSKY, S., WALLBRECHER, E., UNZOG, W., OLESEN, N.O. & FRITZ, H. (2002): Evolution of an eclogitized continental fragment in the Eastern Alps (Siegraben, Austria). *Journal of Structural Geology*, **24**: 339–357.
- RANTITSCH, G. & RUSSEGER, B. (2000). Thrust-related very low grade metamorphism within the Gurktal Nappe Complex (Eastern Alps). *Jahrbuch der Geologischen Bundesanstalt* **142**: 219–225.
- RATSCHBACHER, L., FRISCH, W., NEUBAUER, F., SCHMID, S.M. & NEUGEBAUER, J. (1989): Extension in compressional orogenic belts: The Eastern Alps. *Geology*, **17**: 404–407.
- RATSCHBACHER, L., DINGELDEY, CH., MILLER, CH., HACKER, B.R. & MCWILLIAMS, M.O. (2005): Formation, subduction, and exhumation of Penninic oceanic crust in the Eastern Alps: time constraints from  $^{40}\text{Ar}/^{39}\text{Ar}$  geochronology. *Tectonophysics*, **394**: 155–170.
- REINECKE, T. (1991): Very-high-pressure metamorphism and uplift of coesite-bearing metasediments from the Zermatt-Saas zone, Western Alps. *European Journal of Mineralogy*, **3**: 7–17.
- RUBATTO, D. & HERMANN, J. (2001): Exhumation as fast as subduction? *Geology*, **29**: 3–6.
- RUBATTO, D., GEBAUER, D. & COMPAGNONI, R. (1999): Dating of eclogite-facies zircons: the age of Alpine metamorphism in the Sesia-Lanzo Zone (Western Alps). *Earth and Planetary Science Letters*, **167**: 141–158.
- SASSI, R., MAZZOLI, C., MILLER, C. & KONZETT, J. (2004): Geochemistry and metamorphic evolution of the Pohorje Mountain eclogites from the easternmost Austroalpine basement, Eastern Alps, Slovenia. *Lithos*, **78**: 235–261.
- SCHIFFMAN, P., LIOU, J.G. (1980): Synthesis and stability relations of Mg-Al pumpellyite,  $\text{Ca}_4\text{Al}_5\text{MgSi}_6\text{O}_{21}(\text{OH})_7$ . *Journal of Petrology*, **21**: 441–474.
- SCHIMANA, R. (1986): Neue Ergebnisse zur Entwicklungsgeschichte des Kristallins um Radenthein (Kärnten, Österreich). *Mitteilungen der Gesellschaft der Geologie und Bergbaustudenten Österreichs*, **33**: 221–232.
- SCHMID, S.M., FÜGENSCHUH, B., KISSLING, E. & SCHUSTER, R. (2004): Tectonic map and overall architecture of the Alpine orogen. *Eclogae Geologicae Helveticae*, **97**: 93–117.
- SCHMID, S.M., PFIFFNER, O.A., FROITZHEIM, N., SCHÖNBORN, G. & KISSLING, E. (1996): Geophysical-geological transect and tectonic evolution of the Swiss-Italian Alps. *Tectonics*, **15**: 1036–1064.
- SCHÖNLAUB, H.P. (1973): Schwamm-spiculae aus dem Rechnitzer Schiefergebirge und ihr stratigraphischer Wert. *Jahrbuch der Geologischen Bundesanstalt*, **116**: 35–49.
- SCHUSTER, R. (2004). The Austroalpine crystalline units in the Eastern Alps. Abstract PANGEO 2004, Berichte des Instituts für Erdwissenschaften, Karl-Franzens-Universität Graz, **9**: 30–36.
- SCHUSTER, R. & FRANK, W. (1999): Metamorphic evolution of the Austroalpine units east of the Tauern window: indications for Jurassic strike slip tectonics. *Mitteilungen der Gesellschaft der Geologie und Bergbaustudenten Österreichs*, **42**: 37–58.
- SCHUSTER, R. & STUEWE, K. (2008): Permian metamorphic event in the Alps. *Geology*, **36**: 603–606.
- SCHUSTER, R., BERNHARD, F., HOINKES, G., KAINDL, R., KOLLER, F., LEBER, T., MELCHER, F., & PUHL, J. (1999): Excursion to the Eastern Alps: Metamorphism at the eastern end of the Alps – Alpine, Permo-triassic, Variscan? *Berichte der Deutschen Mineralogischen Gesellschaft, Beiheft zur European Journal of Mineralogy*, **11** (2): 111–136.
- SCHUSTER, R., SCHARBERT, S., ABART, R. & FRANK, W. (2001): Permo-Triassic extension and related HT/LP metamorphism in the Austroalpine-Southalpine realm. *Mitteilungen der Gesellschaft der Geologie und Bergbaustudenten Österreichs*, **42**: 37–58.
- SCHUSTER, R., KOLLER, F., HOECK, V., HOINKES, G. & BOUSQUET, R. (2004): Explanatory notes to the map: Metamorphic structure of the Alps – Metamorphic evolution of the Eastern Alps. *Mitteilungen der Österreichischen Mineralogischen Gesellschaft*, **149**: 175–199.
- SCHUSTER, R., KOLLER, F. & FRANK, W. (2007): Pebbles of upper-amphibolite facies amphibolites in the Gosau Group of the Eastern Alps: relics of a metamorphic sole? Abstract 8th ALPSHOP Davos/Switzerland, 74.



- SELVERSTONE, J. (1993): Micro- to macroscale interactions between deformational and metamorphic processes, Tauern Window, Eastern Alps. *Schweizerische Mineralogische und Petrographische Mitteilungen*, **73**: 229–239.
- SELVERSTONE, J., SPEAR, F.S., FRANZ, G. & MORTEANI, G. (1984): High-pressure metamorphism in the SW Tauern Window, Austria: P-T paths from hornblende-kyanite-staurolite schists. *Journal of Petrology*, **25**: 501–531.
- SELVERSTONE, J., FRANZ, G., THOMAS, S. & GETTY, S. (1992): Fluid variability in 2GPa eclogites as an indicator of fluid behaviour during subduction. *Contributions to Mineralogy and Petrology*, **112**: 341–357.
- SÓLVA, H., THÖNI, M., GRASEMANN, B. & LINNÉ, M. (2001): Emplacement of eo-Alpine high-pressure rocks in the Austroalpine Ötztal complex (Texel group, Italy/Austria). *Geodinamica Acta*, **14**: 345–360.
- STAMPFLI, G.M. (1994): Exotic terrains in the Alps: a solution for a single Jurassic ocean. *Schweizerische Mineralogische und Petrographische Mitteilungen*, **74**: 449–452.
- STAMPFLI, G.M. & BOREL, G.D. (2004): The Transmed transsects in space and time: Constraints on the paleotectonic evolution of the Mediterranean Domain. In Cavazza, W., Roure, F., Spakman, W., Stampfli, G.M. & Ziegler, P.A. (eds): *The TRANSMED atlas: the Mediterranean region from crust to mantle*. Wien, New York: Springer Verlag, 53–70.
- STRAUSS, H. (1990): Kristallisations- und Deformationsgeschichte des Altkristallins nordwestlich von Villach. PhD thesis, University of Graz, Austria.
- TEIML, X. (1996): Die Gesteine der Millstätter Serie – petrologische und geothermobarometrische Untersuchungen. MSc thesis, University of Graz, Austria.
- TEIML, X. & HOINKES, G. (1996): Der P-T-Pfad der Millstätter Serie und ein Vergleich mit dem südliche Ötztal-Stubai-Kristallin. *Mitteilungen der Österreichischen Mineralogischen Gesellschaft*, **141**: 228–229.
- TEIML, X., HOINKES, G. & KONZETT, J. (1995): Joint occurrence of eclogites and white mica-amphibolites in the Austroalpine Basement (Eastern Alps). *Terra Abstracts*, **7**: 318.
- THÖNI, M. (1999): A review of geochronological data from the Eastern Alps. *Schweizerische Mineralogische und Petrographische Mitteilungen*, **79** (1): 209–230.
- THÖNI, M. (2002): Garnet chronometry in the Eastern Alps: insight into the polyphase nature of a composite orogenic structure. *Memorie di Scienze Geologiche*, **54**: 163–166.
- THÖNI, M. (2006): Dating eclogite-facies metamorphism in the Eastern Alps – approaches, results, interpretations: a review. *Mineralogy and Petrology*, **88**: 123–148.
- THÖNI, M. & JAGOUTZ, E. (1993). Isotopic constraints for eo-Alpine high-P metamorphism in the Austroalpine nappes of the Eastern Alps: bearing on Alpine orogenesis. *Schweizerische Mineralogische und Petrographische Mitteilungen*, **73**: 177–189.
- THÖNI, M. & MILLER, CH. (1996): Garnet Sm-Nd data from the Saualpe and Koralpe (Eastern Alps, Austria): chronological and P-T constraints on the thermal and tectonic history. *Journal of Metamorphic Geology*, **14**: 453–466.
- THÖNI, M. & MILLER, CH. (2000): Permo-Triassic pegmatites in the eo-Alpine eclogite facies Koralpe complex, Austria: age and magma source constraints from mineral chemical, Rb-Sr and Sm-Nd isotope data: *Schweizerische Mineralogische und Petrographische Mitteilungen*, **80**: 169–186.
- THÖNI, M. & MILLER, CH. (2009): The “Permian event” in the Eastern European Alps: Sm-Nd and P-T data recorded by multi-stage garnet from the Plankogel unit. *Chemical Geology*, **260**: 20–36.
- TOLLMANN, A. (1977): *Geologie von Österreich. Band 1. Die Zentralalpen*. Wien: Deuticke, 766 p.
- TROPPER, P. & HOINKES, G. (1996): Geothermobarometry of  $\text{Al}_2\text{SiO}_5$ -bearing metapelites in the western Austroalpine Ötztal basement. *Mineralogy and Petrology*, **58**: 145–170.
- USTASZEWSKI, K., SCHMID, S.M., LUGOVIĆ, B., SCHUSTER, R., SCHALTEGGER, U., BERNOULLI, D., HOTTINGER, L., KOUNOV, A., FÜGENSCHUH, B., & SCHEFER, S. (2009): Late Cretaceous intraoceanic magmatism in the internal Dinarides (northern Bosnia and Herzegovina): Implications for the collision of the Adriatic and European plates, *Lithos*, **108**: 106–125.
- VAN DER KLAUW, S.N.G.C., REINECKE, T. & STÖCKHERT, B. (1997): Exhumation of ultrahigh-pressure metamorphic oceanic crust from Lago di Cignana, Piemontese zone, western Alps: the structural record in metabasites. *Lithos*, **41**: 79–102.
- WALTER, F. (1998): Exkursion E4 am 27.9.1998 – MinPet '98 (Pörschach am Wörthersee/Kärnten) – Die Pegmatite des Millstätter See-Rückens. *Mitteilungen der Österreichischen Mineralogischen Gesellschaft*, **143**: 437–450.
- WALTER, F. (2009): Spodumen und Holmquistit in einem Pegmatit von Lug-Ins-Land, Millstätter Seerücken, Kärnten. In Niedermayr, G. *et al.*: *Neue Mineralfunde aus Österreich LVIII. Carinthia II*, **199/119**: 195–196.
- WHITE, R. (1991): Structure of the oceanic crust from geophysical measurements. In Floyd, P.A. (ed.): *Oceanic basalts*. Blackie: Glasgow, 30–48.
- ZACK, T., MORAES, R., KRONZ, A. (2004) Temperature dependence of Zr in rutile: empirical calibration of a rutile thermometer. *Contributions to Mineralogy and Petrology*, **148**: 471–488.
- ZIMMERMANN, R., HAMMERSCHMIDT, K. & FRANZ, G. (1994): Eocene high pressure metamorphism in the Penninic units of the Tauern Window (Eastern Alps). Evidence from  $^{40}\text{Ar}$ - $^{39}\text{Ar}$  dating and petrological investigations. *Contributions to Mineralogy and Petrology*, **117**: 175–186.



## Itinerary for IMA2010 AT1 Field trip

### Saturday, August 28, 2010 (Day 1): Eastern margin of the Alps

|             |   |
|-------------|---|
| 07.00–08.30 | Travel from Budapest to Cák via Győr                                |
| 08.30–10.30 | Field stop 1 (1/1): Quarry in Cák                                   |
| 10.30–10.45 | Field stop 2 (1/2): Travel to Lockenhaus, view on Castle Lockenhaus |
| 10.45–11.00 | Travel to Glashütten/Lockenhaus                                     |
| 11.00–11.20 | Field stop 3 (1/3): Gabbro quarry at Glashütten/Lockenhaus          |
| 11.20–11.40 | Travel to Bernstein   |
| 11.40–12.00 | Field stop 4 (1/4): Quarry Bienenhütte near Bernstein               |
| 12.15–13.15 | Lunch break and view to Bernstein                                   |
| 13.15–13.25 | Travel to Glashütten/Schlaining                                     |
| 13.25–14.25 | Field stop 5 (1/5): Ophicarbonates near Glashütten/Schlaining       |
| 14.25–14.40 | Travel to Unterkohlstätten  |
| 14.40–15.00 | Field stop 5a (1/5a): calcareous micaschist near Unterkohlstätten   |
| 15.00–15.45 | Travel via Schlaining to Rechnitz                                   |
| 16.00–17.00 | Field stop 6 (1/6): Quarry Freinguber close to Rechnitz             |
| 17.00–18.30 | Travel from Rechnitz to Oberwart and Graz, accomodation             |

### Sunday, August 29, 2010 (Day 2): Eclogite bearing Austroalpine units in the Koralpe and Saualpe area

|             |   |
|-------------|---|
| 08.00–08.30 | Travel to quarry Rath near to Bad Gams  |
| 08.30–09.45 | Field stop 7 (2/1): Mylonitic gneiss “Plattengneis”   |
| 09.45–10.15 | Travel to Hohl near to Schwanberg   |
| 10.45–11.15 | Field stop 8 (2/2): Kyanite eclogites   |
| 11.15–11.45 | Travel to Glashütten at the eastern slope of the Koralpe  |
| 11.45–12.15 | Field stop 9 (2/3): Geopark Glashütten  |
| 12.15–13.30 | Lunch break   |
| 13.30–13.45 | Travel to Weinebene at the ridge of the Koralpe   |
| 13.45–15.15 | Field stop 10 (2/4): Schists with large pseudomorphs of kyanite after andalusite, one hour walk in a smooth landscape at the ridge of the Koralpe |
| 15.15–16.30 | Travel to Diex at the southern slope of the Saualpe   |
| 16.30–17.00 | Field stop 11 (2/5): Overview on the Geology of central Carinthia, sightseeing “Wehrkirche”   |
| 17.00–18.00 | Travel to Klagenfurt, accommodation   |

### Monday, August 30, 2010 (Day 3): Austroalpine units in the Nockberge area

|             |   |
|-------------|---|
| 08.00–08.45 | Travel to Puch in the Krastal.  |
| 08.45–09.45 | Field stop 12 (3/1): Quarry Lauster, Marbles from the Millstatt Complex             |
| 09.45–10.15 | Travel to Lug-ins-Land at Baldersdorf and walk to outcrop.                          |
| 10.15–11.00 | Field stop 13 (3/2): Spodumenpegmatit   |
| 11.00–11.45 | Travel to Untertweng  |
| 11.45–13.00 | Field stop 14a (3/3a): Walk on outcrops of garnet micaschists of Radenthein Complex |
| 13.00–13.15 | Travel to Radenthein  |
| 13.15–14.00 | Lunch break   |
| 14.00–15.00 | Field stop 14b (3/3b): GRANATIUM  |
| 15.00–15.30 | Travel to Nöringsattel  |
| 15.30–16.15 | Field stop 15 (3/4): Garnet-Hornblende Schists, Hornblendegarbenschists             |
| 16.15–17.30 | Travel to Winklern  |
| 17.30–18.30 | Field stop 16 (3/5): Mineral exhibition Mautturm Winklern, accommodation            |



